DECONTAMINATING SENSITIVE EQUIPMENT OF TOXIC INDUSTRIAL MATERIALS

LA DÉCONTAMINATION DE L'ÉQUIPEMENT SENSIBLE DES MATIÈRES TOXIQUES INDUSTRIELLES

A thesis submitted to the Division of Graduate Studies
of the Royal Military College of Canada
by

Ross Warner Franklin
Major

In Partial Fulfilment of the Requirements for the Degree of
Master of Applied Science

September, 2016

Acknowledgements

The author gratefully acknowledges the material and technical support granted by Lieutenant-Colonel A. Rollin, Major K. Topping, and Major W. Willmott via the Advanced Technology Investment Reserve Programme, without whom and which none of the following work would have been possible. Likewise, this project would not have grown but for the ambition of partners J. Miedema and J. Robbins in earlier work.

To Professors J. Scott and E. Corcoran, and Drs. D. Kelly and E. Dickson, many thanks are due for ensuring the quality of the product and for guiding the critical transition in mentality from officership to academe. Any omissions or errors that may remain are the sole responsibility of the author.

Thanks also to A. White of the University of Northern British Columbia; J. McDonald of the Sudbury Neutrino Observatory office at Queen's University; S. White of St. Lawrence College; T. Mumby, E. Livermore, A. Qi, Dr. P. Samuleev, and S. Trickey of the Analytical Science Group; Major H. Berghuis of the Canadian Joint Operations Command; Professors P. Chan and R.G. Sabat; Drs. N. Bavarian, M. 'Kommy' Farahani, J. Snelgrove and M. Button, and to B. Ball, C. MacEwen, L. Marois, T. Nash, K. Sampson, D. Twigg, and X. Li and for their concrete contributions.

3M Company (Canada and USA offices) provided thermodynamic data and specifications for FK-5-1-12 without consideration. Some of those data are reproduced here with permission.

Abstract

The trends of aggressive agricultural growth, industrialisation, and urbanisation, combined with degraded industrial hygiene and security in conflict zones, are changing the environment of military operations. This fact is readily acknowledged in military tactical doctrine. The widespread presence of toxic industrial materials in theatres of operation poses risks to deployed personnel. To mitigate risks to personnel, there are established decontamination processes that remove or transform toxic materials, but these processes tend to damage so-called 'sensitive' equipment. When sensitive equipment is contaminated, it therefore becomes a liability. The Canadian Armed Forces lack a decontamination process for sensitive equipment that is both effective at reducing exposure risk for personnel and maintains the equipment's longevity.

The goal of this project was to evaluate the suitability of a commercially available liquid perfluorinated ketone—FK-5-1-12—originally marketed for fire suppression and designed to be minimally deleterious to human and environmental health, to decontaminate sensitive equipment of a range of toxic industrial materials likely to be encountered on deployed Canadian Armed Forces operations.

An inventory of toxic industrial materials was provided by the project sponsor and the toxic materials of greatest concern were identified. Likewise, the properties of sensitive materials and equipment were analysed and suitable challenge contaminants and material coupons for testing were procured. A bench-scale physical decontamination process was designed in which contaminated coupons were immersed in the liquid. The effectiveness of this treatment process was evaluated using neutron-activation analytical techniques for trace contamination.

Measures of suitability of the liquid as a decontaminant, including its operating requirements in hot climates, and the possibility of its reacting with common industrial chemicals, were analysed by numerical methods and by spectroscopic experiments. FK-5-1-12 may be used in hot climates, but would require persistent refrigeration to ensure its availability. It was found to react with both alcohols and amines, but more rapidly with the latter. This behaviour could prejudice its suitability in decontaminating substances with amine functions from sensitive surfaces since such surfaces could be damaged by the resulting evolution of heat and vapour.

Initial determinations of decontamination effectiveness at low contaminant loadings (14 $\mu g \cdot cm^{-2}$) confirmed that the perfluorinated ketone decontaminated surfaces by removing one order of magnitude of organophosphorus contaminant mass from a polyethylene coupon within one hour of treatment. However, at five- and ten-fold higher mass loadings, contaminant was not permanently removed. To test the hypothesis that contaminants tended to be displaced by the perfluorinated ketone, subsequent trials included a parallel separation process. Recovery of arsenical contaminant in cellulose and activated carbon sorptive media within the bounds of uncertainty supported this hypothesis and motivated further process optimisation. Consistent with theories of mass transfer, it was found that applying flow to the liquid, even in a laminar régime, resulted in even higher (> 90 %) rates of removal at time-scales of minutes, which are operationally relevant. Woven Nylon-6,6 substrate material was not as extensively decontaminated as non-woven polymer substrates, likely because of its relatively higher affinity for contaminants.

Devices representative of sensitive equipment used on operations—including laptop computers and night optics—were obtained for operational trials of the decontamination procedure to assess its suitability for treating full-scale equipment. Laptop computers were subjected to software-based stress tests and night optics to spectrometry. In one instance, a laptop hard-disk drive recorded a permanent 3 % loss of volume following its second immersion in the liquid. Some laptops reduced their performance when immersed, but reverted to normal operation afterwards. However, apart from these two failures, the equipment tested appeared to tolerate temporary immersion in the liquid, even when powered-on.

FK-5-1-12 is capable of rapid surface decontamination of typical electronics materials. However, it is not an ideal decontaminant with respect to all the likely requirements of a sensitive equipment decontamination system because of its low boiling point and chemical reactivity, particularly with amines. Nonetheless, it is hoped that the results of this thesis may inform the future procurement of a deployable sensitive equipment decontamination capability.

Résumé

Plusieurs tendances globales concomitantes, y compris une croissance agressive dans le secteur agricole, l'industrialisation et l'urbanisation, ainsi que la dégradation des contrôles d'hygiène et de la sécurité à travers les zones de conflit, créent un milieu d'opérations militaires complexe et dangereux. Malgré la reconnaissance de ce problème au sein de la doctrine militaire, l'omniprésence des matières toxiques industrielles pourrait constituer un défi significatif aux mesures de protection de santé des forces déployées ainsi qu'aux procédures actuelles de décontamination d'équipement en raison des risques inattendus. Par exemple, les composants de plusieurs équipements sensibles et ceux des solutions de décontamination sont incompatibles. Donc, l'équipement contaminé pourrait devenir plutôt un risque qu'un atout pour les forces déployées. Présentement, les Forces armées canadiennes ne possèdent aucun système de décontamination convenable aux tels équipements sensibles.

Le but de la présente recherche était une évaluation de l'aptitude d'une cétone fluorée liquide de disponibilité commerciale, soit la FK-5-1-12, à effectuer la décontamination des équipements sensibles opérés par les Forces armées canadiennes à travers l'enlèvement des matières toxiques industrielles communes. L'enlèvement de plusieurs contaminants d'une variété de surfaces sensibles a été évalué lors de ce travail afin de concevoir un ensemble de démonstration technologique pour les Forces armées canadiennes.

Un inventaire des matières toxiques industrielles a été fourni par le commanditaire. Des coupons de matériel pour les essais d'efficacité d'un processus modèle de décontamination ont été obtenus suite à l'analyse des dispositifs sensibles. Un processus modèle de décontamination superficielle à travers l'immersion des coupons dans 10 mL de la cétone fluorée a été quantifié par les analyses instrumentales de neutrons activés des atomes spécifiques.

Des mesures de la pertinence de l'emploi du liquide, y compris ses besoins opérationnels de stockage et de transport ainsi que ses possibles réactions chimiques avec des substances industrielles communes, ont été analysées à travers les méthodes numériques et par les expériences spectroscopiques. La FK-5-1-12 pourrait être employée aux climats chauds, mais ceci exigera une réfrigération constante. Elle semble plus réactive avec les amines qu'avec les alcools, dégageant de la chaleur et de la vapeur une fois en contact avec les amines en particulier, ce qui pourrait nuire à sa pertinence. Par exemple, la

décontamination des espèces aminées sans endommager les surfaces sensibles pourrait constituer un défi.

Les quantifications initiales de la décontamination des bas fardeaux de contamination (14 $\mu g \cdot cm^{-2}$) organophosphoré ont confirmé l'hypothèse que la cétone fluorée pourrait effectuer la désorption physique superficielle des contaminants. Par exemple, 90 % de la masse initiale de contamination a été enlevé en dedans d'une heure lorsqu'un coupon de polyéthylène était assujetti au processus. Par contre, aux plus hauts fardeaux de cinq et dix fois de plus de densité de contamination, cette action de désorption n'était pas permanente. Donc, dans le but de confirmer l'hypothèse que la cétone fluorée pourrait au minimum déplacer les espèces de contamination, la procédure a été modifiée pour accommoder une étape de séparation en parallèle. La récupération de contamination arsénique dans les médias de séparation (le charbon activé et la cellulose) a confirmé cette dernière hypothèse et a motivé l'optimisation du processus. Par exemple, l'augmentation du débit de la cétone, même dans un régime d'écoulement laminaire, a transféré plus de masse de contamination (> 90 %) et celle-ci, plus rapidement que lorsque la cétone était en repos. Les coupons en Nylon-6,6 n'ont pas été décontaminés aussi rapidement que les coupons en polymères non-tissés, ce qui s'explique par l'affinité supérieure de Nylon aux contaminants.

La compatibilité du processus aux dispositifs représentatifs de l'équipement sensible, y compris les ordinateurs portatifs et les monocles à vision nocturne, a été essayée lors de 17 essais opérationnels. Les ordinateurs portatifs ont subi des essais de stress par logiciel, tandis que les monocles ont été essayés par la spéctrométrie. Une panne transitoire, soit l'incapacité de transmission des données par laser lors de l'immersion, a été observée. Exceptionnellement, il y avait une perte permanente de 3 % du volume d'un disque dur qui s'est produit après un deuxième essai d'immersion. Il n'y avait ni d'autres résultats inattendus, ni d'autres pannes transitoires ou permanentes au bilan des essais.

La FK-5-1-12 est capable de décontaminer rapidement les superficies des matériaux électroniques. Pourtant, elle ne répond pas à l'ensemble des besoins opérationnels probables d'un système de décontamination sensible en raison de son point d'ébullition bas et de sa réactivité avec les amines. Néanmoins, les résultats communiqués dans le présent travail pourraient contribuer à l'acquisition d'un système déployable qui convient à la décontamination de l'équipement sensible.

Table of Contents

List of Tables

List of Figures

List of Equations

Note on Units and Nomenclature

Preference is given to base and derived units of the *Système international d'unités* (SI), with the exception of some manufacturing specifications and tolerances for which metrology is reported in United States customary units. For instance, computer screen diagonal dimensions are reported in inches (in), and polymer thicknesses may be given in thousands of an inch (thou). SI equivalents are given in all instances to avoid ambiguity.

For organic chemical nomenclature, preference is given to rules established by the International Union of Pure and Applied Chemistry. Exceptions are for classes of mass-manufactured pure substances and mixtures for which a relevant, industrially recognised designation exists. For instance, refrigerants and some engineered fluids are named according to the rules of the American Society of Heating, Refrigeration, and Air-Conditioning Engineers, and weaponised chemical agents are assigned two-letter military designations. Organisms at the species level are named according to the rules of binomial nomenclature.

The constant e is 2.71828… and j is $\sqrt{-1}$.

Glossary

2ME	2-mercaptoethanol, 2-thioethanol
AES	Auger electron spectroscopy
B3LYP	Becke, 3-parameter, Lee–Yang–Parr (density functional)
BAET	2-(butylamino)ethanethiol
BIOS	built-in operating system
BITE	built-in test equipment
BrPMe	bromophos-methyl, 4-bromo-2,5-dichlorophenyl dimethyl phosphorothionate
CAF	Canadian Armed Forces
CARC	Chemical Agent Resistant Coating
CAS	Chemical Abstracts Service
CB	cyanobiphenyl
CBRN	chemical, biological, radiological, and nuclear
CCD	charge-coupled device
CEES	2-chloroethyl ethyl sulfide, half-mustard
CEPA	Canadian Environmental Protection Act
CFC	chlorofluorocarbon
CF CBRN D S	Canadian [Armed] Forces Chemical, Biological, Radiological, and Nuclear Decontamination System
CFDS	*Canada First* Defence Strategy

CG	carbonyl dichloride, phosgene
cgs	centimetre–gram–second base units
CK	chloroformonitrile, cyanogen chloride
COTS	Commercial-off-the-Shelf
CPU	central processing unit
CW	chemical warfare
DA	diphenylchloroarsenic
DC	diphenylarsanecarbonitrile
DCM	dichloromethane, methylene chloride
DEP	diethyl phthalate
DFATD	[Canadian] Department of Foreign Affairs, Trade, and Development
DFT	density functional theory
diglyme	bis(2-methoxyethyl)ether
DIMP	diisopropyl methylphosphonate
DMMP	dimethyl methylphosphonate
DMSO	dimethyl sulfoxide
DWCP	Directory of World Chemical Producers
EC	Enzyme Catalogue
ECBC	Edgewood Chemical Biological Centre
ED	ethylene diamine, ethane-1,2-diamine
EDAX	energy-dispersive X-ray spectroscopy

EEPROM	electrically erasable programmable read-only memory
EG	ethylene glycol, ethane-1,2-diol
EPDM	ethylene propylene diene monomer
EtOH	ethanol
FID	flame ionisation detection
FK-5-1-12	1,1,1,2,2,4,5,5,5-nonafluoro-4-(trifluoromethyl)-3-pentanone/3M Novec 1230/3M Novec 649
FoV	field of view
FTIR	Fourier-transform infrared [spectroscopy]
GA	Tabun, (*RS*)-Ethyl *N*,*N*-dimethylphosphoramidocyanidate
GAC	granular activated carbon
GB	Sarin agent, (*RS*)-propan-2-yl methylphosphonofluoridate
GC	gas chromatography
GD	Soman agent, 3,3-dimethylbutan-2-yl methylphosphonofluoridate
HCFC	hydrochlorofluorocarbon
HD	distilled sulfur mustard agent, bis(2-chloroethyl) sulfide
HDD	hard disk drive
HDPE	high-density polyethylene
HFC	hydrofluorocarbon
HFE-7100	methyl-nonafluoro[iso]butyl ether (azeotrope)

HFE-7200	ethyl-nonafluoro[iso]butyl ether (azeotrope)
[I]NAA	[instrumental] neutron-activation analysis
IPCC	Intergovernmental Panel on Climate Change
IPE	Individual Protective Ensemble/Equipment
i-PrOH	isopropanol, 2-propanol
IR	infrared
ISO	International Organisation for Standardisation
IUPAC	International Union of Pure and Applied Chemistry
[Agent] L	Lewisite, 2-chloroethenylarsonous dichloride
LC[D]	liquid crystal [display]
LD_{50}	lethal dose to 50% of exposed population
LDPE	low-density polyethylene
LFTSP	Land Force Technical Staff Programme
LOQ	limit of quantitation
LUMO	lowest unoccupied molecular orbital
MEA	monoethanolamine, 2-aminoethanol
MeOH	methanol
MES	methyl salicylate
Mil-Spec	military specification
MNVG	monocular night-vision goggles

MOTS	Military-off-the-Shelf
MS	mass spectrometry
MTBF	mean time between failures
MTTF	mean time to failure
MTTR	mean time to repair
NATO	North Atlantic Treaty Organisation
NMR	nuclear magnetic resonance [spectroscopy]
OMPA	octamethylpyrophosphoramide, Schradan, *N*-[bis(dimethylamino)phosphoryloxy-(dimethylamino)phosphoryl]-*N*-methylmethanamine
OP	organophosphate/phosphorus
OSPM	Operating System-driven Power Management
PFC	perfluorocarbon
PFPrA	1,1,1,2,2-pentafluoropropanoic acid
PFPE	perfluoropolyether
PM	particulate matter
PrCB	printed circuit board
QL	*N*-[2-(ethoxy(methyl)phosphanyl)oxyethyl]-*N*-isopropyl-propan-2-amine
QoS	Quality of Service
RAM	random-access memory
RMCC	Royal Military College of Canada
rms	root–mean–square

SEDS	Sensitive Equipment Decontamination System
SEEDP	Sensitive Electronic Equipment Decontamination Project
SI	*Système international d'unités*
SIMS	Secondary-ion mass spectroscopy
SLOWPOKE-2	Safe LOW-POwer [K]ritical Experiment reactor
SMART	Self-Monitoring and Reporting Technology
SNR	signal-to-noise ratio
SOR	Statutory Orders and Regulations; Statement of [Operational] Requirements
t-BuOH	*tert*-butanol, 2-methyl-2-propanol
TDG	thiodiglycol, 2,2′-thiodiethanol
TDP	technology demonstration package
TFA	trifluoroacetate
TFT	Thin-Film Transistor
TIM	Toxic Industrial Material
TPhAs	triphenylarsine
TWA	Time-Weighted Average
USB	Universal Serial Bus
UV	ultraviolet
VASE	variable-angle spectroscopic ellipsometry
VHP	vaporous hydrogen peroxide

VOC	volatile organic compound
VX	ethyl ({2-[bis(propan-2-yl)amino]ethyl}sulfanyl)(methyl)phosphinate
WSXGA+	Widescreen Super-Extended Graphics Array Plus
XPS	X-ray photoelectron spectroscopy

1. Introduction

1.1 – Foreword

The Canadian Armed Forces (CAF) do not currently possess a sensitive equipment decontamination capability. When task forces of the CAF are deployed in Canada or abroad, their use of Commercial-off-the-Shelf (COTS) electronics and other sensitive equipment can become a liability in the event of exposure to chemical, biological, radiological, and nuclear (CBRN) materials or to toxic industrial materials (TIMs). If such sensitive equipment becomes contaminated with CBRN or TIMs, it cannot be decontaminated with existing methods (to reduce risk to personnel) without being destroyed itself. Because of the logistical burdens of disposing of and replacing COTS equipment, it is desired to design a field-expedient decontamination system suitable for them. This capability gap has motivated the current project.

1.2 – Thesis Scope

The aim of this section is to introduce three themes that inform the sensitive equipment decontamination problem. First, the notions of 'contamination', 'decontamination', and 'sensitivity' all depend upon material properties: the properties of contaminants themselves, of surfaces, and of the interactions between them. Second, the measures of effectiveness of any decontamination process are described by the extents of removal or transformation of a contaminant. Unfortunately, a process to remove or transform contaminant may cause the underlying material to fail—an undesired result. Finally, the measures of suitability particular to sensitive equipment decontamination are described by reliability, i.e. the probability that equipment subjected to a decontamination process will function as intended instead of failing.

1.2.1 – Material Properties

The risk of TIMs is a consequence of their physico-chemical properties. Globally, TIMs are present in wide variety, large quantity, and often without adequate industrial hygiene protocols, which increases the risks of exposure to deployed military forces.[1] Personnel may be exposed, acutely or chronically, to substances either banned or obsolete in Canada, or to higher ambient concentrations than would otherwise be the case. Some TIMs, e.g. activated organophosphate (OP) pesticides and radioactive particulate matter (PM), may act in similar ways as classic CBRN agents, and result in illness or death of personnel.[2] Of particular concern are TIMs that tend to remain on

affected surfaces (are persistent), because of the prolonged risks they pose. These TIMs, in priority, must be decontaminated somehow in order to reduce residual risk to personnel. Hence, the means by which surfaces become contaminated, and may be decontaminated, are germane to the problem. Likewise, knowledge of surface and material properties describes the ability of certain chemicals to achieve decontamination of persistent TIMs, and distinguishes the sensitivity of some surfaces from the durability of others.

A surface, e.g. of a piece of equipment, is *contaminated* when an unwanted chemical tends to remain on it. With some materials, there is a risk that the chemical will escape and harm nearby personnel. With others, a chemical bound to the surface will remain more definitely, and risks of harm are reduced. Depending on its composition and the nature of its surface interactions, a harmful chemical species can be removed or transformed into benign products. These techniques are generally called *physical* and *chemical* methods of decontamination and are distinguished by the presence of such a transforming chemical reaction.

A material is *sensitive* through its tendency to be damaged as a result of a treatment process, such as a decontamination process intended to remove or transform harmful chemical species. A material may suffer weakening physical damage or chemical reaction even as the harmful chemical species is removed or transformed. When sensitive materials are incorporated into equipment parts, as is often the case for COTS electronic equipment, the equipment itself may fail and require replacement if it is subjected to an unsuitable decontamination process. By relating both sensitivity and contamination/decontamination to surface and material properties, quantitative measures of the effectiveness and suitability of any decontamination process may be defined.

1.2.2 – Decontamination Effectiveness and Deficiencies

As it stands, there are effective methods available to decontaminate vehicles, personnel, and the environment. Contamination may, to large extent, be removed from such surfaces or transformed into benign products. Moreover, the methods pose minimal risk of enduring harm to the underlying (substrate) materials. Typically, these methods include contact with water- or alcohol-based solutions of electrically conductive chemicals. However, the distinct properties of sensitive equipment impose particular requirements for decontamination that make the foregoing unsuitable. For instance, sensitive equipment often contains electronic, electro-optic, and mechanical parts, as well as thin coatings, adhesives, and lubricants that are readily damaged by

electrically conductive, corrosive, and inflammable chemicals. Even though the equipment would be rendered safe and not pose a residual risk to unprotected personnel if subjected to typical decontamination methods, it would be unusable and require replacement. A more attractive possibility is to mitigate risk by decontaminating the equipment such that it is both safe and serviceable. To do so, atypical decontamination methods require investigation.

1.2.3 – Suitable Methods for Sensitive Equipment Decontamination

In principle, the possibilities for sensitive equipment decontamination include methods that do not rely upon the electrically conductive, corrosive, or inflammable compounds that are well-established for use on vehicles, the environment, or personnel. Indeed, there are both physical and chemical methods that have been designed expressly for the goals articulated earlier. These methods strike a balance between removing or transforming contaminants on one hand, and preserving the material integrity and function—the reliability—of sensitive equipment on the other. There are also families of compounds related to established decontaminants that have not been studied or marketed for sensitive equipment decontamination, but which may prove useful for this purpose.

Thus, there are three themes that describe the sensitive equipment decontamination problem. First, the meanings of sensitivity, contamination, and decontamination are all unified through an understanding of material properties. Knowing these properties provides both the design challenge and insight into possible solutions. Second, the effectiveness, but unsuitability, of existing decontamination methods with respect to sensitive equipment imposes constraints on feasible design options. Third, the suitability of a novel decontamination process intended for sensitive equipment may be described in terms of the enduring reliability of the equipment.

1.3 – Outline of Activities

The aim of the project was to evaluate the effectiveness and suitability of a physical decontamination method for sensitive equipment through experiments. Before any experiment or design was undertaken, however, a review of the literature provided focus to the course of the project.

Within the theme of material properties, the project sponsor provided an inventory of the TIMs of greatest concern to the CAF. TIMs in this inventory were rationalised into a representative sample against which

decontamination could be tested. The second effort was to learn about the material properties that give rise to sensitivity, contamination, and decontamination. Sensitive materials, representative of genuine equipment, were sought for testing. The properties of surfaces provided insight on the range of technologically feasible options for decontamination, and why methods may be both effective in decontamination and yet unsuitable for particular materials. Quantitative requirements for the effectiveness of a decontamination process were obtained from literature and military doctrine. The literature was also searched for examples of available technologies, particularly those designed for sensitive equipment, so as to comment on their fitness for the deduced requirements. To answer the question of decontamination effectiveness, appropriate analytical techniques were sought. Finally, the operation of sensitive equipment was researched to understand how performance and reliability could be attributed to it before, during, and after any model decontamination process.

The first stage of experiments was to evaluate some properties of a commercially available fluid that may be both effective and suitable for physical decontamination of sensitive equipment. The likely limitations to large-scale field deployment of this fluid were considered through its chemical and thermodynamic properties. Since ecological effects, commercial availability, cost, and regulatory status may also constrain use, these factors were considered as well.

The second stage of experiments was to test the effectiveness of the fluid in decontaminating surfaces. Having arrived at a group of challenge contaminants, representative materials, and analytical methods for a bench-scale process, tests were designed and executed. Test results were interpreted against the requirements deduced for field-expedient, large-scale decontamination. Changes were made at the bench scale in an effort to optimise decontamination effectiveness against the operating environments and time constraints of a deployable process.

The final stage of experiments was to design and execute a test plan that would quantify the effects of the model decontamination process itself on the performance and reliability of full-scale sensitive equipment. Performance and reliability statistics on the equipment were accumulated alongside data on its possible physical failure modes. The statistical results of a reliability test plan, combined with physical data on failure modes, would provide critical measures of suitability about the decontamination process and complement the results of its effectiveness in decontaminating surfaces.

Through a literature review into the TIMs of greatest operational concern and existing decontamination methods, it was possible to select appropriate challenge contaminants for decontamination experiments and obtain measures of effectiveness, such as the extent of removal or transformation. In addition, through a review of the common material properties of sensitive equipment, it was possible to obtain operational testing procedures and measures of suitability, such as the confidence that equipment would function as intended after being subjected to a decontamination process. A process which is both effective and suitable could meet the aim of the project and be scaled-up to address the current capability gap in sensitive equipment decontamination.

In summary, deployed CAF task forces may have no option but to operate near TIM-contaminated zones as missions dictate, and are unlikely to stop using COTS and other sensitive equipment to fill operational requirements. The risks of personnel exposed to TIMs through many pathways will rise as a result. For some of these pathways, including hardened equipment, vehicles, and the environment, there are existing methods to decontaminate to the extent required by the mission and mitigate risk to personnel, while avoiding damage to the underlying material. However, no such methods have yet been fielded for sensitive equipment, which has motivated the current project.

2. Literature Review

The purpose of this section is to review the aspects of decontamination that pertain to sensitive equipment in general, beginning with the materials that characterise the problem. The requirements and methods for decontamination, as found in the literature, informed the design, execution, and interpretation of the bench-scale experimental procedures undertaken in this project. Similarly, an understanding of the normal operation and reliability of sensitive equipment provided objective criteria with which to evaluate the suitability of a model decontamination process. The final objective of this section is to describe a specific compound that may achieve some of the requirements deduced for sensitive equipment decontamination.

2.1 – Materials Relevant to Sensitive Equipment Decontamination

The materials relevant to sensitive equipment decontamination are presented, starting with contaminants, moving next to the contaminant–substrate interface, and then to the substrates themselves. In the first place, among the TIMs of greatest concern to the CAF, representative classes of chemicals were selected for testing based on their persistence and toxicological risk. The properties of typical sensitive materials (including what makes them 'sensitive') and of surface interactions provided insight into the nature of contamination and into possible mechanisms for decontamination. Requirements for sensitive equipment decontamination were derived from military doctrine. Examples of decontamination systems, both in service and in development, were found in the literature to illustrate the state of the art.

2.1.1 – TIMs of Greatest Operational Concern

In order to obtain meaningful results from a bench-scale sensitive decontamination process, a representative sample of contaminants was needed. To guide the project, the sponsor (the CAF Directorate of CBRN Defence) provided an inventory of TIMs posing acute inhalation toxicity risks. The list, compiled and analysed by the United States Naval Research Laboratory, includes five classes of chemicals: oxidisers, reducers, volatile organic compounds (VOCs), self-polymerisers, and biocides, collectively accounting for hundreds of different chemicals.[3] However, it is not practical to 'decontaminate' TIMs that disperse or react rapidly, which includes the majority of oxidisers, reducers, and self-polymerisers. For instance, if the top priority TIM of concern, ammonia, were released in a significant quantity (70 m^3), it would cease to pose an acute health risk to personnel at distances

of 1-5 km downwind, 15 min after release, depending upon meteorological conditions.[4] While such chemicals are indeed acutely toxic, they do not persist (adsorb) on surfaces. In contrast, it is required to decontaminate more persistent or accumulative toxic chemicals, which include the VOCs and biocides, and in turn, most classical chemical warfare (CW) agents.[5] The basic properties of these classes are described in further detail in the following paragraphs.

2.1.1.1 – VOCs

VOCs may be defined as compounds of carbon having vapour pressures > 69 Pa at room temperature (up to 25 °C), boiling points < 260 °C at 1 atm (101.325 kPa), and that tend to react with other compounds in the atmosphere in the presence of visible and ultraviolet light.[6] VOCs include short-chain linear, cyclic, and branched aliphatic hydrocarbons, aromatic hydrocarbons, and similar compounds with functional groups (e.g. hydroxyl, amine, and carbonyl). Alone, they present several risks for human and environmental health, including acute inhalation toxicity.[7] They also react with oxides of nitrogen in the presence of light to yield ground-level ozone, a significant air contaminant.[8] Although 'volatile' and readily evaporated, they are relatively more persistent than other classes of TIMs, such as fumigant gases and vapours, because they have a higher tendency to adsorb or remain on surfaces, including synthetic materials.[9] The tendency to remain on surfaces and then gradually change into the vapour phase, where they damage respiratory health, imposes residual risks on personnel. To mitigate such risks may require that VOCs be decontaminated.

2.1.1.2 – Biocides

Biocides are noted among the TIMs for their relatively greater "stability and ease of dispersion" than the other four classes and, as suggested by their name, are primarily intended to destroy life.[3] Although their combination of high stability, ease of dispersion, and propensity to kill is beneficial in agriculture and pest control, their decontamination is particularly important to minimise residual risks to personnel. Biocides are collectively represented in the NRL list by an organophosphate (OP) pesticide, octamethyl diphosphoramide (OMPA), whose structure is shown in Figure 1.[3]

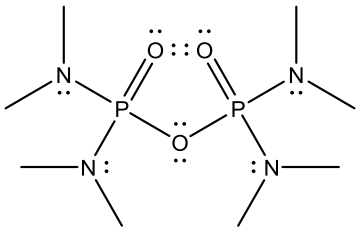

Figure 1: Octamethyl diphosphoramide

In addition to knowledge of the identities of the TIMs of greatest concern, the relevant amounts of these chemicals, and the risks they can pose, serve to quantify contamination and decontamination.

2.1.2 – Risks of Exposure to TIMs

The purpose of this section is to review the risks posed by TIMs, and, in turn, the measures of effectiveness of any process whose goal is to decontaminate them from sensitive equipment. In a risk calculation, sensitive equipment is a possible pathway for a contaminant source to reach a final human receptor. The human receptor, if given sufficient warning of the presence of a contaminant, can take steps to mitigate its own exposure. For instance, it could avoid travel across the contaminated zone, or adopt protective measures. If, however, warning is not available and exposure is inevitable, then appropriate hazard-management steps, including decontamination, must be taken.[10] Mitigating the final branch of the risk pathway and preventing casualties is therefore the ultimate goal of decontamination, but there must be criteria with which to judge its success. The figures of merit in evaluating decontamination effectiveness against challenge contaminants in the current project have been derived from literature on human toxicology.

Evaluating the source term in a risk estimate of deployed forces to TIMs is problematic: voluntarily reported data are available in the Directory of World Chemical Producers (DWCP), but chemical-production facilities are not always inspected to verify this reporting.[3] Probabilistic estimates are one practical method of arriving at a source term in risk analysis.[11] The source and receptor terms must also be linked by an environmental pathway for the hazard to be exerted. If no pathway exists, or if it is removed, then risk has been mitigated.[12] For these reasons, estimates will likely be conservative and at a level of precision no better than an order of magnitude. Even so, with conservative assumptions, it is possible to draw upon toxicological data to arrive at working figures. Common figures of merit in assessing environmental and human toxicity are the *dose* (or concentration) *lethal to*

50 % of the exposed population.[13] Such doses are usually expressed as LD_{50} or LC_{50} and correspond to dose-mass per unit of body-mass integrated over exposure time. Human responses to toxic loads can span several orders of magnitude of contaminant mass concentration.[13]

While the relationship between toxic load and local concentration or time of exposure is not necessarily linear, a decrease in either variable usually results in less toxic load, and therefore less risk to the receptor. For instance, a concentration–time toxicity value for OMPA, expressed as the *Acute Exposure Guideline Level 3* (a life-threatening risk), is 0.30 ppm (3.51 $mg \cdot m^{-3}$) over 1 hour of exposure at 25 °C.[14] Since deployed forces may be required to remain in a contaminated zone for such lengths of time, the duration of exposure cannot necessarily be controlled. To ensure safety, conservative assumptions are made in the time dimension. Hence, a process (decontamination) is needed to decrease the local concentration of contaminant and lower the risk to personnel. The quantity remaining at the end of a process is the most important figure in the risk calculation because it imposes the risk, but it is a function of the initial load and the extent of removal. For example, 99 % removal of 100 units initially on an affected area, and 99.99 % removal of 10 000 units on the same area, both yield the same result—1 unit remaining. Therefore, in addition to reporting an achievable extent of removal in a given time, it is important to note the initial load when comparing the efficacy of decontamination processes.

The concentration–time relationship in the toxicity of TIMs provides figures of merit with which to estimate risks to personnel, as well as the effectiveness of decontamination, in terms of contaminant mass loading and achievable extents of removal. In addition to objective criteria that quantify the risks of health effects of TIMs and overall measures of the effectiveness of their decontamination, the literature contains insight into the very nature of contamination, decontamination, and sensitivity, through the study of surface phenomena and material properties.

2.1.3 – Decontamination

The purpose of this section is to provide a working definition for 'decontamination' and the root of the problem of sensitive equipment decontamination. Decontamination may be defined generally as the "removal or neutralisation of chemical, biological, radiological, and nuclear contamination."[15] In Canadian military doctrine, decontamination includes TIMs, but is expressed in CBRN terms as the

> "process of making any person, object, or area safe by absorbing, destroying, neutralising, making harmless, or removing chemical or biological agents, or removing radioactive material clinging to or around it."[16]

Even with the broader Canadian military definition that gives five methods, the aim of decontamination could apparently be met by making an affected area safe. However, while safety is necessary, it alone is insufficient. There is an implicit goal that any contaminated surface (whether human tissue, armoured vehicle, or sensitive equipment) be restored to normal use. In other words, serviceability is desired in addition to safety.

A frustration between safety and serviceability quickly emerges. A decontamination process can remove or transform an underlying (substrate) material just as it can a contaminant. If it reacts with both, and transforms the contaminant, but damages the substrate, then the first purpose of decontamination has been achieved, but at the cost of rendering the substrate unserviceable. It seems preferable not only to create safety, but to preserve serviceability whenever practical. Otherwise, large quantities of equipment would be disposed of, and require costly replacement, if ever they became contaminated. While some COTS electronics are so inexpensive and rapidly obsolete as to be disposable, the same cannot be said for all equipment, such as sensitive electro-optics. Canadian military task forces, in contrast to domestic emergency responders, may face longer and costlier supply chains simply by virtue of being deployed in austere conditions.[17] As a result of this diminished supply capacity, it would be preferable to preserve the functioning of mission-critical equipment. A decontamination process for sensitive equipment that is both effective and suitable can resolve this frustration.

2.1.4 – Model of Contamination

In assessing how to decontaminate a surface effectively and safely, it is helpful to understand the cause of contamination in the first place. Such understanding is gained through surface science, which also provides the theoretical framework for understanding the material properties of sensitive equipment, to be described in the following section.

Figure 2 depicts a conceptual model (not to scale) of a solid surface, and defines several characteristics. Attached species or *adsorbates* include gases, vapours, liquids as drops or films, and solid particulate matter. Surfaces usually hold some moisture, and may be treated with lubricant or adhesive.[18]

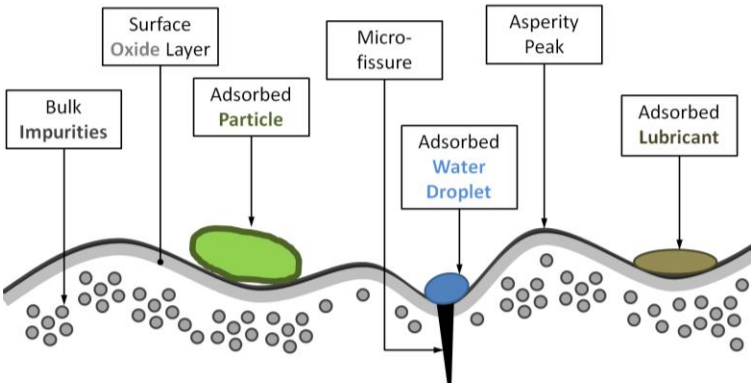

Figure 2: Conceptual Model of a Real Surface

The interactions at a surface are governed by many thermodynamic parameters, not all of which may be readily measured. Solids have surface energy and liquids have surface tension (the free energy per unit area), which are measurable quantities, but these are lumped physical parameters. An appropriate physical model can provide insight both into the causes of contamination, and into their reversal, so as to achieve decontamination.[19] As shown in the figure, an unwanted particle or liquid drop that has adsorbed onto a surface has contaminated it. The endurance of contamination means that the sum of driving forces tending to remove it is less than that of the forces keeping it attached. An optimally applied driving force could upset the equilibrium that favours contamination and lead to a decontaminated surface. However, while it may be acceptable to remove adsorbed water along with a contaminant particle, it may be unacceptable to remove a required surface treatment, such as lubricant or adhesive, because damage to the surface may result. A suitable decontamination technique would preferentially remove 'contaminant' adsorbates, even though their properties may resemble those of required surface treatments.

A contaminant may be removed from a surface by some combination of driving forces that causes it to be pushed or pulled off, or else chemically transformed. Engineered examples of these methods are surveyed in the literature review but their principles will be introduced briefly. A push or pull may be accomplished by exerting high or low pressure on the contaminant, e.g. by fluid flow or vacuum. A fluid that has some chemical affinity for the contaminant may dissolve it, as when water dissolves inorganic salts or particles. A fluid without such affinity may displace contaminant from the surface and achieve a similar result, as when lubricant displaces water from the microstructure of metal. Grease on a polished surface resists removal by

water, even with a surface-active agent (surfactant, e.g. a detergent) to lower the surface tension, which requires a more aggressive decontamination scheme. By adjusting the pH of the system, the surfaces of the surfactant micelles and the contaminants become mutually repulsive, which greatly hastens cleaning.[20] Conversely, as the decontamination scheme involves ever larger physico-chemical driving forces, it may increasingly imperil the integrity of the substrate by depleting a required surface treatment, such as a lubricant.

The molecule poly(tetrafluoroethylene), PTFE (Teflon), provides an example of the physico-chemical behaviour desired for general-purpose decontamination. PTFE is used in solid 'non-stick' surface coatings because of its low surface energy and self-lubricating properties.[21] As a result, it resists contamination by many types of molecules. If a liquid with such properties were to flow between a surface and a contaminant, it could result in less long-range attraction between them, leading to separate, distinct phases.[22] Such a property of 'repulsion' could then be usefully applied to the problem of decontamination. Indeed, liquid perfluorocarbons have been used to displace both water and hydrocarbons.[23] For instance, liquid- and vapour-phase perfluorocarbons, as well as other minimally reactive fluids, are among the preferred agents for intraocular tamponade, in which they prevent other fluids from entering a torn retina for a specified length of time after surgery.[24]

A physically decontaminating liquid must also have the ability to penetrate the region of the surface close to the contaminant. Given enough momentum, a liquid becomes turbulent, and can drag or detach a film or drop from a contaminated surface.[25] However, if supplied too much momentum, the liquid will change phase to a vapour (cavitate). Likewise, if the liquid is shaken at high frequencies, it can clean some sensitive substrate materials and components effectively, but will damage those that are vibration- or heat-sensitive through cavitation.[26] This apparent competition between effectiveness and suitability is further revealed through the material properties of sensitive equipment.

2.1.5 – Material Properties of Sensitive Equipment

The purpose of this section is to describe the material properties commonly encountered in sensitive equipment, which distinguish them from other kinds of materials for which effective decontamination methods have already been developed. Classes of sensitive equipment in military use have been defined in previous work to include many Commercial-off-the-Shelf (COTS) electronic devices, optics, membranes, and composite materials, typically those with

mixtures of synthetic polymers and micro- or nanomaterials.[27] Sensitivity in all of these materials arises from two factors: first, small characteristic dimensions, and second, lack of hardening to different chemical environments. The designed-for chemical environment for most COTS equipment is atmospheric air with some water vapour and minimal contamination.[28] Most COTS equipment has not been designed to tolerate immersion in liquid water, or in conductive or corrosive aqueous solutions, such as those which have been used successfully to decontaminate other (non-sensitive) surfaces. One should not expect COTS equipment to function in such conditions. The tendency of equipment to operate correctly or to fail in any given condition may be measured and compared through reliability metrics. These metrics will be defined in the discussion on equipment trials.

The first factor contributing to sensitivity is the prevalence of small characteristic dimensions. Surface areas of micro- and nanometric dimensions are many times less resistant to both physical and chemical degradation simply because of their size than are materials with larger characteristic dimensions. This is a result of geometry rather than chemical interactions, but it worsens any process that also leads to loss of substrate material. As a characteristic dimension is reduced, the surface-to-volume ratio of the material (i.e. the specific surface area) is increased. This, in turn, increases the importance of surface effects, including chemical reaction and mechanical wear.[18]

The second factor contributing to sensitivity is chemical compatibility. Chemical compatibility is the tendency of two or more materials to react, and if so, to what extent and result. Reactions can affect material properties, foremost through surface effects. Corrosion, chemical sorption, lubrication, adhesion, friction, and wear are all possible consequences of surface changes in molecular structure.[18] Such changes can lead to off-specification behaviour, and eventually failure, of the material and the equipment of which it is part.

It will be shown in following sections that sensitivity (i.e. the risk of reduced reliability) in COTS equipment in particular is a consequence of using small-scale solid-state electronic, mechanical, optical, and electro-optical components. These components may have surface treatments, including adhesives, non-volatile lubricants, and coatings, which are essential for their correct functioning. Any sufficiently aggressive decontamination procedure increases the risk of non-selectivity for contaminants, and may undesirably remove such treatments along with any contaminant. In turn, a crucial function could be damaged, either transiently or permanently.

In addition to coping with the balance between effectiveness and preserving the integrity of the material to which it is applied, there are other important requirements for any decontamination system. These include the environment in which it can operate, its intrinsic safety, and its efficiency.

2.1.6 – Requirements for Sensitive Equipment Decontamination

The purpose of this section is to describe both general requirements for decontamination and specific requirements for sensitive equipment. Some general requirements for an 'ideal' decontaminant have been proposed in the CBRN literature. One list includes the following characteristics: high efficacy (independent of environmental conditions), rapid speed of action, easy portability, low human and environmental toxicity, low cost, long shelf-life, and low capacity to spread contamination.[2]

Sensitive equipment decontamination requirements are bound to follow similar lines as the generic requirements for non-sensitive equipment. An ideal sensitive equipment decontaminant will preserve the performance and reliability of all sensitive equipment exposed to all TIMs in all circumstances, while selectively removing only contaminants. To the extent that this ideal is unachievable in reality, the decontaminant would at least be able to preserve some of the capabilities provided by the equipment while lowering the burden of safe disposal of irreversibly contaminated equipment. The best achievable decontamination process will likely be a trade-off between the least logistical burden on one hand, and the least damaging effect on the operation of sensitive equipment on the other. Existing military doctrine and requirements further quantify the acceptability of such trade-offs and these follow.

The CAF have already articulated specific performance requirements for decontamination of "tactical level equipment of land, sea, and air units, their personnel, supporting bases and non-sensitive personal equipment" in a Statement of Operational Requirement for Project 00002253—the CF CBRN Decontamination System (CF CBRN D S).[29] The CF CBRN D S is essentially a field-deployable plug-flow reactor with separate decontamination 'lines' for vehicles, personnel, and non-sensitive equipment. Within the overall plug flow of a contaminated unit that enters and becomes progressively decontaminated, there are provisions for Quality Control. Decontamination operators equipped with chemical detectors can reject insufficiently decontaminated personnel or vehicles and 'recycle' them for further treatment (e.g. an additional shower for personnel). In principle, a sensitive equipment decontamination system (SEDS) would constitute yet another

decontamination line to complement the others and would maintain an acceptable throughput of treatment. Some of the minimum operational requirements captured in the CF CBRN D S have been selected to guide the current work and are summarised in the following paragraphs.

First, a SEDS should achieve the required extent of decontamination. The CF CBRN D S requires *Thorough*-level decontamination of vehicle-, camp-, or personnel-borne equipment in parallel with the *vehicle exterior* and *Individual Protective Equipment (IPE) doffing* stages of decontamination.[29] On account of the wide variety of contaminants and health risks, there is no single metric for Thorough-level decontamination, and the extent of decontamination in field conditions would require validation in a full-scale test plan. For the current project, the minimum target extent of removal was 90 % (one order of magnitude), with a desired removal of 99 % or greater, at initial and final loadings close to the limit of detection of any contaminant. This requirement flows logically from the need to minimise the source term in the contaminant risk assessment. An extent of 99 % removal, given 100 starting units, results in the same residue—1 unit—as 99.99 % removal from 10 000 starting units, and this residue exerts the risk. Since the doctrinal time budget for cleaning vehicle exteriors and doffing IPE is 30 min, it follows that a SEDS operating in parallel should be capable of destroying, transforming, or neutralising contaminants from equipment within 30 min of treatment time.

Second, a SEDS should be field-deployable. The design parameters for the environmental suitability of deployable equipment are given in North Atlantic Treaty Organisation (NATO) doctrine.[30] Consistent with this doctrine and the requirements of the CF CBRN D S, a SEDS should operate between −21 °C (the minimum temperature of NATO climate condition C0) and +49 °C (the maximum temperature of NATO climate condition A1). It should tolerate storage between −33 °C (the minimum temperature of NATO climate C1) and +49 °C, and be capable of full performance at 2000 m altitude in any of the foregoing climates.

For instance, given these constraints, a system that can operate across all design climates and can neutralise a contaminant by removing 95 % of its initial load from an affected material within 25 min would meet the basic requirements. Some or all of these requirements, even as they apply to sensitive equipment in particular, may be met by commercially available technology. Examples of such technology are surveyed in the following section.

2.1.7 – Possibilities for Sensitive Equipment Decontamination

The purpose of this section is to survey the operating principles, benefits, and shortcomings of various decontamination methods—physical, chemical, enzymatic, and directed-energy—that may be applied to sensitive equipment in particular. Commercial examples are also presented, and comments are offered on their fitness for the requirements deduced previously.

2.1.7.1 – Physical Methods

First, a purely physical decontamination method implies the absence of chemical reaction. Such methods achieve decontamination typically by removal from the substrate into another phase, or sorption to another surface. A physical method does not preclude adding one or more 'inert' or minimally reactive chemical species to a system to achieve these results. One consequence of the lack of chemical reaction is the need to manage, or treat separately, any removed contaminant. This is not a trivial issue, since the contaminant may still exert toxic effects on human and environmental health until it is transformed into benign products. Hence, if it is not possible to transform contaminants, it is preferable to concentrate them and safely dispose of a small volume. Conversely, a lack of reaction offers several benefits: it avoids 'activation', which occurs when the toxicity of a biocide is increased through a reaction before it is degraded into benign products.[31] Since a reduction/oxidation (redox) potential difference is the driving force for electrochemical corrosion, minimising this potential difference also limits the extent of corrosion.[32] Minimal reactivity also minimises the formation of reactive free radical species that may lead to substrate deterioration. However, deterioration of sensitive substrates may still occur by means other than chemical reaction, such as by temperature, pressure, or mechanical erosion, which may be inherent in the physical decontamination technology.

2.1.7.1.1 – Vacuum Aspiration

Vacuum aspiration is an operationally mature technology for selective removal of particulate matter from a surface. Indeed, as part of an industrial hygiene programme, vacuum removal of particulate matter that harbours biological contaminants from surfaces is both effective and cost-efficient.[33] Particulate matter near an area of lowering pressure will follow streamlines in the direction of lowering pressure as described by Bernoulli's principle.[34] Removal of surface-deposited liquid contaminants is also possible, but limited by the contaminant's volatility at a given barometric pressure relative to its affinity for the surface. The vacuum must also be maintained long enough to

ensure the required extent of contaminant removal. Kärcher Futuretech (Schwaikheim, Germany) has marketed a chemical/biological decontamination system for sensitive equipment based upon this principle.[35] The apparatus generates, within a cavity, a pressure drop from ambient pressure to 1 Pa, and raises the internal temperature to between 70-75 °C to remove contaminants. It is reported to achieve 6-9 $\log_{10}$ removal of biological warfare agents from contaminated surfaces within 30 min of treatment time, which is consistent with allied doctrinal requirements.[35] It is possible that chemical treatments on some sensitive substrates may also be degraded, melted, or volatilised by these temperature–pressure conditions, as they fall outside the parameters of typical storage and use. Since the Futuretech system is currently in-service in the German, French, and Turkish armed forces, it may be feasible for the CAF as a Military-off-the-Shelf (MOTS) procurement option. However, quantitative studies on the risks it imposes on the reliability of sensitive equipment, such as electronics, have not been found.

A related system for decontamination of small sensitive equipment and enclosed spaces involves a two-stage process: a proprietary spray treatment followed by vacuum aspiration. This system, SX34, is marketed by Cristanini CBRN Decontamination Systems (Rivoli Veronese, Italy).[36] It has been tested and shown to remove 90 % or greater of a 200-1000 $\mu g \cdot cm^{-2}$ initial load of OP contaminants from butyl rubber and polymer-laminated textiles within a single treatment cycle, typically of 30 min.[36] The extents of removal of other chemical contaminants and biological and radioactive particulate matter were not as high during those tests. A logistical disadvantage of this approach is that the spray treatment is consumed in the process. Operational stocks of this commodity would require maintenance and rapid replacement to ensure the ongoing availability of treatment. In contrast, a system based upon a recyclable working fluid (or one not requiring a working fluid at all) would impose a lower logistical burden.

2.1.7.1.2 – Positive Pressure

A variation of drawing a vacuum is to apply positive pressure to the system through the use of air, noble gases, or minimally reactive vapours at high speed. Removal of contaminant is achieved by the bulk movement of such fluids and the tendency of the contaminant to dissolve into them. Such techniques are well-developed for fixed industrial applications, e.g. movement and separation of airborne contaminants from process air streams.[6] Hot-Air Decontamination systems (STERIS Corporation, Ohio) are currently marketed for large-scale military applications, including aircraft, on deployed operations.[37] In such a system, the equipment to be treated is enclosed in a

volume, and compressed, heated, and purified air is blown across it. In principle, the contaminant is removed into the bulk of the fluid, which is later filtered to entrap the contaminant. A major advantage of this approach is that the reliability of the equipment should not be affected to the same extent as it would be in a novel chemical environment or in a vacuum. Imposing higher-than-normal temperature and humidity conditions for the duration needed for decontamination may be acceptable if the effects on reliability are well-characterised. Civilian airframe manufacturers have also recently been granted patents on such technology, principally aimed at microbiological decontamination.[38] Various high-temperature (> 75 °C)–high-humidity (> 70 %) combinations have shown effectiveness in achieving required extents of inactivation of pathogens from typical aircraft material surfaces.[39] One available study on the removal of chemical contaminants and simulants from military aircraft showed 99 % removal of 100 $\mu g \cdot cm^{-2}$ initial loads of mustard, thickened mustard, and VX over the course of 3, 4, and 20 hours, respectively.[40] Such times are much longer than the doctrinal time budget associated with Thorough decontamination in the CF CBRN D S. Nonetheless, on the bases of effectiveness and suitability, Hot-Air Decontamination may be among the few currently feasible options for both small equipment and larger equipment, typified by aircraft.

2.1.7.1.3 – Supercritical Fluids

At a sufficiently high temperature–pressure condition, above the critical points of these two parameters, a fluid exists in the so-called supercritical phase, where it exhibits some properties characteristic of its liquid phase and some of its gas phase simultaneously.[41] Supercritical CO_2 (temperature ≥ 31 °C, pressure ≥ 72.9 atm) has been successfully commercialised as a solvent in several applications, notably in garment dry-cleaning as a 1,1,2,2-tetrachloroethene replacement, in beverage decaffeination as a benzene and dichloromethane (DCM) replacement,[42] and as a biological steriliser.[43] Supercritical CO_2 has been patented for decontamination of electronics[44] and polymer substrate materials[45] in industrial applications. For these reasons, it, too, has been proposed as a sensitive equipment decontaminant. However, achieving such large pressure values in field-expedient decontamination, as opposed to a well-developed manufacturing setting, could prove a logistical burden to a deployed task force with access to austere infrastructure (if any). At such pressures, which deviate significantly from the normal operating conditions of equipment, there is also a higher risk that the fluid may start to erode the substrate material in addition to removing the contaminant, by the high-speed impact of particulate matter. On the other hand, if supercritical pressures are not attained, liquid CO_2 on its own has shown limited ability for

highly effective decontamination at the required throughput. A bench-scale 0.5-L liquid CO_2 reactor was able to remove 90 % of oil contamination from 5.6-g polymer coupons after 3 hours of treatment, but its rates of removal were inferior to washing with a non-pressurised solvent.[46]

2.1.7.1.4 – Gases and Aerosols

At cryogenic temperatures and high-vacuum pressures, surface cleaning of sensitive electronics substrates may be achieved with aerosolised and highly pure N_2 and Ar gases.[47] CO_2 snow has also been employed for simultaneous removal of particulate matter and of organic drops or films, because of the solvent effect of liquid CO_2 produced at the surface when solid CO_2 melts. To date, these techniques have been successfully applied at relatively small scales in cleanrooms for surface decontamination, including removal of hydrocarbons, of individual sensitive components (e.g. silicon wafers, hard-disk drives, and optics).[47] However, such techniques, while selective, are admittedly limited in throughput, and cannot currently compete on that basis with any regenerated liquid solvent-cleaning scheme. Another disadvantage of this approach is that maintaining temperatures and pressures that deviate significantly from the ambient could require power consumption beyond the capabilities of a field-deployed force to generate. Other logistical requirements, including cleanrooms and gloveboxes, are not prohibitive in industry or research, but are not as easily deployed on military operations.

2.1.7.1.5 – Ultrapure Water

Ultrapure water is, in principle, a minimally destructive solvent if applied temporarily, even to energised electronics. This is explained because of the high resistivity (low conductivity) of water with low ionic activity and low contaminant concentrations, and such water is standardised for cleaning electronics materials.[48] Indeed, the purity requirements for water become increasingly stringent as the characteristic dimension of the electronics material decreases, in order to ensure compatibility. However, long-term exposure to moisture of hygroscopic polymers, adhesives, and composites, as found in full-scale sensitive equipment, is to be avoided.[49] Such exposure introduces risks of swelling in different directions and of structural degradation from the chemical reaction of hydrolysis. The purity of water is difficult to maintain in field conditions because it tends to dissolve a wide range of ambient substances, including gases such as CO_2, which yields ionic activity as $[CO_3]^{2-}$, $[H_3O]^+$, and $[HCO_3]^-$ in aqueous solution. In addition, water's high surface tension (72 $mN \cdot m^{-1}$) within the operational temperature domain is significantly more polar (51 $mN \cdot m^{-1}$) than dispersive (21 $mN \cdot m^{-1}$) in

character.[50] This limits water's ability to penetrate so-called 'hydrophobic' surfaces, and contaminants such as VOCs.

2.1.7.1.6 – Liquid Organic Solvents

Liquid organic solvents with oxygen-bonded groups, including water-free short-chain (C_1 to C_4) alcohols and C_3-C_4 ketones, possess low surface tensions, typically of 20 $mN \cdot m^{-1}$, in contrast to that of water.[51] Hence, they can more efficiently displace both polar and non-polar chemicals from polymer surfaces without having to add soaps or detergents (surfactants) or scrubbing inaccessible places, with the accompanying risks of mechanical wear. They remain liquid throughout the operationally relevant temperature domain of 21 to 49 °C. For instance, 2-propanol, either pure or in aqueous solution, is compatible with common electronics materials such as polycarbonate and polystyrene for limited-duration solvent-cleaning and is used to clean full-scale medical devices and aerospace parts in civilian applications.[52] However, all such solvents are volatile (VOCs) and will readily produce inflammable vapour concentrations at operational temperatures. Inflammability is one of the considerations governing the choice of solvent in large-scale cleaning operations.[47] The risk of a fire when immersing large quantities of electronic equipment in an austere environment is a particular concern, and may limit the deployment of inflammable solvents on such a scale. This is another example of divergent requirements between civilian and deployed military users.

2.1.7.1.7 – Liquid Halogenated Compounds and Replacements

Other organic compounds of interest to sensitive equipment decontamination contain halogen substituents. These compounds also possess low surface tension and exist in the liquid phase in most ambient conditions, including the operational and storage temperatures required for a decontamination system. An increasing degree of halogenation, particularly with some fluorination, and no double-bonded carbons, renders them characteristically unreactive and non-flammable in many conditions.[53] Such properties avoid the problems described for common organic solvents. Indeed, halogenated compounds have historically been used in sensitive equipment and electronics cleaning applications, but their use has been significantly restricted, and banned in many jurisdictions, because of environmental concerns.[54] Chlorine and bromine atoms within an organic molecule bestow useful solvent properties, but degrade stratospheric ozone when they are photolysed to free radicals in the upper atmosphere.[55] For instance, CFC-113 (1,1,2-trichloro-1,2,2-trifluoroethane), a chlorofluorocarbon with a boiling point of 47 °C, was used

successfully in industrial-scale electronics immersion degreasing until the 1980s, when it was banned by regulations that implemented the aims of the Montréal Protocol.[56]

During the search for a CFC-113 replacement suitable for cleaning of weapons-grade electronics during manufacture, United States government laboratories compiled a familiar list of requirements: minimal environmental health and safety impact, cleaning efficacy, low corrosivity, non-depletion of adhesives, and resistance to high-voltage breakdown.[57] By 1990, deionised water, 2-propanol, and terpenes were considered among the most likely candidates to fulfil this role.[57] By 1993, an aqueous solution of citrus-derived terpenes and non-ionic surfactants for wood-rosin flux removal from electronic printed circuit boards (PrCBs) was commercially viable.[58] Non-ozone depleting organic fluorinated gases, both polar and non-polar (e.g. CHF_3, CF_4, C_2F_6) continue to be used for selective cleaning of sensitive silicon-containing substrate materials, such as the glass screens of visual displays.[59] However, a technique which has proven suitable for high-technology manufacturing may not be amenable to a field-expedient application because of the austere infrastructure in the field. Likewise, techniques aimed at production of individual parts are not necessarily suited for maintenance of full-scale assemblies.

One suitable family of less-halogenated CFC replacement compounds is the hydrofluorocarbons (HFCs), which are thermally stable in typical ambient conditions.[60] Proprietary blends of liquid HFCs, such as 2,3-dihydrodecafluoropentane, with co-solvents, including 2-propanol, are currently marketed specifically for cleaning electronic and medical equipment by E.I. du Pont de Nemours and Company.[61] Such COTS technologies, designed for similar goals as envisioned in this project, may provide the most feasible design solution for sensitive equipment decontamination.

In other recently developed families of 'engineered' fluids, including the hydrofluoroethers (HFE) and the fluorinated ketones (FK), a compromise has been struck among inflammability/reactivity, environmental persistence, and human health concerns. HFEs and FKs have been conceived for a variety of end uses, including solvent-cleaning of sensitive materials.[62] Moreover, HFE-7100 and HFE-7200 (marketed as Novec 7100, Novec 7200, and other proprietary blends by 3M Company) have both shown potential in small-scale sensitive materials decontamination studies.[63] For instance, the combined mass-transfer and adsorption behaviour of HFEs and textiles impregnated with activated carbon has been developed into a surface wipe for application to sensitive substrate material surfaces by the Edgewood Chemical Biological

Centre (ECBC) with industry partners.[64] As seen from the academic and patent literature, HFEs remain an area of productive research in sensitive equipment decontamination, likely because they satisfy the overarching substrate compatibility requirement.

Andrle et al. explored the use of HFE-7200 in a bench-scale bulk decontamination system using poly(butadiene) coupons as a substrate material and distilled mustard agent (HD) as a challenge contaminant.[63] The group sought to maximise decontamination by introducing ultrasonic vibration at 40 kHz for a highly turbulent flow régime, and by stripping and recycling the contaminant-enriched HFE-7200 through reactive filter media. To do so, the group incorporated separate stages for stripping the HD-enriched solvent fraction and then for oxidising the HD, so as to minimise the risk of discharging it. From initial HD loads of 254 $\mu g \cdot cm^{-2}$ on the coupons, after 45 min of treatment, the group achieved 88.95 % decontamination without ultrasonication and 90.12 % with ultrasonication. For reasons previously mentioned, solvent-bathing some sensitive parts at frequencies that are intended to produce cavitation may be detrimental to their reliability.[26] The marginal increase in decontamination effectiveness from ultrasonication would likely not warrant its use on pressure- and vibration-sensitive parts. Nonetheless, these families of replacement halogenated solvents apparently satisfy many of the general requirements of a sensitive equipment decontaminant.

A commercially available FK (FK-5-1-12, marketed as Novec 1230 and Novec 649 by 3M Company), originally developed for fire-suppression and immersion heat-transfer in sensitive applications such as archives and electronic data centres, has been the subject of previous decontamination trials (see 2.4 – Previous Research).[27] The results of those trials appeared promising and have, in part, motivated the current project.

2.1.7.1.8 – Nanoparticles

A final group of physical decontamination methods is physical sorption by solid organic or inorganic nanoparticles. In order for the sorption method to be effective, the nanoparticles must be able to achieve solid–solid or solid–fluid contact with the contaminant, and be removed from the affected surface after treatment. The fitness for large-scale application of nanoparticles that may show efficacy of contaminant sorption or transformation must be weighed against such constraints. The heterogeneous catalytic degradation pathways of organophosphorus and sulfur vesicant compounds by MnO_x, TiO_2, and MgO nanoparticles are described in literature.[65] Since the mid-2000s,

these nanoparticles have marketed for sensitive decontamination as FAST-ACT (NanoMaterials, Inc., Manhattan, Kansas) in an example of technology transfer from research studies to a commercial application.[15] TiO_2 nanoparticles have been studied more recently for both decontamination efficacy and suitability on a printed circuit board assembly.[66] From an initial load of 45.8 $\mu g \cdot cm^{-2}$ of HD, 99.3 % surface removal was achieved after 1 hour of contact time with the particles. Furthermore, the circuit board functioned as intended after decontamination. Operational disadvantages of the method used in this study were the requirements to ensure homogeneous coating of the substrate and for mechanical removal of the nanoparticles, which was done manually. The study authors conceded as much, but proposed the use of nanoparticles in series with a vacuum-based removal method.

Sol–gel synthesised Al_2O_3 nanoparticles, both with and without reactive impregnants, have been studied for sequential physical sorption and in-place neutralisation of mustard agent.[67] However, these particles have not been subjected to complementary trials on equipment reliability and the rate of mustard destruction was not quantified in the same study. ZnO nanoparticles have been studied *in vitro* for OP decontamination efficiency and shown pseudo-first order decomposition of Sarin (GB) with varying half-lives of 0.16 hours and 1.92 hours at 30 °C.[68] This study also did not consider mass transfer of particles onto a contaminated surface, subsequent removal of the particles, or quantification of material compatibility or reliability.

Organic particles, including sugar alcohol and methyacrylate polymers, have been studied for their ability to physically sorb a range of contaminants with different properties (both non-polar HD and polar VX) and transform some contaminants within minutes.[69] Transformation may occur either by virtue of the composition of the particles themselves, or by a general-purpose decontaminant that uses multiple liquids and solids to achieve mass transfer and a range of chemical reactions. Indeed, nanoparticles may be most useful for separation operations, in which they are not required to be in contact with (and be removed from) sensitive substrates. Their function would be to sorb or transform contaminant that is present in a fluid phase. Such a design approach would use two distinct treatment stages: the first optimised for contaminant removal and substrate compatibility, and the second optimised for purification of the working fluid for the first stage using the sorptive–reactive capabilities of nanoparticles. Through such a compromise, the demonstrated efficacy of some organic or inorganic nanoparticles in rapidly transforming contaminants may be combined with a solvent or surfactant that has been selected for optimal substrate compatibility and surface removal of contaminants.

In the foregoing survey of physical decontamination methods, the prevailing operation was removal of contaminant, which may be followed by sorption or filtration. In these cases, the effect of a contaminant may be neutralised, but the chemical composition of the contaminant has not necessarily been transformed. In contrast, chemical decontamination methods all involve transformation of contaminants into relatively less toxic products. These methods are surveyed in the following section.

2.1.7.2 – Chemical Methods

Chemical methods of decontamination include applying reagents, catalysts, enzymes, or directed energy to make or break particular chemical bonds. A combination of removal and sorption—two physical methods—can achieve the goal of decontamination through mass transfer of the contaminant, but the contaminant itself has not been transformed because no chemical reaction has occurred. Transformation requires chemical reaction, and may be achieved by partial transformation of contaminants (towards less-toxic products)[70] or complete mineralisation of organic or biochemical contaminants, i.e. breaking down into simple, benign, inorganic products such as H_2O and CO_2.[31]

In non-sensitive applications, a chemical reaction that results in the prompt destruction of contaminant is usually favourable, because risk is rapidly reduced. The predominant chemical reactions for decontamination of chemical warfare agents have included some form of oxidation or nucleophilic substitution and these are well-developed.[70] In the context of sensitive equipment, however, any tendency to react must be weighed against the competing need to preserve the integrity of the substrate. Variations on the theme of chemical reactions include inorganic and enzymatic catalysis and directed-energy methods, in which reaction occurs but only the contaminant itself is transformed.

For field-expedient decontamination, a liquid decontaminant is particularly useful. The fundamental properties of liquids allow them to be pumped, sprayed, penetrated, coated, and removed from contaminated materials (unlike solids), and to be transported in bulk at atmospheric pressure (unlike gases). These requirements have been incorporated into traditional decontamination technologies. Aqueous solutions with high oxidation potential (free chlorine and peroxides) are suggested for field decontamination of non-sensitive equipment, e.g. vehicles and building surfaces, with high throughput and reliable destruction of contaminants.[14] Solutions that promote free chlorine are nonetheless acknowledged to be

entirely unsuitable for sensitive equipment, particularly COTS electronics, because of the inevitability of corrosion.[71]

More recently, chemical decontamination technologies have been developed for materials other than the painted metals and ceramics found on vehicles, in view of the different properties of the target substrates. For instance, lotions that promote a nucleophilic substitution reaction (using oximes) have been developed for use on the human epidermis.[72] Vapours and gases, typically with free chlorine or peroxide, have also been used for specific applications, notably the biological decontamination of buildings.[73] Some compounds, such as vaporous hydrogen peroxide (VHP), are expressly marketed on the basis of their suitability with sensitive substrates, but they are not necessarily effective against the wider range of non-biological contaminants.[74] While VHP has shown compatibility with some common structural materials (steel and aluminium), hydrogen peroxide in the condensed phase has been shown to damage a common electronic circuit board material.[75] Achieving a consistent level of effectiveness, whether by removal or transformation, against a broad range of challenge contaminants, while avoiding damage to sensitive substrates, is a design goal for sensitive equipment decontamination. This goal has not been met by the aforementioned examples of field-deployable chemical-based systems.

2.1.7.2.1 – Substrate Compatibility Problem

The problem of substrate compatibility on a chemical level is bound to emerge for any chemical decontamination method. Thick metal surfaces that have been treated with Chemical Agent Resistant Coating (CARC)[15] and the human epidermis that regenerates routinely will both tolerate washing and rinsing with some ionic surfactants and oxidants.[2] In contrast, sensitive equipment has not necessarily been designed to function during and after exposure to such conditions. Indeed, vehicle surfaces and human tissues have different decontamination requirements from each other on the basis of substrate material properties alone, which leads to separate treatment 'lines' for them in decontamination doctrine.[16] On this basis, it seems reasonable to create another treatment line expressly for sensitive equipment, which is also supported in doctrine.[10] This line may use a chemical decontaminant that achieves transformation, but the substrate compatibility problem may limit the application of a chemical method on the wide variety of COTS and other in-service sensitive equipment, and tilt the balance in favour of a physical method.

2.1.7.2.2 – Reduction/Oxidation

Redox activity is well-established as a means to transform contaminants into benign products. Changing the oxidation states of chemical species changes their properties, and oxidation usually results in products that are benign, such as H_2O and CO_2. Oxidising agents (bleaches) are cheap and effective for mass decontamination, but readily damage surfaces in addition to transforming contaminants.[43] More recent substitutes for hypochlorite bleach are based on hydrogen peroxide; these may use benign reagents, such as polyglycols, sodium bicarbonate, and ethanol, to effect transforming chemical reactions.[71] However, use of any such decontaminant introduces the significant risk of substrate material loss through corrosion because it is electrochemical in nature. For sensitive equipment in which metallic soldering provides both electrical continuity and structural connections, such corrosion may lead to increased failures.[76] For similar reasons, aqueous ionic surfactants or any liquid with sufficient ionic activity (and therefore electrical conductivity) may be detrimental for energised electronics.

2.1.7.2.3 – Nucleophilic Substitution

Nucleophilic substitution, e.g. through hydrolysis and oxime reactions, offers rapid transformation of contaminants. Rapid transformation alleviates the problems of removal and disposal inherent in a physical decontamination method which, by definition, does not induce any chemical reaction. In nucleophilic substitution, the nucleophile (which may be readily available water, an alcohol, or alkoxide) attacks the contaminant and substitutes for the leaving group, resulting in a molecule of lower toxicity to personnel.[70] Since this reaction may evolve charged species, and such species are good conductors of electricity, there remains the risk of corrosion. Water-free alcohol-based wipes with metal (Zn(II) and La(III)) catalysts have been developed for the removal from sensitive surfaces and simultaneous transformation of a variety of contaminants, notably organophosphorus (OP) species.[77] These wipes are intended to yield pH levels close to the self-ionisation equilibria of the short-chain alcohols in an effort to minimise damaging conductivity effects while they catalyse reactions. The reaction catalysed by the wipes was tested for efficacy of decontamination in a decoupled process.[78] First, the contaminant was desorbed from genuine electronics substrate materials, and then the extent of the catalysed reaction was followed in time by analytical methods. From a maximum contaminant loading density of 5800 $\mu g \cdot cm^{-2}$, recoveries of contaminant from surfaces with methanol all exceeded 90 % within 10 min. Subsequent destruction of one contaminant (paraoxon) by the catalysed reaction was approximately 80 %

after 30 min and greater than 90 % after 1 hour; the other contaminant (diazinon) was not detectable after 0.5 min of treatment. It is not known whether the wipes themselves have been evaluated for their suitability on full-scale sensitive equipment in a field trial. Nonetheless, the throughput of a method that relies on a manual cleaning stage (cf. CO_2 snow, nanoparticles) is not likely to exceed that of bulk cleaning, as is the case for immersion in a solvent, surfactant, or other fluid.

2.1.7.3 – Enzymatic Methods

The active site of an enzyme provides a location for structurally similar molecules to bind temporarily and then to undergo a particular chemical reaction. In principle, enzymatic treatment may be less 'aggressive' to sensitive substrate materials than high-pH, redox, or free-radical based chemistries. For instance, naturally occurring phosphotriesterases (EC #: 3.1.8.1) have been isolated to degrade phosphoric acid esters, including OP pesticides, GB, GD, VX, Vx, and similar compounds, and all with predictable by-products.[79] Such enzymes have been commercialised as DEFENZ Decon Enzymes (Genencor/Danisco USA).[80] It is possible to prepare suspensions or foams of these enzymes as needed for decontamination. Since enzymatic methods necessarily involve chemical reaction, however, there is still the possibility of damage to the substrate material, depending on the contaminant and the reactions catalysed by the enzyme. Enzymatic cleavage of phosphoric acid esters such as paraoxon yields corrosive and conductive phosphoric acid as one product.[70] Given the characteristic specificity of enzymes, the utility of any one against a range of challenge contaminants is questionable. DEFENZ Decon Enzymes were tested for decontamination efficacy in a range of environmental conditions.[81] Steel coupons were loaded with 100 $\mu g \cdot cm^{-2}$ of an HD simulant or an OP pesticide (paraoxon) and treated according to the manufacturer's directions with appropriate field decontamination times (15-30 min). After 15 min, the enzyme formulation achieved 74 (± 31) % removal of paraoxon and 30 (± 6) % removal of HD simulant—not even one order of magnitude from the non-porous surface material. The coupons themselves were not tested for material compatibility, such as corrosion or weight loss, in this study. Since enzymes are catalysts, they offer the benefit of neutralising the process effluent of a decontamination process without being chemically transformed themselves, and so are recyclable to an extent. As with nanoparticles, enzymes might be most effectively used as part of a decoupled decontamination scheme in which they are not required to be in contact with sensitive materials, but their specificity in transforming highly toxic contaminants may be exploited.

2.1.7.4 – Directed-Energy Methods

Another possible area of technologies is directed energy, which is based upon the tendency of photons of particular energy to make and break chemical bonds by promoting electrons. Photons are emitted onto a contaminant and transfer their energy to the electrons in certain types of bonds. Directed energy is a chemical method of decontamination, and has been used successfully for biological disinfection of water supplies and of sensitive surfaces for health care.[82] Emissions of mercury-based ultraviolet lamps occur at wavelengths of approximately 260 nm. When this wavelength strikes adjacent pyrimidine groups in genetic material, such as thymine–thymine pairs, the UV photons induce cyclobutane dimers or 6–4 carbon photoproducts.[83] When the number of such genetic defects is greater than a pathogen's ability to 'proofread' and excise them, the enduring risk of contamination is reduced. Mercury-vapour lamps can effectively cause 4-$\log_{10}$ or greater inactivation of the pathogen *Giardia lamblia*.[82] However, directed energy is limited in application to chemical compounds that absorb and are transformed at certain wavelengths. For a directed-energy system to achieve chemical transformation, it must produce such wavelengths. Even so, the method does not involve mass transfer, and so would not remove radioactive contaminants or particulate matter. Although the technology has matured for UV disinfection of pathogens on surfaces and in water,[83] it faces some intrinsic limitations. For instance, it is constrained by radiation phenomena, such as the line of sight of the beam, and is not able to surround complex geometries of contaminated surfaces as can fluids (gases, vapours, or liquids). In contrast to civilian hospitals that have, in principle, been designed for ease of decontamination, sensitive equipment has not been so designed. It is not known whether UV disinfection has been tested for field-expedient sensitive equipment decontamination, but at present, it is unlikely to be broadly useful for contaminants other than pathogens.

In spite of a number of means to achieve rapid transformation of contaminants through chemical reaction, there appear to be more physical methods available that would be suitable for the particular problem of sensitive equipment decontamination. In such systems, one physical process, e.g. removal from the sensitive substrate, may be followed by another, e.g. physical sorption, to achieve the required extent of decontamination and to preserve substrate integrity. A physical removal step followed by chemical transformation also seems to be a feasible design philosophy. Appropriate analytical testing techniques are needed to quantify the extent of any decontamination process so as to determine the residual risk to personnel. Such techniques are discussed in the following section.

2.2 – Decontamination Testing Methods

The purpose of this section is to survey the chemical analytical methods through which the extent of decontamination, and hence its effectiveness, may be quantified. Since contaminants may exert toxic health effects at very small exposures (e.g. at fractions of 10^{-6} to 10^{-9} or less of a sample), and over several orders of magnitude, the precision, bias, sensitivity, selectivity, and limits of detection, quantitation, and linearity of response of analytical techniques are all important considerations.[84] Moreover, analytical techniques can provide qualitative and quantitative data on the structure and fate of contaminants, as well as on decontaminants, if they are also chemical species.

Well-established instrumental methods such as mass spectrometry (MS), Fourier-transform infrared (FTIR) spectroscopy, and nuclear magnetic resonance (NMR) spectroscopy offer detection capabilities for the analytes typically encountered in suspected CBR or TIM events and are recommended for this purpose.[85] MS involves fragmenting analyte molecules and reporting the relative numbers of fragments by mass. With knowledge of the most massive (molecular) ion, the masses of fragments typically encountered in organic molecules, and masses of elemental isotopes, structural information may be deduced. Samples with masses of nanograms may be quantitated with MS, which is useful for trace analysis.[86] FTIR may be used for quantitative analysis, but is typically reserved for qualitative identification of the bonds of a molecule.[87] Since the energy levels of mid-infrared photons correspond to the vibrational modes of many bonds of interest, IR absorption by molecules may indicate the presence of such a bond (and non-absorption, its absence). Harmonics of these vibrations are similarly detectable in the near-infrared region. NMR may be used for both qualitative and quantitative analyses. It probes the relaxation of nuclear spin angular momenta after certain nuclei (typically ^{1}H, ^{13}C, ^{19}F, or ^{31}P) are pulsed with radio frequencies. Relaxation decays are heavily influenced by neighbouring nuclei and by the extent of magnetic shielding provided by electrons. Thus, transformation of these decays to the frequency domain provides a plot of the number and types of neighbouring nuclei arranged by frequency (chemical shift).[88] From this plot, the structures of many organic compounds may be deduced, and their abundances tracked over time. Radiochemical methods, including neutron-activation analysis (NAA), may be suitable for detection of radiological or nuclear materials by virtue of radioactivity, and also for certain contaminants having thermal-neutron capturing atoms.[89] This latter property is well-suited to determinations of contamination.

The NAA apparatus is particularly useful for trace elemental analysis. NAA can detect elements with isotopes that emit prompt and delayed gamma radiation by impinging upon their nuclei with a variable thermal neutron flux of up to 10^{13} neutrons·cm^{-2}·s^{-1}.[90] By irradiating several millilitres of sample volume over the course of minutes or hours, it offers low limits of detection (μg to pg) for elements that readily absorb thermal neutrons. Instrumental NAA (INAA), that is, irradiation and analysis in series, with no radiochemical treatment in between, allows rapid determination of some seventy elements, irrespective of their chemical arrangement, at a relatively minor penalty of a 10^3 reduction in sensitivity compared to the basic limits of NAA. NAA cannot quantify low-mass atoms such as C, H, O, N, P, and S, which collectively comprise the majority of organic compounds.[89] If a substance absorbs neutrons abundantly and is highly volatile at given test conditions, enough heat may be evolved during irradiation to cause a phase change or activate a reaction. NAA also has infrastructure requirements, such as a source of neutron emissions and the attendant safety measures, which make it less ubiquitous than the smaller-scale MS, FTIR, and NMR. However, the intrinsic benefit of NAA is that the presence of one detectable or 'tracer' atom as a substituent in an organic structure also renders the larger structure detectable. Thus, the rapidity and sensitivity of NAA may be used in decontamination studies with a judicious choice of challenge contaminant.[91]

The complementary detection characteristics of MS, FTIR, NMR, and NAA may be combined in the following manner: in initial quantifications of decontamination, the relative insensitivity of INAA to interference will produce conservative results, with 'contamination' indicated by the mere presence of tracer atoms, regardless of chemical structure. In subsequent determinations to estimate actual risks of exposure, the sensitivity of MS and NMR to chemical structure can improve confidence in decontamination protocols and maintain a high throughput of samples. Finally, FTIR, NMR, and MS collectively provide multiple lines of evidence for the structures of chemicals to determine if reactions have taken place, and to what extent.

Chemical analytical techniques, while useful in determining the extent of decontamination and detecting the products of chemical reactions, cannot directly be used to evaluate effects on the reliability of full-scale equipment. Doing so requires other apparatuses and operational trials, which are presented in the following section.

2.3 – Operational Trial Parameters

The purpose of this section is to provide an overview on operational trials of equipment. The goal of operational trials is to determine equipment compatibility with a given process. In this project, evaluating equipment compatibility required considering how it might fail in a decontamination process. A general definition of failure is given first, followed by specific possibilities of failure that were gleaned from literature on the equipment.

2.3.1 – Reliability, Failure, and Degradation

Reliability is the conditional probability that an item will "perform a required function, without failure, under stated conditions, for a stated period of time."[76] It includes performance and environmental conditions as well as operator behaviour, and it may be influenced by the degree of built-in redundancy and the operational tolerances of the components themselves. Reliability metrics for equipment are, like risks of exposure to toxicity, difficult to predict and to analyse deterministically. Impurities in finished products, variable operating environments, and human operator behaviour throughout the equipment life-cycle all confound determinism. Hence, statistical methods are preferred, and any statement about the reliability of equipment must be interpreted with the caveats for probabilistic models. As a result, the physics of failure is useful to validate such models and ensure that they are reasonable.[92] If failure is described by statistics, it should also be defined by a physical parameter associated with the 'normal' operation of the equipment, e.g. strength, conductivity, or rate of information processing.

Failure is essentially a break in the enduring operation of equipment. Ideally, equipment can be demonstrated *not* to fail under conditions of interest, but since failures are bound to happen, they ought to be described quantitatively with some level of confidence. Failures in the performance of electronics and other sensitive equipment may be transient or permanent.[76] Sudden, permanent failures may also be considered catastrophic if capabilities are rapidly lost, with little or no warning, or possibility of replacement or repair. Otherwise, repair or replacement is a suitable corrective action. Depending upon the scale of observation, failures may be undetectable, or they may exhibit drifting or progressive degradation. An item may cease to operate transiently, but revert to normal operation at a later time, even without corrective action.[93] Transient failure could occur, for example, if equipment overheats and does not function as intended, but continues to function later on, after heat has been dissipated.

The two states of *successful operation* and *failure* may be described by binomial statistics, i.e. statistics about two mutually exclusive states. The reliability fraction R of a population of equipment at a given confidence level C may be calculated from binomial test data. A sample of N total items tested and k items failed gives R and C according to Equation 1.[76]

$$C = 1 - \sum_{i=1}^{k} \frac{N!}{i!\,(N-i)!} R^{(N-i)}(1-R)^{i}$$

Equation 1: Confidence as a Function of Reliability

For instance, if a sample of 10 items were tested and 2 items failed, one could report with no more than 42 % confidence that the reliability of the larger population would be 90 %. The equation may be solved for other values relevant to a reliability test plan. In order to demonstrate that a population of equipment will function 97 % of the time (be 97 % reliable), at a level of confidence of 50 %, a sample size of at least 23 representative items must be tested. If all 23 items perform without an arbitrary failure for the equivalent of one lifetime, as defined by the tester, then 97 % reliability at 50 % confidence has been demonstrated. Likewise, successfully testing 22 items without failure may demonstrate 90 % reliability at 90 % confidence. These numbers are a consequence of statistics rather than any physical phenomenon, but this means that they apply to any system. The corollary is that physical quantities such as the length of a lifetime and the conditions for success and failure must be defined by the tester. Another consequence of statistical distributions is that, without the benefit of large sample sizes, it is necessary to test items to failure under stress conditions that exceed likely lifetime levels in return for equal statistical power.[76]

For electronic equipment that has both hardware and software, as well as a human operator, success and failure may be considered at a given *layer of abstraction*. Layers of abstraction provide a framework for understanding the range of phenomena responsible for data communications, from the electrons within a material (physical phenomena) to the user interface of a device (the application layer). Users are normally concerned whether or not the equipment is functioning, without knowing the operating details of hardware and software, such as electrical potential, the integrity of data signals, or the layout of a network. However, when it comes to design or troubleshooting, it is helpful to determine what kinds of problems may occur and where. In the event of equipment failure, it would be fruitless to repair software if hardware

were actually at fault. For these reasons, a standard model of layers of abstraction has been developed and is summarised in Table 1.[94]

Table 1: ISO/IEC 7498-1 Layers of Abstraction

Layer Number	Description
7	Application Layer
6	Presentation Layer
5	Session Layer
4	Transport Layer
3	Network Layer
2	Data Link Layer
1	Physical Layer

In practice, it may prove difficult to measure operations at every such layer, particularly the middle layers, to sense precisely where performance or reliability has changed within a device. By measuring 'above the top' and 'below the bottom' layers, e.g. the performance of a software application and the electrical power consumption of the equipment, any changes can at least be bounded. Through the use of specialised built-in or installed test equipment (hardware or software), some operations in the middle layers can be measured by a user.

Reliability predictions based solely upon past behaviour at given conditions, and attempts to attribute all failures to definite causes, are problematic. Instead, equipment-level reliability for given operating conditions should be quantified through time-based metrics: the mean time to failure (MTTF) for non-repairable items, and mean time between failures (MTBF), mean time to repair or replace (MTTR), and overall availability for repairable items. The dimensionless *availability* (A) for repairable components, assemblies, and devices is given in terms of these metrics in Equation 2.[76]

$$A = \frac{MTBF}{MTBF + MTTR}$$

Equation 2: Overall Availability (A)

While a COTS laptop computer part that has failed (e.g. fan motor burn-out) may be repairable in principle, repairing it in practice could prove logistically challenging to deployed military task forces. For essentially irreparable items, the timeliness of replacement becomes more important to overall availability than the time requirement for repair. Aside from irreversible failures, degraded operation is also possible. To the extent that degradations are detectable, Quality of Service (QoS) metrics are intended to quantify them, and

these also typically involve time as a parameter. QoS may be measured by throughput bottlenecks, cost increases, or time delays to overall operations.[94] Since the QoS of equipment may be affected, transiently or permanently, by exposure to a decontamination process, recording QoS parameters provides a way to quantify the impact of the process, even if it does not cause any apparent failures.

This project considered decontamination process suitability, beginning with solid-state components, and mechanical, magnetic, optical, and structural components in turn. The successful operation and likely failures of these components, especially as they may be influenced by decontamination methods, and ways they may be tested, are presented in the following sections.

2.3.2 – Components of Sensitive Equipment

2.3.2.1 – Solid-State Electronics

Integrated circuits contain millions or billions of discrete, solid-state components. These components rely upon small differences in conductivity (a physical phenomenon) to manipulate information digitally. Digital information must then be presented in a form understandable by a user, typically as an application. Since failures of solid-state circuits are routinely captured in Quality Control before product shipment, early in the equipment life-cycle, mechanical failures of soldering points and electrical mismatches or shorts are their most likely remaining failure modes.[76] Any operating environment that tends to bias the electrical operating points of discrete components outside of specifications will lead to an increased rate of transient, if not permanent, failures.[95] Depending upon the capacitance and resistive–capacitive (RC) time constant of electronic circuits, they may also retain accumulated electrical charge after having been 'switched off'. It may not be practical to immerse solid-state electronics in conductive liquids long enough for such liquids to achieve decontamination, because a circuit's operation may be compromised. However, solid-state devices could be immersed in minimally conductive liquids, even when energised, with minimal risks of electrical discharge, fire, corrosion, and the like. It is therefore not surprising that many proposed sensitive equipment decontamination techniques, if they involve liquids, demand minimal conductivity. The conductivity of a candidate decontaminating liquid could be measured by a standard method[96] and correlated to the risk of promoting corrosion in electronics materials.[32]

Other assemblies commonly found in sensitive equipment include the electro-mechanical/-magnetic (cooling fans, hard-disk drives), optical (video displays, optical-disk lasers), and electro-optical (photomultiplier tubes). Such assemblies rely upon physical phenomena other than electrical conductivity to work as intended. The successful operation, and possible failure modes, of each type of assembly as they affect overall equipment availability are considered in turn.

2.3.2.2 – Mechanical Parts

Sensitive equipment contains more than electronic circuits. Even so-called electronic equipment often contains mechanical parts to move fluids (air) and solids (recording media). Failure of these parts can endanger reliability in ways described in this section.

2.3.2.2.1 – Cooling

In electronic equipment, cooling is critical to maintain reliable performance.[76] By packing more circuits into a smaller area to achieve better performance, more heat is produced in a given time.[97] Sudden heating may cause melting of metallic solder, which endangers electrical continuity, placing equipment at risk of failure. Non-metallic, combustible materials may melt or catch fire, which is dangerous to the equipment and to personnel near it. Heat sinks are commonly employed for combined conductive–convective heat-transfer, but their effectiveness is limited by their material composition, geometry, and the space they occupy.[98] For these reasons, laptops are usually equipped with a fan or fans for cooling, in addition to heat sinks on particularly heat-sensitive components. Electromechanical fans are lightweight and provide forced convective heat transfer from surfaces, such as the large surface areas of heat sinks, but they must be powered, controlled, and appropriately lubricated to work as intended. In general, moving a fluid (air) across a hot surface is more effective in a given time at removing the heat from the surface than by conduction alone because the motion in convection replaces a warmer fluid element with a cooler one. However, if a fan fails, this forced convection is lost, and heat may be transferred to heat-sensitive components. Heat not transferred promptly out of the system may cause parameters to drift out of specification, or thermal-stress related failures of components.[99] To prevent such failures from occurring, fans should be protected from both electrical shorts and delubrication. A decontamination process for sensitive equipment should therefore be selective enough to remove contaminants of concern without depleting essential lubricants for mechanical parts. Depletion of lubricants may be tested by analysing the residue of a decontamination

process for the chemical constituents of lubricants. Lubricants may be extracted from residue with a suitable solvent.

2.3.2.2.2 – Storage Drives

The mechanical reliability of recording media concerns hard-disk drives (HDD) using magnetic platters and optical (compact disc and digital versatile disc) drives (which will be described in greater detail in the next section), since both depend upon mechanical components. In both cases, the spindle drive rotates the recording medium (a disk), and the actuator arm translates the reader or recorder above the disk. For these machines to operate, the rotating recording medium must be retained by fluid or solid bearings. In turn, bearings require lubrication to function reliably. These common mechanical requirements may lead to common points of failure. For instance, HDD spindle motors typically spin at 5 000-8 000 rpm. Synthetic mono- and polyester oils, combined with surfactants and antioxidants, are the preferred lubricants for these applications.[100] However, if lubricant is depleted or thinned, it may increase shear forces and stresses, causing seizure-related failure.[101] Loss of spindle bearing lubricity could lead to bearing overheating, and possibly burnout of the assembly.[102] Depletion of such lubricants could be tested by analysing the residue of a decontamination process as described previously.

Apart from spindle lubrication, there are other potential areas of failure in an HDD, as seen at the interface of the HDD platter. A diagrammatic cross-section of the platter of a magnetic HDD, not to scale and with exaggerated asperities, is depicted in Figure 3.[103]

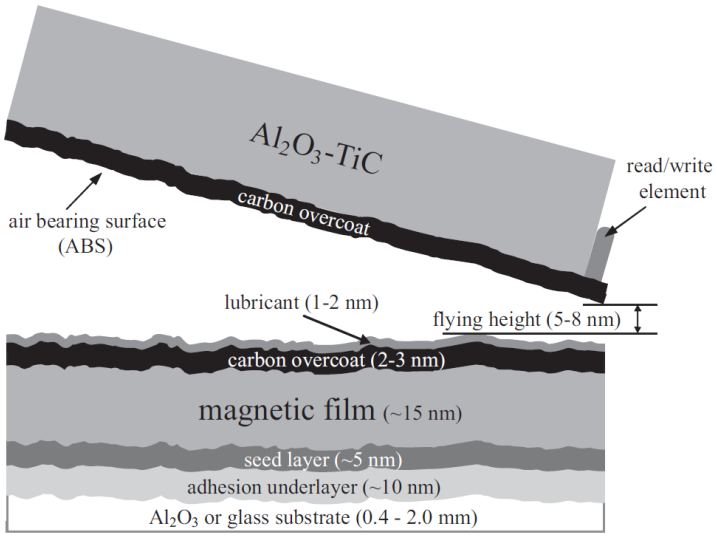

Figure 3: Typical Hard Drive Platter Interfacial Cross-Section (Reproduced from Brunner (2009))

From bottom to top, the Al_2O_3 or glass substrate provides rigidity for the remaining layers, all of which must rotate intact at thousands of rpm. The adhesion underlayer of nickel and phosphorus supports the chromium seed layer and the magnetic film in which digital data are recorded. The magnetism of the film is changed electromagnetically by the read/write element over a distance. This distance is maintained by diamond-like carbon coatings on both sides of the interface, a layer of lubricant on the platter side, and a flying height in the centre.[103]

The probabilities of both transient and permanent failures of HDDs because of losses of lubricity at the platter are assumed to be high for a number of reasons. At the read/write element, a drop in flying height could result in a surface ploughing action and a permanent deformation of the recording layer, leading to physically unreadable ('bad') sectors of the magnetic film.[102] Loss of platter lubricity could also increase the risk of deformation from contact by the element.[104] The ambient air at the interface is pressurised to provide yet another kind of bearing: the air-bearing surface. This air may also be 'depleted' if it is displaced by another fluid, such as a decontamination fluid. Replacement of pressurised air (a compressible fluid) by a liquid (a minimally compressible fluid) would result at least in off-specification performance from the balance of forces acting at the interface. In practice, it may prove difficult to measure ingress of a fluid other than air because HDD assemblies are

hermetically sealed and admit atmospheric air only through a filtered valve. An HDD could be fabricated with pressure transducers and fluid sensors to study this possibility. However, the possibility of depletion of lubricant from the platter could be measured more directly by analysing an HDD platter coupon by surface microscopy or spectroscopy before and after exposure to a decontaminant.

The head–platter interface is critical, and to ensure its reliable operation, it is usually lubricated with perfluoropolyethers (PFPEs). PFPEs are polymers of molecular mass between 500 and 1500 g·mol^{-1} that remain liquid between −100 °C and +400 °C, have low vapour pressures (< 133 Pa at 20 °C), and resist oxidation.[105] For these reasons, they have been useful for HDD lubrication to protect the alumina or glass substrate and the adhered magnetic recording-medium film over the lifetime of the equipment, without reapplication. One example structural formula, that of Zdol 1000, is shown in Figure 4, with m and n denoting variable lengths of common backbone monomers.[106]

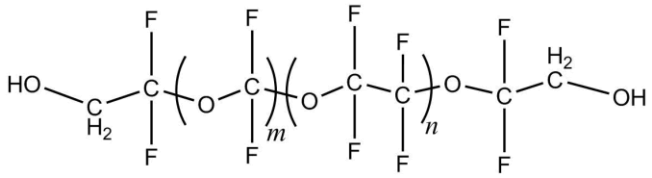

Figure 4: Example Perfluoropolyether (Zdol 1000) Structural Formula

PFPEs have been selected for their superior lubrication properties, but even the normal operating environment created at the HDD platter may challenge their reliability. Al^{3+} cations and Cl^- and F^- anions are naturally present as contaminants in the environment. They create the Lewis acids $AlCl_3$ and AlF_3, which catalyse the oxidation and cleavage of PFPEs.[105] PFPE backbones are sometimes substituted with trifluoromethyl groups to prevent polymers from being attacked by Lewis acids. However, repeated wearing of parts can reveal regions of clean aluminium which generate additional ions and degrade PFPEs in turn.[105] Partly degraded PFPEs have higher vapour pressures than the original molecule and evaporate more quickly, which in turn increases the likelihood of a damaging ploughing action.[103] PFPE degradation and depletion should not be accelerated by a decontamination process.

A specific concern for sensitive equipment decontamination arises at the head–platter interface. HFEs, which showed promise in decontaminating sulfur mustard agent from poly(butadiene) coupons,[63] have been employed to

deposit lubricants in HDD manufacture, just as they have been used experimentally to de-lubricate HDD platters. In one instance, platter de-lubrication was achieved by immersion in HFE-7100 for only 10 min.[104] HFE-7200[107] and FK-5-1-12[108] are also known solvents for a common PFPE, Zdol. Decontamination operations in the field consisting of immersing an HDD in HFEs or FK-5-1-12 could increase the risk of HDD lubricant depletion. This consideration may limit the use of either of these families of chemicals for field-expedient decontamination of HDDs on a large scale.

Accelerated failures, whether attributed to decontamination or any other process, must be distinguished from the normal failure rate of HDDs. Analysis of HDD populations in use has revealed bimodal failure: very few failures in the first 12 months of use, and a Weibull-type probability density function ($R^2 = 0.94$) peaking at 46 months.[109] One method to account for such confounding factors is to collect data with built-in test equipment (BITE).[76] The HDD industry developed a form of BITE, the Self-Monitoring and Reporting Technology (SMART), in 1994-95 to provide warning of drive failure within 24 hours.[110] SMART is itself susceptible to false positives and negatives, but has been improved over successive years of HDD production.[111]

SMART incorporates multiple data sets, including raw, sensor-fed data, and normalised data. Suitably designed parametric hypothesis tests, such as Analyses of Variance or paired *t*-tests (explained in Appendix B), may use discrete changes in some SMART-sensed raw data, rather than the SMART failure algorithm, to test null hypotheses about HDD performance.[111] Such an approach treats SMART as any other sensor. For instance, the null hypothesis that an HDD subjected to decontamination treatment will not have significant variance in its behaviour, compared to an HDD without treatment, and given an identical set of instructions, may be tested. Any changes in reliability metrics may also be correlated to changes in performance metrics. The SMART identities most closely associated with accelerated failure rates include reallocated sectors, seek errors, and offline reallocations, followed by probational counts, scan errors, and cyclic redundancy check errors.[112] Measuring these identities before, during, and after decontamination provides a way to monitor the health of the HDD. A statistically significant change in the SMART identities after an HDD has been subjected to a particular treatment could be attributed to that treatment. Statistics could help to quantify the impact of such changes on the long-term reliability of the HDD.

2.3.2.3 – Electro-Optical Parts

2.3.2.3.1 – Optical Media

Optical drives, like magnetic HDDs, depend upon consistent electromechanical properties because they also require rotation of a recording medium. As suggested by their name, they also depend upon optical properties to function. They are more susceptible to the dielectric behaviour of the materials themselves, particularly at optical frequencies, along the signal path. The phenomena of reflection, refraction, and absorption (extinction) all reduce the integrity of the intended signal. The use of rapidly changing and narrow laser pulses at wavelengths < 700 nm is needed to read or write bits of information at micrometric spacing without interference between adjacent bits. Precise control, provided by feedback-controlled servos and motors, is also necessary to read and write data. With typical error-correction codes, error rates for compact disc (CD) drives are reduced from 10^{-5} down to 10^{-13} byte–error·byte read^{-1}: on average, fewer than one byte in error per terabyte read.[113] As a result, such drives are normally highly reliable.

The index of refraction of air is the normal condition for such drives. In a standard atmosphere, the index is close to unity.[51] However, a medium in the laser propagation path between lens and disc surface with an index of refraction that is much larger than unity could lead to transient failures from refracted laser pulses (described by Snell's law).[114] At a minimum, one would not expect such a drive to function if immersed in a fluid other than air. Since optical drives also rely on mechanical rotation, the same concerns about bearing lubricity apply to them as to fans and HDDs. Because optical drives use removable recording and storage discs, and are not equipped with BITE, their performance and reliability must be gauged by less automated methods, such as the success or failure of reading from or writing to a disc.

2.3.2.3.2 – Liquid Crystals

Liquid-crystal (LC) technology now predominates in the field of visual displays. Liquid-crystal displays (LCDs) use the temperature- and direction-dependent polarisability of twisted-nematic liquid crystals to change refractive indices in picture elements (pixels) of a screen.[59] The ability to change both colours and light levels at high resolution allows them to display images. LCs exhibit some properties of liquids and some of solid crystals: in addition to surface tension, LCs may flow in response to applied shear and have viscosity.[115] Typical LC constituents include cyanobiphenyls (CB), as

shown in Figure 5, whose substituent may be a linear alkane. For example, 5CB is the industry designation for 4-cyano-4'-pentylbiphenyl.

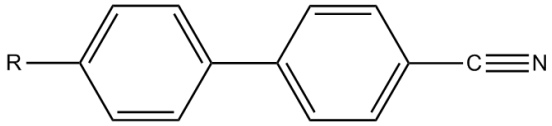

Figure 5: Generic Cyanobiphenyl Structure

During manufacture of LCDs, proprietary mixtures of LCs are applied in thin layers between polarising sheets and surrounded by thermally cured adhesive.[59] Depletion of LCs, whether through mechanical removal, dissolution, or chemical reaction, would therefore result in aberrant display of graphics (if they are displayed at all). Such failures may be measured by the intensity and colour of emitted light as well as by the operation of individual pixels. As long as the adhesive seal remains intact, the LC fill should not be depleted. Thus, a decontamination system suitable for use with LCD-containing devices should not corrode, deplete, or react with any of the layers, seals, or fill.

2.3.2.3.3 – Night Observation Devices

Night observation devices (NOD) are a separate application of electro-optical phenomena. They are indispensable for military missions that require round-the-clock activity. NODs use the photoelectric effect and vacuum amplification on a microchannel plate within the image intensifier (II) tube to amplify 'low' intensities of ambient light, i.e. intensities at which natural human visual acuity is poor.[116] Colour is not reproduced with fidelity, but instead in a limited number of blues, greens, and yellows, depending on the wavelengths emitted by the phosphor coating.[117] However, the shape of the reproduced image resembles the original thanks to the spatial consistency of the process. NODs therefore rely upon powered electronics, but they are also classical optical devices in that they have objective and ocular lenses. The respective functions of these lenses are to collect available ambient light and to form an image to be projected into the observer's eye.

Performance measurements for such devices are quantum (quantum efficiency, work function), electronic (gains, distortions), and optical (image location and magnification), as well as overall characteristics that quantify the

'quality' of image reproduction (field of view (FoV), signal:noise ratio (SNR)).[116] The reliability of NODs may be characterised by maintenance of the baseline SNR, FoV, image properties, and vacuum-tube amplifier gain/distortion characteristics. Catastrophic failures may include electrical shorts, loss of vacuum in the II tube, and mechanical breakage of an optical lens.[116] Permanent, though not necessarily catastrophic, failures include chemical transformation of the phosphor coating, resulting in loss of image reconstruction, and mechanical abrasion of the optical lenses.[59] Thus, a decontamination technique suitable for use with these devices should not cause such events as shorting, lens etching, or phosphor depletion. Electrical behaviour may be measured by probing the circuits of the device, requiring disassembly. Optical behaviour may be measured without disassembly by comparing the spectra transmitted by the device before and after any treatment.

2.3.2.4 – Structural Materials

The use of composite materials in equipment is another likely sensitivity. Examples of composites in sensitive equipment include printed circuit board materials, of which the most common are paper-backed phenolic resin and fibreglass-reinforced epoxy resin.[118] Such composites depend upon adhesives to maintain their integrity. Adhesion, in turn, depends upon maintaining the design length and functional groups of constituent molecules. De-polymerisation may occur through hydrolysis, substitution, and radical-forming reactions.[49] Hence, as previously discussed, long-term exposure of many adhesive polymers to liquid water leads to irreversible degradation.

Material loss through mechanical and electro-chemical wear must also be limited for parts to maintain their structural integrity. An organic solvent that dissolves sensitive materials in addition to contaminants is evidently not a suitable choice for decontamination. Water, in addition to depleting material through hydrolysis, can accelerate corrosion in both vapour and liquid forms.[32] For water vapour in ambient air, a relative humidity of 60 % may be critical in allowing a corrosive electrolytic solution to form on the surface of an electronic material from the combination of moisture vapour and ionic species as adsorbates. Given the small characteristic dimensions of metallic members in electronic assemblies, their exposure to corrosion over even a short time could result in failure. The impact of a decontaminant on structural materials may be tested by evaluating properties such as tensile strength before and after exposure to a treatment, or by determining the weight loss or gain of material coupons after such exposure.

Adhesives themselves, and composite materials that include adhesives, may be readily attacked by organic liquids, water, and ionic particulate matter. Even if outright material loss (through dissolution) is not a concern, the gradual loss of adhesive integrity or corrosion may lead to accelerated failure rates. Thus, both water-based and organic decontamination solutions may be detrimental to composite materials that contain adhesives, even over short durations of exposure. On the other hand, exposure of composites to air or inert fluids may present no quantifiable acceleration of failure over the time required to achieve decontamination.

2.3.3 – Summary

A decontamination process appropriate for use on sensitive substrate materials will be selective and preferentially remove (or transform) contaminant adsorbates. Ideally, such a process would minimise physical and chemical driving forces on sensitive equipment so as not to harm its reliability, and would not damage ecological or human health. The technique would also be amenable to scale-up and deployment into operational conditions, achieving rapid decontamination of sensitive equipment and reducing risks to personnel. The effectiveness of a decontamination process may be evaluated through chemical analyses, and its suitability evaluated through operational trials.

2.4 – Previous Research

2.4.1 – 2012-13 Sensitive Electronic Equipment Decontamination Project

The 2012-13 Sensitive Electronic Equipment Decontamination Project (SEEDP) was carried out by candidates on the Canadian Army's Land Force Technical Staff Programme (LFTSP).[27] The aim of the project was to determine whether the fluids HFE-7200 or FK-5-1-12 could be used to remove chemical warfare (CW) agents from sensitive electronic equipment. If they could, such fluids might improve the CAF's ability to decontaminate sensitive equipment and preserve its function after exposure to contamination. Experimental design and results of the 2012-13 project are presented in Appendix A.

The project determined that immersion of contaminated low-density polyethylene (LDPE) coupons in liquid FK-5-1-12 caused contaminant to move into the decontaminant phase. Notably, one of the fastest rates of removal was observed for mustard agent (HD), which was produced and handled locally in accordance with a licence from the then-Department of Foreign Affairs, Trade, and Development (currently Global Affairs Canada). A

rate of removal of 99.7 % from a coupon was determined after 30 min of immersion time by instrumental neutron-activation analysis of chlorine, the tracer atom for HD contamination. Concurrent sampling of the liquid FK-5-1-12 and its analysis by gas chromatography with mass spectrometry (GC-MS) failed to account for contaminant in the fluid, which did not permit an independent confirmation of decontamination. However, HD is known to react in the ambient and it can form products that are challenging to detect, even by GC-MS.[119] This outcome suggested, first, that FK-5-1-12 could feasibly be applied to decontamination, and second, that better accounting for the fate of contaminants would be needed to improve confidence in the procedure.

Bench-scale experiments were complemented by reliability trials on small-scale sensitive equipment. Trials of Universal Serial Bus (USB) memory devices exposed to various decontaminants showed a range of effects on performance and reliability, from the statistically undistinguishable to the catastrophic. For USB memory devices energised to 5 V_{dc} and immersed in conductive decontaminating solutions, electrochemical corrosion at soldering points likely caused both transient and catastrophic failures. For a USB device immersed in 6 % by weight $NaOCl_{(aq)}$ solution (a typical bulk decontaminant[14]), the test was not completed successfully: the physical hardware was beyond repair, and the data stored on the device were corrupted beyond recovery. This would not be acceptable for operational decontamination whose implicit goal is to maintain critical capabilities. On the other hand, USB devices that were immersed solely in FK-5-1-12, or that were exposed to 2-chloroethyl ethyl sulfide (CEES), a simulant for HD, and then immersed in FK-5-1-12, did not experience catastrophic or irreversible performance degradation. These two results—rapid contaminant removal and no apparent detrimental effect—motivated the larger scope of the current thesis.

2.4.2 – Properties of FK-5-1-12

The purpose of this section is to provide a summary of the physical, chemical, and ecological properties of FK-5-1-12, as well as its regulatory status and commercial availability in Canada.

2.4.2.1 – Physical Properties

Several of the previously published physical properties of FK-5-1-12 at 25 °C are summarised in Table 2.[120, 121]

Table 2: Properties of FK-5-1-12

Systematic IUPAC Name	1,1,1,2,2,4,5,5,5-nonafluoro-4-(trifluoromethyl)-3-pentanone
Molecular Formula	$C_6F_{12}O$
Structural Formula	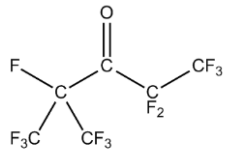
CAS #	756-13-8
Molecular Weight ($g \cdot mol^{-1}$)	316.04
Density at 25 °C, 1 atm ($g \cdot cm^{-3}$)	1.6
Dielectric Strength (relative to dry N_2)	2.3
Dynamic Viscosity (cP)	0.64
Melting Point (°C/K)	-108/165
Boiling Point (°C/K), 1 atm	49/322
Solubility of Water in Fluid ($\mu g \cdot g^{-1}$)	20
Vapour Pressure at 25 °C (atm)	0.324
Surface Tension at 25 °C ($mN \cdot m^{-1}$)	10.8
Atmospheric Half-Life (days)	3-5
Ozone Depletion Potential by IPCC Method	0
Global Warming Potential ($CO_2 \equiv 1$)	1
Airborne Acute Toxicity (ppm)	10 000
Airborne Chronic Exposure Limit, 8-hour Time-Weighted Average (ppm)	150

Since FK-5-1-12 is a branched, perfluorinated ketone containing twelve σ_{C-F} bonds and one $\pi_{C=O}$ bond, its properties may be expected to resemble those of the short-chain aliphatic perfluorocarbons (PFCs), the aliphatic ketones, and other perfluorinated ketones. FK-5-1-12 is, as are PFCs, insoluble in many common industrial solvents, including water and short-chain aliphatic hydrocarbons.[108] The simultaneous hydro- and lipophobicity of PFCs is a direct consequence of carbon–fluorine bonding. The molecular polarisability of the simplest PFC, CF_4, is only 25 % that of a hydrocarbon of comparable size.[122] This lower polarisability limits the likelihood of attractive dispersive interactions among PFCs and hydrocarbons. In water, a solvent not dominated by dispersive interactions, the sum of the water–CF_4 solvent interaction energy and the energy of cavity formation (i.e. to 'host' a CF_4 molecule in the water) is positive, and therefore thermodynamically unfavourable.[122] In consequence, CF_4, larger PFCs, and perfluorocarbon groups tend to repel both hydrocarbons and water.

FK-5-1-12 in the condensed and vapour phases has a higher dielectric strength than air. It resists conducting a potential of up to 15 kV in the vapour phase and 48 kV in the liquid phase over a 2.7-mm spark gap at 1 MHz, which is 2.3-fold higher than dry $N_{2(g)}$ (6.8-kV breakdown voltage).[123] This physical property also shows the relatively low polarisability of the CF_x groups compared to others (in this case, the N≡N bond).[124] As a result, liquid-phase FK-5-1-12 is more resistant to electricity, and safer from electric breakdown, than air itself.

2.4.2.2 – Observed Reactions and Environmental Fate

The strong C-F bonds in PFCs generally result in very low reactivity with other functional groups.[125] However, the presence of a carbonyl group in FK-5-1-12 makes it more likely to react by addition or substitution than symmetric perfluorocarbons with no functional groups (CF_4, C_2F_6, etc.).[126] FK-5-1-12 is indeed more reactive than the PFCs, to the extent that it will more readily degrade in the environment.[127] This property makes it more attractive from ecological and life-cycle perspectives, but demands a more nuanced view for its suitability as a decontaminant. The possibility of chemical reactions is usually beneficial in decontamination if it results in transformation of a contaminant into benign products. Conversely, any greater tendency to react introduces higher risks of substrate incompatibility, as in the examples of corrosion and lubricant or adhesive depletion presented earlier. Some of the previously observed reactions of FK-5-1-12 are summarised in the following sections and their effects on suitability for decontamination are considered.

2.4.2.2.1 – Acyl Substitution

In previous studies, FK-5-1-12 has been observed to react with weaker nucleophiles, e.g. water and methanol,[128] and with stronger nucleophiles, such as a bifunctional amine and thiol.[27] Jackson et al. have described this behaviour through a nucleophilic acyl substitution mechanism.[128] Their proposed mechanism resembles that of an acyl derivative, with addition and elimination steps and a tetrahedral intermediate (Figure 6). In this mechanism, HNuc represents the nucleophile, and the leaving group in the elimination step is invariably 1,1,1,2,3,3,3-heptafluoropropane (the refrigerant vapour HFC-227ea), analogous to the electronegative leaving group of an acyl halide.

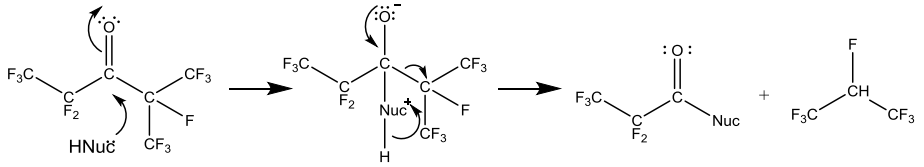

Figure 6: Nucleophilic Acyl Substitution of FK-5-1-12

In the first step, the electron density of the nucleophile (e.g. from a lone pair of electrons) is capable of attacking the positive charge density of the carbonyl group carbon. Electron density shifts from the $\pi_{C=O}$ bond to form a single bond, resulting in a tetrahedral carbon intermediate. In the second step, the bond between the carbonyl carbon and the electronegative leaving group cleaves heterolytically, the carbonyl $\pi_{C=O}$ bond is restored, and the nucleophile bond to the proton is cleaved. The central carbon of the leaving group bonds to the proton from the original nucleophile, resulting in the formation of two neutral products.

This mechanism may explain how FK-5-1-12 will hydrolyse in typical environmental conditions, at both pH 5.6 (naturally acidic carbonic acid-saturated rainwater) and pH 8.5 (naturally basic seawater).[128] A hydrolysis mechanism is shown in Figure 7.[128]

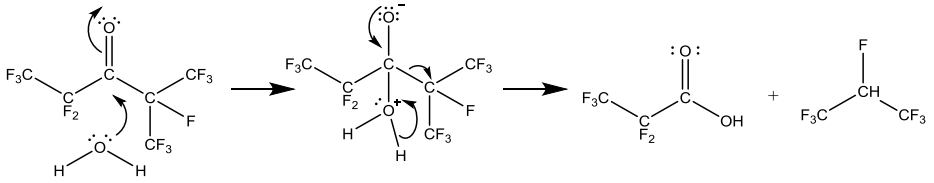

Figure 7: FK-5-1-12 Hydrolysis

The nucleophilic water attacks the carbon of the carbonyl group, expelling HFC-227ea vapour as the leaving group and generating liquid 1,1,1,2,2-pentafluoropropanoic acid (PFPrA).[128] Hydrolysis of a carbonyl group is relatively insensitive to pH because it may be initiated at either atom. It may occur in acidic conditions if the high electron density on the carbonyl oxygen attacks a nearby H^+ ion, or in basic conditions if the low electron density on the carbonyl carbon is attacked by an OH^- ion.[129]

FK-5-1-12 in contact with water exhibits first-order hydrolysis rate constants at both pH values (Table 3) that equate to a lifetime of hours. The generation of PFPrA from degraded FK-5-1-12 would likewise be rapid.

Table 3: FK-5-1-12 Hydrolysis Kinetics in Buffered pH Solutions

pH	First-Order Hydrolysis Rate Constant (s^{-1})
5.6	$(1.9 \pm 0.1) \times 10^{-4}$
8.5	$(3.1 \pm 0.3) \times 10^{-4}$

The PFPrA product from discharged FK-5-1-12 could exert ecological effects on land or in water bodies. PFPrA has an acute toxicity value (24-hour LC_{50}) of 80 $mg \cdot L^{-1}$ to a model organism, the aquatic rotifer *Brachionus calyciflorus*.[130] For comparison, the smallest naturally occurring perfluorinated carboxylic acid, trifluoroacetic acid (TFA), has a 24-hour LC_{50} value of 70 $mg \cdot L^{-1}$.[130] The 24-hour LC_{50} values reported for *B. calicyflorus* from some common industrial solvents are of the same order of magnitude, at 51 $mg \cdot L^{-1}$ for acetone, 113 $mg \cdot L^{-1}$ for toluene, and 68 $mg \cdot L^{-1}$ for hexane.[131] Therefore, if FK-5-1-12 were to be used in the field, spill precautions suitable for such solvents ought to be taken to mitigate ecological effects. FK-5-1-12 itself is relatively volatile, with a vapour pressure of 0.324 atm at 25 °C (Table 2). Hence, its atmospheric reactions and fate are also relevant in deciding its suitability.

2.4.2.2.2 – Photochemical Reactivity

In the atmosphere, FK-5-1-12 may be attacked by water and by sunlight.[127] The photon absorption spectrum of FK-5-1-12 exhibits Gaussian distribution in the ultraviolet region (between 240-360 nm), with a prominent maximum at 305 nm.[132] UV radiation in general can promote *n* (non-bonding) and π (bonding) electrons in the carbonyl group to the π^* (anti-bonding) molecular orbital. Moreover, FK-5-1-12 at 296 K and a partial pressure of 1.5 Torr (200 Pa) has been shown to photolyse by UV photons at 305 nm in simulated tropospheric conditions.[132] Either of the σ_{C-C} bonds adjacent to the carbonyl may be broken by the 305-nm wavelength to yield radicals. The results of successive photolytic degradations give FK-5-1-12 an atmospheric half-life of the order of days (Table 4).[132]

Table 4: FK-5-1-12 Photolysis Kinetics in Simulated Troposphere

Partial Pressure of Diluent Air (Torr)	First-Order Photolysis Rate Constant (s^{-1})
700	8.5×10^{-7}
200	2.1×10^{-6}
50	8.3×10^{-6}

The effective photolytic rate constant declines to approximately one order of magnitude lower as the total ambient pressure approaches that of mean sea level.[132] This behaviour means that, while FK-5-1-12 should be protected

from UV light to limit its degradation, exposure to UV for minutes or hours will not result in significant losses.

The ultimate products of FK-5-1-12 photolysis in the simulated troposphere have been shown to include CF_3COF and COF_2. These, in turn, are unstable, and are rapidly hydrolysed to TFA, CO_2, and HF.[132] This fate mechanism is important because the relatively high vapour pressure and low boiling temperature of FK-5-1-12 will cause it to evaporate readily into the atmosphere, where it will be partly mineralised. TFA is known to occur naturally in the oceans,[133] and, although it may be attacked by the hydroxyl radical (e.g. in the atmosphere),[134] its predominant fate appears to be deposition to oceans or terrestrial salt-lakes.[135] The carbon–fluorine bond can be made and broken biochemically, as observed in naturally occurring fluorinated short- and long-chain fatty acids, fluoroacetone, and fluorinated nucleic and amino acids.[136] However, there remain acknowledged information gaps on the environmental cycling of fluorine, and particularly of the trifluoromethyl moiety.

The results presented above suggest that FK-5-1-12, when discharged into the environment, is likely to be mineralised to HF and CO_2 and yield TFA (if evaporated and photolysed),[132] or to be degraded to PFPrA (if spilled into ground- or surface-water and hydrolysed).[127] The total mass of naturally occurring TFA in the hydrosphere has been estimated to the order of 10^{11} kg, which is far larger than the mass of synthetic fluorocarbons discharged during the 20th century.[137] In this view, the total environmental load of short-chain perfluorocarboxylic acids from the degradation of discharged FK-5-1-12 would not be significant, but point sources of spilled FK-5-1-12 in soils may require some form of remediation.

2.4.2.2.3 – Thermal Homolytic Decomposition

Although FK-5-1-12 has been marketed as a fire-suppression agent,[121] there are limits to this capability in fires that evolve enough thermal energy to cause it to decompose.[138] For instance, FK-5-1-12 will react by thermal decomposition into perfluoropropyl and perfluoropropanoyl radicals, shown in Equation 3, with an Arrhenius pre-exponential factor of 8.5×10^{16} s^{-1} and activation energy of 288.7 $kJ \cdot mol^{-1}$.[138] Readily combustible (thermally unstable) materials have activation energies of approximately half this value, e.g. 100-150 $kJ \cdot mol^{-1}$.[139]

$$C_2F_5C(O)C_3F_7 \rightarrow C_3F_7\cdot + C_2F_5(O)C\cdot$$

Equation 3: Thermal Homolytic Decomposition of FK-5-1-12

This behaviour is in contrast to the performance of Halon 1301 (CF_3Br), a fully halogenated extinguishant banned by the Montréal Protocol for its persistence and ozone-depletion potential.[140] Indeed, FK-5-1-12 has been shown to enhance combustion in certain situations, such as the United States Federal Aviation Administration's aerosol-can explosion test, that evolve such quantities of thermal energy.[138] In these situations, FK-5-1-12 would act as a fuel, rather than an extinguishant. Halon 1301 replacements, in which some halogenations have been replaced with non-halogen substituents, such as hydrogen or oxygen, are more readily combustible than Halon itself.[138] The possibility of reaction, including combustion, seems an inevitable trade-off with increased degradability of halogenated molecules. However, if precautions are taken, the thermal decomposition of FK-5-1-12 need not limit its suitability for field-expedient decontamination.

2.4.2.3 – Regulatory Status and Availability

As of the time of writing, the regulatory status of FK-5-1-12 in Canada is permissive. FK-5-1-12 is in the Public portion of the *Canadian Domestic Substances List* and does not fall within the ambit of the *Federal Halocarbon Regulations, 2003* (SOR/2003-289).[141] It is not among the *Speciated Volatile Organic Compounds* for mandatory discharge reporting under the National Pollutant Release Inventory.[142] However, it is not explicitly excluded from the list of Volatile Organic Compounds within Schedule 1 of the *Canadian Environmental Protection Act* (CEPA).[143] Thus, any future regulation made under sections 92.1 or 93, or an order made under section 94 of CEPA, would compel reporting and remedial requirements for discharges into the environment.

FK-5-1-12 is currently available for sale in Canada in bulk from suppliers of fire-protection products at prices of approximately $\$70\cdot kg^{-1}$.

Since FK-5-1-12 had previously shown evidence of both efficacy in physical decontamination of a chemical warfare agents and suitability towards energised sensitive equipment, its application in a general-purpose sensitive equipment decontamination system was tested in further detail in this thesis project. Some of its physico-chemical properties, such as reactivity, were also explored, given the opportunity of a wider project scope.

3. Experimental

Experiments to assess the fitness of FK-5-1-12 for sensitive equipment decontamination were devised in keeping with the three themes presented earlier. The first was to evaluate the physico-chemical properties of FK-5-1-12, including its hygroscopicity, electromagnetic and thermodynamic properties, and chemical reactivity. The second was to determine the effectiveness of FK-5-1-12 in a bench-scale decontamination process using representative contaminants and sensitive substrate materials. The third was to test the suitability of FK-5-1-12 for full-scale, field-expedient decontamination through reliability trials on sensitive equipment and experiments on fluid recovery. Experimental uncertainties and error propagation are discussed in Appendix B.

3.1 – Properties of FK-5-1-12

The FK-5-1-12 used in all experiments was purchased from a vendor of fire-protection products (Control Fire Systems, Toronto, Ontario) in 75-lb (34-kg) carboys, and not from the original manufacturer (3M Company). Physico-chemical properties of FK-5-1-12 have been published in open literature, including product information,[144] patents,[145] and third-party studies.[146] Tabulated thermodynamic properties are available from the manufacturer upon request.[123] Other properties that might be germane to its decontamination effectiveness or suitability, such as its molecular interactions and chemical reactivity, were not found from these sources. Hence, experiments to determine these properties were among the logical goals of this project.

3.1.1 – Methods

3.1.1.1 – Hygroscopicity and Purity

The aim of experiments testing the purity of FK-5-1-12 was to determine whether or not it would be suitable in the field if used 'as delivered' from a supplier. If not, additional purification steps could be required for it to perform according to its published specifications. Impurities of interest included water, which can dissolve ions and conduct electricity, and solid particulate matter, which could be deposited onto equipment during treatment.

The free water content in a sample may be determined by Karl Fischer potentiometric titration.[147] In the Fischer method, free water in a sample

reacts with pyridine–I_2 and pyridine–SO_2 complexes until none remains. This point is accompanied by a measurable increase in electrical potential, which is related to the original volume of water in the sample. The water content of four batches of FK-5-1-12, as delivered by the same commercial supplier (Control Fire Systems), was determined by this method. Determinations were made by ALS Environmental Labs (London, Ontario) at three replications per batch in December 2014. The first batch had been delivered in March 2013, and the three others in September 2014.

Solids found in as-delivered FK-5-1-12 were collected on filter paper, air-dried, and analysed. 35.7 (± 0.1) mg of solids were recovered from approximately 12 kg of FK-5-1-12. Elemental composition of the solids was determined by INAA (SLOWPOKE-2 facility, Royal Military College) using an accredited method for trace element identification[148] and by scanning electron microscope (SEM)/energy dispersive X-ray spectroscopy (EDAX, both XL30, FEI Company). The solids were pulverised manually with a glass rod on a watchglass and the melting point of the resulting powder was determined by a melting-point apparatus with electronic oven control (EZ-Melt, Stanford Research Systems) according to the manufacturer's directions.[149]

3.1.1.2 – Electrical and Magnetic Properties

Some of the electrical and magnetic properties of FK-5-1-12 could help to explain or predict its behaviour when in contact with sensitive equipment (particularly those having electrical or magnetic parts) and with contaminants. Since these properties were not found during the literature review, it was logical to determine them experimentally.

3.1.1.2.1 – Optical and Spectral Properties

Optical and spectral properties such as refraction, transmittance, and absorption provide insight into the macroscopic properties and interactions of matter. This is a consequence of the strength and location of electrical charges within molecules and their interactions with photons (vibrations of the electromagnetic field). For instance, elliptically polarised photons in the ultraviolet–visible region yield information about the long-range interactions of molecules, and infrared photons are correlated with the vibrations of specific bonds that confer reactivity.[150]

3.1.1.2.1.1 – Visible–Ultraviolet Ellipsometry

In preparation for visible–ultraviolet ellipsometry, FK-5-1-12 was gravity-filtered through Whatman No. 1 filter paper to separate suspended particles.

It was analysed by a series of published methods for the determination of fluid dielectric properties (by J. A. Woollam Company, Omaha, Nebraska).[151] Liquid-phase FK-5-1-12 was pipetted either onto a silica substrate of known surface roughness or into a hollow equilateral silica prism. Elliptically polarised light was emitted at an incident angle θ_1 with respect to the normal of these surfaces and the polarisation angles Δ and Ψ were measured using variable-angle spectroscopic ellipsometry (VASE) with RC2 and VUV-VASE ellipsometers (J.A. Woollam). The VASE apparatus scanned the wavelength domain between 191 nm (the far-ultraviolet region) and 1699 nm (the near-infrared region). In this convention, Ψ describes the shape of the polarisation ellipse and Δ describes the angular displacement of polarisation in time.

Complex indices of refraction $\tilde{n}$ were modelled by Equation 4 in the angles Ψ, Δ, and the incident and reflected ray angles θ, represented by indices 1 and 2.[152] The real part of $\tilde{n}$ (n) represents refraction, and the imaginary part (jk) represents absorption.

$$\frac{\tilde{n}_2 \cos\theta_1 - \tilde{n}_1 \cos\theta_2}{\tilde{n}_2 \cos\theta_1 + \tilde{n}_1 \cos\theta_2} \cdot \frac{\tilde{n}_1 \cos\theta_1 + \tilde{n}_2 \cos\theta_2}{\tilde{n}_1 \cos\theta_1 - \tilde{n}_2 \cos\theta_2} = \tan\Psi\, e^{j\Delta}$$

Equation 4: Indices of Refraction as a Function of Ellipsometric Angles

The index of refraction (n) of the liquid FK-5-1-12 was fit as a function of wavelength λ by an expansion in m terms of the Cauchy (Equation 5) or Sellmeier (Equation 6) series with arbitrary coefficients A and B.[153] The real and imaginary parts of the index of refraction as a function of wavelength were reported to the author.

$$n = A_0 + \sum_m \frac{A_m}{\lambda^{2m}}$$

Equation 5: Cauchy Expansion

$$n = \sqrt{1 + \sum_m \frac{B_m \lambda^2}{\lambda^2 - \lambda_{0,m}^2}}$$

Equation 6: Sellmeier Expansion

Given a polynomial function of the index of refraction of FK-5-1-12 in wavelength λ in the visible region of light, the strength ${n_{UV}}^2 - 1$ and relaxation frequency ω_{UV} of the molecule's UV oscillator were calculated. Photon wavelengths were converted to frequencies, and the term $n(\omega)^2 - 1$

was fit to the product $\omega^2 \cdot (n(\omega)^2 - 1)$ through linear least-squares regression. The UV oscillator strength and relaxation frequency were solved from the slope and intercept of the resulting linear function.[154]

3.1.1.2.1.2 – Infrared Spectroscopy

The near-IR absorption modes of FK-5-1-12 were also measured using a VUV-VASE ellipsometer at J.A. Woollam. Liquid FK-5-1-12 was added to silica cuvettes with interior path lengths of 0.2, 1.0, and 10 mm, and its absorption spectrum was scanned across the aforementioned wavelength domain ([191, 1699 nm]). Cuvettes without FK-5-1-12 were scanned as blanks. Absorption–wavelength data were reported to the author.

The mid-IR absorption spectrum of FK-5-1-12 was measured by Fourier-transform IR spectroscopy (Nicolet iS10 spectrometer with OMNIC software, Thermo Scientific). Liquid samples were pipetted onto a polished KBr disc with a second disc overlaid to retain the sample in the spectrometer cell. Spectra were obtained as the average of 8 scans. The same KBr discs without liquid added were used to determine blank spectra.

3.1.1.2.2 – Magnetic Properties

Many organic liquids exhibit isotropic diamagnetism, meaning that their relative permeability μ_r is less than unity in all directions and they move in the opposite direction of an applied magnetic field.[155] The relative permeability μ_r of FK-5-1-12 had not been published previously and so it was determined in this project through another dimensionless magnetic property: the volume susceptibility. Both permeability and volume susceptibility are intensive properties, that is, independent of sample size or shape for homogeneous substances.[155] In this sense, they are similar to mass density or specific gravity. Just as the mass density of a quantity of liquid may be determined by the deflection of a hydrometer of a suitable size, so too may the magnetic susceptibility be measured by the deflection of a susceptibility balance. In the Evans balance, the deflection of an unknown sample in a magnetic field is measured by a photocell and compared to that of a reference sample and of a sample of air.[156] The procedure allows determination of the susceptibility of the sample to an accuracy of 1-2 %.

A magnetic susceptibility balance (MSB Mark I, Johnson Matthey) was calibrated before use according to the manufacturer's directions.[157] Reading the deflection of a reference sample provided a calibration factor C_{Bal} (0.9698 ± 0.0008) and reading the deflection of an empty tube provided the value R_0.

Filtered FK-5-1-12 was pipetted into the sample tube and its height was measured to ensure that it would satisfy the minimum height required for the procedure. A correction term for the volume susceptibility of air, $\chi_{V|Air}$, was included.[158]

A formula for volume magnetic susceptibility (Equation 7) was used based on the assumptions that FK-5-1-12 presented a homogeneous, isotropic, incompressible liquid of constant composition in a sample tube of constant plan area. Readings R and R_0 from the apparatus (deflection), measurement of the sample tube's inner plan area A_{XS} in square centimetres, and the calibration factor together allowed calculation of the sample's volume magnetic susceptibility $\chi_{V|FK}$. The factor 10^{-9} expresses the deflection in terms of 'dimensionless' Gaussian cgs units, which are still used in this application. The Gaussian cgs susceptibility is multiplied by 4π to give the 'dimensionless' SI value.

$$\chi_{V|FK} = \frac{C_{Bal} \cdot (R - R_0)}{10^9 \cdot A_{XS}} + \chi_{V|Air}$$

Equation 7: Volume Magnetic Susceptibility (cgs)

The permeability μ_r (relative to vacuum, μ_0) was then obtained by Equation 8.

$$\mu_r = \frac{(1 + \chi_V)}{\mu_0}$$

Equation 8: Relative Permeability

3.1.1.2.3 – Bulk Electrical Resistance

The resistance of liquid-phase FK-5-1-12 to AC mains voltage typical of a field application was determined experimentally. An IEC 60320-1 C13 (female) cable was submerged in approximately 0.5 L of gravity-filtered liquid FK-5-1-12 in a polycarbonate container and connected to a 15-A mains circuit energised to a nominal 120 V_{AC} (root–mean–square). The resultant current from the cable conductors through the liquid was measured by a high-resistance electrometer (Keysight B2987A) with conductivity probes spaced at 10.00 (± 0.02) mm. The actual rms voltage function from the mains was determined by a power quality analyser (Fluke 435).

3.1.1.3 – Thermodynamic Properties

The durability of FK-5-1-12 as an operational decontaminant was evaluated by comparing its temperature-dependent physical properties to the basic requirements deduced for sensitive equipment decontamination. The proximity of the 0.987-bar (101.325-kPa) boiling point of FK-5-1-12 (49.2 °C) to the upper limit of expected operating temperatures (49 °C in NATO climate A1) introduced a concern of unacceptable rates of fluid loss through evaporation. Thus, the feasibility of field deployment of the fluid was tested by mathematical modelling and experiment.

The goal of transient heat-transfer calculations was to estimate the behaviour of FK-5-1-12 in limiting climate conditions. A minimally insulated reactor volume and a quiescent FK-5-1-12 fluid volume were both represented by spherical geometry. A one-dimensional, symmetric heat transfer problem was formed according to Fourier's law of heat conduction (Equation 9). Fourier's law relates heat flux $\phi''_{H|i}$ to the temperature gradient ∇T via the thermal conductivity through the i^{th} layer of a system, $k_{cond|i}$.

$$\phi''_{H|i} = -k_{cond|i}\nabla T$$

Equation 9: Fourier's Law of Heat Conduction

An energy balance of n layers of a system in terms of internal energy U, density ρ, volume V, and constant-pressure specific heat capacity c_p of the i^{th} layer is given in Equation 10.

$$U_t = \frac{d\left(\rho_i V_i c_{p|i} T_i\right)}{dt} = \sum_{i=1}^{n}\left(\phi''_{H|i}\right)$$

Equation 10: Energy Balance of System

The spherical system, drawn in SolidWorks 2014 (Dassault Systèmes), is shown in Figure 8.

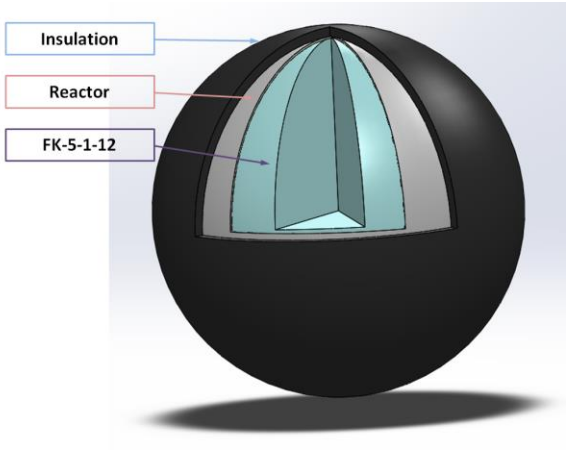

Figure 8: System Geometry for Transient Heat Transfer

Numerical simulation parameters, including material property constants, temperature-dependent equations, and initial and boundary conditions of the layers of the system are presented in Table 5.

Table 5: Parameters and Initial and Boundary Conditions for Transient Heat Transfer

Ambient	
Boundary Condition (T_∞)	49 °C
Insulation Layer	
Material	Closed-cell EPDM (Ethylene propylene diene monomer)
Outside Surface Area	0.7150 m^2
Thickness	0.0127 m
Mass	4.27 kg
Specific Heat Capacity	2000 $J \cdot kg^{-1} \cdot K^{-1}$
Density	900 $kg \cdot m^{-3}$
Thermal Conductivity	$k_{EPDM} = 10^{-6}T[\mathrm{K}]^2 + 8 \cdot 10^{-5}T + 0.0328$ [$W \cdot m^{-1} \cdot K^{-1}$]
Initial Temperature	49 °C
Insulation–Wall Interface	
Initial Temperature	42 °C
Reactor Wall	
Material	HDPE (High-density polyethylene)
Outside Surface Area	0.6621 m^2
Thickness	0.003175 m
Mass	1.845 kg
Specific Heat Capacity	1900 $J \cdot kg^{-1} \cdot K^{-1}$
Density	890 $kg \cdot m^{-3}$
Thermal Conductivity	0.49 $W \cdot m^{-1} \cdot K^{-1}$
Initial Temperature	40 °C
Interior	
Material	FK-5-1-12
Diameter	0.4527 m
Outside Surface Area	0.6438 m^2
Volume	0.04858 m^3
Mass	77.816 kg
Specific Heat Capacity	$c_{p\|FK} = 1.2946 - 1.8246 \cdot 10^{-3} \cdot T[\mathrm{K}] + 3.964 \cdot 10^{-6} \cdot T^2$ [$J \cdot g^{-1} \cdot K^{-1}$]
Density	$\rho_{FK} = -2.904 \cdot T[°\mathrm{C}] + 1674.415$ [$kg \cdot m^{-3}$]
Thermal Conductivity	$k_{FK} = -0.188 \cdot T[°\mathrm{C}] + 63.403$ [$mW \cdot m^{-1} \cdot K^{-1}$]
Kinematic Viscosity	$\upsilon_{FK} = e^{\left(\frac{660.0991}{T[°\mathrm{C}]+200} - 3.8731\right)}$ [cSt]
Initial Density	1601.815 $kg \cdot m^{-3}$
Initial Temperature	25 °C
Coefficient of Thermal Expansion (Volumetric)	0.0018 K^{-1}

The problem was discretised into 10-s timesteps and solved explicitly using the Forward Euler method.[97] Dimensionless groups, an overall heat-transfer coefficient for the FK-5-1-12 fluid element, and resultant heat fluxes and temperature increments through the layers were computed for each timestep. Further details on numerical modelling are found in Appendix B.

3.1.1.4 – Chemical Reactivity

Chemical reactivity is neither required nor forbidden in decontamination. Admittedly, it may cause more damage than benefit to sensitive equipment, which has been acknowledged not to tolerate chemical environments other than ambient air. Published studies have advanced the hypothesis that FK-5-1-12 will react with nucleophiles by acyl substitution, and have shown evidence that it is attacked by common chemicals such as H_2O.[127] Some VOCs and biocides among the TIMs of operational concern also have nucleophilic functions, meaning that FK-5-1-12 might react with these species. With contemporary tools, such reactions may be predicted by numerical methods, and analysed by instrumental methods of spectroscopy, to complement macroscopic observations.

3.1.1.4.1 – Structural Calculations

Since the number and arrangement of atoms in a molecule determine its chemical properties, including reactivity, an understanding of molecular structure may be useful as a predictive tool.[159] The structure of a molecule is analogous to that of a building, and molecular geometry at equilibrium may be solved using appropriate equations of mechanics. By the definition of equilibrium, the sum of forces acting on a building must equal zero for it to stand upright, and the same is true of forces acting on a molecule for it to hold together. Such values are obtained for atoms and molecules by solving the Schrödinger equation. The Schrödinger equation requires a basis set of electron density and a function for the total energy of the system, which is to be minimised at equilibrium.[160] As with large classical systems, quantum systems are often solved numerically. An initial estimate of the molecular shape is input, and this is refined by optimisation so as to satisfy the Schrödinger equation and the physical constraints on atoms and electrons. The resulting arrangement of the molecule may be depicted as a contoured map of the electrostatic potential, the separation of charges (the net dipole moment vector), and the density of electrons (orbitals). To save calculation time, electron-density functionals ('functions of functions'), rather than functions themselves, are often used as approximations.[160]

To guide chemical reactivity experiments in this project, electrostatic potential maps, net dipole moments, and the highest-occupied/lowest-unoccupied molecular orbitals (HOMOs/LUMOs) were calculated. FK-5-1-12 was compared to its analogous non-fluorinated saturated ketone (2-methyl-3-pentanone) and the smallest perfluorinated ketone (1,1,1,3,3,3-hexafluoropropan-2-one, HFA). Molecular geometry was input in Spartan '08

software (Wavefunction Inc.). It was first solved at the ground state in vacuum by the *ab initio* Hartree–Fock method with a 3-21G basis set, which is suitable for calculations of atoms in the first row of the periodic table.[161] Since Becke–Lee–Yang–Parr electron-density functionals have been used in previous attempts to predict some properties of FK-5-1-12, B3LYP density functional theory with a 6-31G+* basis set was used in subsequent calculations.[127]

3.1.1.4.2 – Reagents

The reactivity of FK-5-1-12 with nucleophiles that could be encountered on operations was tested experimentally to determine whether such reactions would impair its suitability as a decontaminant. Analytical-grade reagents were obtained from suppliers (typical purity > 99 %) and used without further purification (Table 6). When possible, analogous compounds were sought to study differences in the behaviour of functional groups while controlling for the length of the molecule. Where reagents are also TIMs of operational concern, their rankings in terms of acute inhalation toxicity according to the United States Naval Research Laboratory's sensitivity analysis are noted in the table.[3]

Table 6: Reagents in FK-5-1-12 Reactivity Studies

Category:	Reagent:	Supplier:	Ranking:*
1° alcohol	Methanol (MeOH)	Fisher	37
1° alcohol	Ethanol (anhydrous) (EtOH)	Commercial Alcohols	23
1° diol	Ethane-1,2-diol (EG)	Sigma-Aldrich	n/a
1° diol/thioether (HD breakdown product)	2,2′-Thiodiethanol (TDG)	Sigma-Aldrich	250
1° amine	Propan-1-amine ($PrNH_2$)	Sigma-Aldrich	n/a
1° diamine	Ethane-1,2-diamine (ED)	Sigma-Aldrich	180
1° alcohol/1° amine	2-Aminoethanol (MEA)	Sigma-Aldrich	76
1° alcohol/1° thiol	2-Thioethanol (2ME)	Sigma-Aldrich	315
2° alcohol	2-Propanol (*i*-PrOH)	Fisher	58
3° alcohol	2-Methyl-2-propanol (*t*-BuOH)	Fisher	273
3° amine/OP biocide	Octamethylpyrophosphoramide (OMPA) – 94.7 % purity	Chromatographic Specialities	8
OP ester (GB breakdown product)	Diisopropyl methylphosphonate (DIMP)	Alfa Aesar	n/a
OP ester (GB breakdown product)	Dimethyl methylphosphonate (DMMP)	Sigma-Aldrich	n/a

**Ranking* refers to the highest ranking of acute inhalation toxicity in the United States Naval Research Laboratory sensitivity analysis of Toxic Industrial Materials

Reagents were added in two iterations. The first iteration was intended to minimise the evolution of gases in glass vials and the risk of an explosion. In this iteration, reagents were added volumetrically at 100 (± 10) µL to 15-mL glass vials with PTFE seals. FK was added to these vials volumetrically at 10 (± 0.1) mL (an FK–reagent ratio of 100:1). OMPA was added gravimetrically at 0.0053 (± 0.0001) g OMPA to 0.5224 (± 0.0001) g FK-5-1-12.

A subsequent iteration used 22 % molar excesses of FK-5-1-12 with respect to the hypothetical amount of reagent consumed in nucleophilic substitution. For instance, to test the reactivity of one equivalent of a bifunctional nucleophile (ethane-1,2-diamine), two equivalents plus 22 % excess of FK-5-1-12 were used. In these experiments, the volumes of both FK-5-1-12 and reagent were adjusted to give a total volume of 8 mL. Both quiescent and turbulent flow régimes were studied. For the turbulent case, glass vials were rotated at a velocity of 200 (± 1) rpm on a platform shaker-table (Brunswick Innova 2100) at ambient laboratory temperature. Qualitative signs of reaction in the vials were noted with time, and 100-µL or 100-mg aliquots, for liquids and solids, respectively, were drawn for spectroscopic analysis by

NMR and FTIR spectroscopy. For comparison, neat reagents were also sampled.

3.1.1.4.3 – Spectroscopy

^{1}H NMR spectra were obtained with an Oxford 300-MHz NMR (Agilent Technologies), typically operating at 23.5 (± 1.0) °C. Either 99.8 % deuterated chloroform ($CDCl_3$, Sigma-Aldrich) or 99.8 % deuterated dimethylsulfoxide (DMSO-d6) with tetramethylsilane (Canadian Isotopes) was used as a locking solvent. ^{1}H NMR spectra were obtained at a duty cycle of 1.998 s of acquisition time and 1.000 s of relaxation time over 16 repetitions.

NMR spectra were Fourier-transformed by processing software (ACD Labs 2D Processor) and converted to arrays for analysis by spreadsheet (Microsoft Excel 2010) and by linear algebra software (Mathworks MATLAB R2012b). Peak intensities in a given spectrum were normalised with respect to the maximum intensity to allow spectrum-by-spectrum comparisons. The chemical shifts and coupling constants were read from these spectra. Proton abundances were determined by integrating numerically. Sensitivity analysis into the effects on chemical shifts from different temperatures and locking solvents was conducted using published formulae.[162, 163] Spectral line-shapes were also interpreted for evidence of reaction, e.g. proton exchanges.[164]

IR spectra of products were obtained with a Nicolet iS10 Fourier-transform IR spectrometer interfaced with OMNIC software (Thermo Scientific). Liquid samples were pipetted onto KBr discs. Solids were hand-milled with IR-grade KBr powder (Sigma-Aldrich) at a ratio of 1 % sample by mass and the mixture was pressed into new discs. FTIR spectroscopy was used strictly to qualify the presence of functional groups and changes among them, without quantitation.

3.1.1.5 – Fluorinated Lubricant Depletion

In the literature review, a likely conflict between sensitive equipment decontamination effectiveness and suitability emerged when examining hard-disk drives. Hydrofluoroethers and fluorinated ketones have been used to dissolve critical hard-disk platter lubricants, and yet have also been applied to the problem of sensitive equipment decontamination in small-scale trials because they satisfy many particular requirements of SED. In this view, any fluorinated solvent or surfactant could do more harm than good by depleting fluorinated (and other) lubricants, along with contaminants, from sensitive surfaces. Surface analyses of hard disk platters were intended to test this question experimentally.

Laptop HDDs (n = 4) at the end of their service lives were obtained from electronic waste for delubrication tests. HDDs were disassembled and both platters from each drive were shattered into coupons. Coupons from one platter were submerged in either neat FK-5-1-12 or neat HFE-7200 for 20 min (treatment group), and then withdrawn and sealed in polyethylene bags. Coupons from the other platter (control group) were not subjected to any treatment and were immediately sealed in polyethylene bags. Treated and control coupons were shipped to Surface Science Western (University of Western Ontario, London, Ontario) for surface analyses.

At Surface Science Western, Auger Emission Spectroscopy was performed using a Phi-660 Scanning Auger Microprobe (PerkinElmer). Auger analysis used a 5-keV electron beam rastered over a 100-µm × 100-µm coupon surface area. The depth of a coupon was profiled at a rate of 14 nm·min^{-1} over a 2-mm × 2-mm surface area using Ar^+ at 3 keV for up to 1.54 min. Data were reported as the abundances of elements profiled with time by coupon.

Time-of-Flight (ToF) Secondary-Ion Mass Spectrometry (SIMS) analysis was conducted using a TOF-SIMS IV apparatus to characterise secondary ions of interest within the first 1-3 nm of the surface, including any adsorbates. A 25-keV Bi^{3+} cluster primary ion beam pulsed at 10 kHz was used to bombard coupon surfaces, thereby generating secondary ions. The positive or negative secondary ions were extracted from the sample surface, mass-separated and detected via a reflectron-type ToF analyser, allowing parallel detection of ion fragments having mass/charge ratios (m/z) up to ~900 within each 100-µs cycle. A pulsed, low-energy electron flood was used to neutralise sample charging. Positive and negative secondary ion mass spectra were collected at each of 128 × 128 pixels over a scanned area of 500 µm × 500 µm. Data were reported as the abundances of secondary ions by coupon.

X-ray photoelectron spectroscopy (XPS) with an AXIS Nova spectrometer (Kratos Analytical) operating at 160 eV was used to probe a maximum depth of 10 nm over a coupon area of 300 µm × 700 µm. Data were reported as the total abundance of a given element within this volume by coupon.

3.2 – Decontamination with FK-5-1-12

To assess the decontamination effectiveness of FK-5-1-12 required appropriate choices of both contaminants and sensitive substrate surfaces. The choice of contaminant would inevitably be subject to the constraints of safe handling and detection methods, and the choice of surface materials

compelled by the need for faithful representation of full-scale equipment. These materials are introduced in the following section. Thereafter, the methods of contamination, decontamination, and chemical analysis are presented.

3.2.1 - Materials

3.2.1.1 – Contaminants

The inventory of TIMs provided by the project sponsor was rationalised into the classes of TIMs posing the greatest risks of enduring contamination. While some VOCs may be less reactive and more persistent than oxidants, reductants, and self-polymerisers, biocides were noted above all others in the combination of persistence, stability, ease of dispersion, and toxicity. Biocides were therefore a logical contaminant with which to challenge the decontamination effectiveness of FK-5-1-12. Two biocides, bromophos-methyl (BrPMe, 4-bromo-2,5-dichlorophenyl dimethyl phosphorothionate) and triphenylarsine (TPhAs), were obtained as analytical standards (Fluka) for these tests.

3.2.1.2 – Substrate Materials

Coupons for decontamination testing were specified with nominal dimensions of 40 mm × 7 mm × 1.5 mm. These were obtained in materials representative of sensitive equipment. Virgin HDPE was obtained commercially (Plastic World, Toronto, Ontario) as a baseline substrate material for proof-of-concept testing. The polycarbonate (PC) and acrylonitrile–butadiene–styrene (ABS) alloy FR3021, used in computer shells, keyboards, and the like, was obtained from diverted electronic waste. This waste was machined into coupons for testing. Virgin Nylon-6,6 webbing coupons, conforming to Type VII, MIL-W-4088K specifications, were obtained commercially (Bally Ribbon Mills, Bally, Pennsylvania).[165] Two types of coupons representative of the most commonly used printed circuit board substrate materials in COTS electronic equipment were also obtained: G-10/FR-4 specification fibreglass with epoxy resin and XXX specification paper-backed phenolic resin (Franklin Fibre, Wilmington, Delaware).[118]

Upon receipt, coupons were cleaned using compatible solvents: 2-propanone for fibreglass-reinforced epoxy and phenolic resin, and 2-propanol for the remainder. Coupon surfaces were profiled by a diamond-tipped stylus profilometer (SRG-4000, Phase II Plus) with 5-nm sensitivity. Average surface-roughness values R_a, R_q, R_t, and R_z, as functions of asperity heights y_i, were determined according to Equation 11 to Equation 14.

$$R_a = \frac{1}{n}\sum_{i=1}^{n}(|y_i|)$$

Equation 11: Arithmetic Average Roughness

$$R_q = \sqrt{\frac{1}{n}\sum_{i=1}^{n} y_i^2}$$

Equation 12: Root–Mean–Square Roughness

$$R_t = R_{peak} - R_{valley}$$

Equation 13: Maximum (Peak-to-Valley) Roughness

$$R_z = \frac{1}{5}\sum_{i=1}^{5} R_{peak|i} - R_{valley|i}$$

Equation 14: Average Peak-to-Valley Roughness

The woven Nylon-6,6 coupons were not profiled this way. Instead, their surface properties were estimated using SEM images and EDAX elemental analysis (XL30 SEM/EDAX, FEI).

3.2.2 – Methods

3.2.2.1 – Proof-of-Concept—OP Pesticide and HDPE Substrate

Bromophos-methyl (BrPMe) was selected as the initial contaminant to challenge the capability of FK-5-1-12 decontamination. BrPMe is an OP pesticide and is detectable by INAA since it contains Br as a tracer atom.[91] The general relationship between analysis and the extent of decontamination was as follows: first, the background abundance of Br in all parts of the decontamination system was determined by INAA. Br was added ('contaminating' coupons) as spikes of a known quantity of BrPMe, and a decontamination process was attempted. Determinations of Br in the parts of the system after each process then served to measure the extent of decontamination.

Substrate coupons and samples of FK-5-1-12 were analysed by INAA for background Br abundance using an accredited determination method for petroleum hydrocarbons, with a 15-min typical irradiation time.[148] All counts were verified against a Br^- standard of 10.0 (± 0.1) $\mu g \cdot g^{-1}$ and a Br^- control of 10.0 (± 0.1) $\mu g \cdot g^{-1}$ (SCP Science, traceable to NIST). This method was applied to blanks, controls, and coupon and liquid samples subjected to treatment.

The effect of 'no fluid flow' conditions on contaminant partitioning was determined by a three-step process: one, contaminating a coupon; two, immersing a contaminated coupon into quiescent liquid FK-5-1-12 and holding for different time intervals; three, withdrawing the coupon, allowing FK-5-1-12 to evaporate. After this process, the coupon itself was irradiated to determine its residual abundance of Br.

A contaminant solution of 2.0 (± 0.1) mg of BrPMe was prepared in 25 (± 1) mL of dichloromethane (DCM, Fisher Scientific). Once cut to nominal dimensions, HDPE coupons were washed, first in water and detergent, then in 2-propanone, allowed to air-dry, and sealed in polyethylene bags. FK-5-1-12 was gravity-filtered through a Whatman No. 1 filter paper. It was pipetted in 10-mL (± 0.5-mL) volumes into 15-mL glass vials. These vials were the bench-scale decontamination systems that were to contain the contaminated coupons. Immediately before contamination, coupons were washed again in ethoxyethane, air-dried, and weighed on an analytical balance (Mettler AE 163). 50 (± 0.1) µL of BrPMe contaminant solution were spiked onto coupons by micropipette and the coupons were 'aged' undisturbed for 10 min, allowing evaporation of the DCM solvent. These spikes totalled a BrPMe mass loading density of 14.3 $\mu g \cdot cm^{-2}$.

Coupons were decontaminated by immersing them in vials with FK-5-1-12, holding for set time intervals (replacing the vial cap for intervals > 10 s), withdrawing the coupons, and allowing them to air-dry for 3 min. An FK-5-1-12 liquid sample and the treated coupon were both analysed for total Br concentration by the same method used for trace elemental quantitation in petroleum hydrocarbons. Control coupons were spiked with contaminant but not subjected to the decontamination process, and blank coupons were not spiked with any contaminant. These coupons were all analysed by the aforementioned method.

The ratio of the residual Br abundance in a decontaminated coupon to the Br abundance in a control coupon, with blank responses subtracted, served as a measurement of the effectiveness of decontamination by immersion for a given time interval.

The BrPMe loading density was increased by factors of 5 and 10 in two subsequent series of determinations. HDPE coupons were again used as substrate material and there was no mechanical power input except for the actions of immersing and withdrawing the coupon. In these series, contaminant-enriched FK-5-1-12 was not sampled and the extreme transient and steady-state cases of immersion for 1 second and 24 hours were not determined.

3.2.2.2 – Contaminant Mass Balance

To account for the fate of contaminants with confidence motivates a contaminant mass balance approach. As a consequence of the law of conservation of mass, the mass of contaminant entering a system must equal the mass that leaves. In principle, one unknown quantity in a balanced system may be calculated from knowledge of all the others, accounting for reaction and other possible fate mechanisms.[166] However, every practical determination of mass or concentration is accompanied by experimental uncertainty, and these uncertainties accumulate. To increase confidence in results, one may measure dependent quantities and verify that they indeed sum together, as expected from a mass balance, within the bounds of experimental uncertainty.

Previous attempts to sample the FK-5-1-12 phase and analyse it by GC-MS or by INAA either failed to yield mass balance, or yielded mass balance only within relatively large bounds of uncertainty of 20-30 %. Thus, a parallel separation process was included in the experimental design to increase confidence in the possible fates of the contaminants.

For separation, laboratory-grade sorptive media, including cellulose-based paper (Kimwipes, Kimberly-Clark) and granular activated carbon passing Mesh Nos. 6-14 (GAC, Fisher Scientific) were used without purification. Samples of these were analysed for background abundances of contaminant tracer atoms (Cl, Br, As) by INAA. HDPE coupons were used again as the target substrate material. The coupons themselves were also irradiated to provide an additional dependent value in the calculation of contaminant mass balance.

Cellulose–GAC mass ratios were specified at 9 mg cellulose and 27 mg GAC per g of FK-5-1-12, and the media were always used together. These ratios corresponded to 96.5 mg cellulose and 435 mg GAC per vial containing nominally 10 mL of FK-5-1-12. Sorptive media were weighed after being

added to the empty 15-mL vials for quality control, with typical Coefficients of Variation of 4.1 % in cellulose mass and 0.98 % in GAC mass. FK-5-1-12 was then dispensed into the vials at nominally 10 mL using a bottletop dispenser (Brinkmann, Metrohm AG), and the vials were weighed again to ensure quality control (mean FK-5-1-12 mass 16.052 g, Coefficient of Variation 3.8 %). A challenge contaminant solution of 18.9 (± 0.1) mg of 97 % purity triphenylarsine (TPhAs) was prepared in 25 (± 1) mL of chromatography- and pesticide-grade mixed hexanes (Fisher Scientific).

To replicate contamination, coupons were spiked by micropipette with 50 µL of challenge contaminant solution, typically with two 25-µL spikes to ensure even loading on coupon surfaces. Contaminated coupons were allowed to 'age' for ≥ 10 min for carrier solvent evaporation. To replicate decontamination, coupons were then immersed in the vials containing FK-5-1-12 and sorptive media for 5, 10, or 20 min. Control sorptive media and coupons were spiked with contaminant but not subjected to the decontamination process. Blank sorptive media and coupons were not deliberately contaminated.

After these time intervals had elapsed, the contaminated coupons were withdrawn and the FK-5-1-12 was allowed to evaporate from the vial over the course of 18 hours, after which the sorptive media were withdrawn and analysed. 4.0 (± 0.5) mL of hexane and 96.5 mg of fresh cellulose were added to the empty vials, which were then agitated at 200 rpm for 2 hours. The hexane phase and fresh media were also analysed for residual contaminant abundance.

The extent of decontamination was determined in the bulk of coupons and sorptive media, including blank, control, and treated samples, through INAA of the As tracer atom. Internal inorganic controls and standards for As (Inorganic Ventures, Christiansburg, Virginia) were used for every INAA determination.

3.2.2.3 – Factorial Contaminant–Substrate Studies

A factorial contaminant–substrate study sought next to generalise the effectiveness of the decontamination process from a single challenge contaminant applied to a single substrate material. Coupons of representative materials, e.g. FR-4 circuit board substrate and Nylon-6,6 webbing, having been procured and machined to suitable sizes, were solvent-washed (either with 2-propanone or 2-propanol), air-dried, and kept segregated in sealed containers until used.

Challenge contaminant solutions of 17.8 (± 0.1) mg of neat bromophos-methyl (BrPMe), and 18.9 (± 0.1) mg of 97 % purity triphenylarsine (TPhAs) were prepared in 25 (± 1) mL of chromatography- and pesticide-grade mixed hexanes (Fisher Scientific). FK-5-1-12 was dispensed into 15-mL glass vials and sorptive media were added as specified in 3.2.2.2 – Contaminant Mass Balance. Likewise, the contamination, decontamination, and sampling protocols used in mass balance determinations were unchanged. Spikes of contaminant solution directly onto sorptive media were used as controls. Blank media were also analysed as described previously.

The extents of contamination and decontamination were determined through INAA, with internal inorganic controls and standards for Br and As (SCP Science; Inorganic Ventures). However, coupons themselves were not analysed at this stage because of the possibility of interfering atoms (e.g. Br in so-called 'bromine-free' substrate).

3.2.2.4 – Process Optimisation

To determine the possible trade-off between decontamination efficiency and power input, the flow régime of FK-5-1-12 liquid in the test vials was varied from quiescent conditions. HDPE coupons were contaminated with TPhAs solution and subjected to decontamination with parallel sorption using cellulose and GAC. 15-mL vials containing FK-5-1-12, a contaminated coupon, and sorptive media were placed into the grooves of a platform shaker. The rotational velocity of the shaker was set to 100, 200, or 300 rpm, to reproduce laminar to transitional flow conditions. Other experimental parameters were unchanged. Coupons in all vials were analysed for As abundance after 10 min of immersion/agitation time.

3.3 – Suitability of FK-5-1-12

The suitability of FK-5-1-12 as part of a field-deployable decontamination system refers to its ability to satisfy requirements other than simply the removal or transformation of contaminants. Among these supporting requirements, listed in the literature review, are compatibility with the materials found in sensitive equipment and the ability to operate in diverse environmental conditions. To answer these problems required complementary experimental methods, which are presented here.

3.3.1 – Methods

The aim of operational trials on full-scale sensitive equipment was to evaluate the suitability of the model decontamination process towards the equipment itself, rather than the effectiveness in removing or transforming contaminant. Eight commercially available laptop computers and one set of monocular night-vision goggles (MNVG), representative of field-deployed equipment, were obtained for these trials. A trial plan with all equipment is presented in Table 7, with details in the following sections.

Table 7: Operational Trial Plan

Trials	Item	Make/Model	Functions Tested	Methods
1	Laptop #1	Compaq Presario C762NR	CPU, RAM, cache, HDD, CD-R	Windows Reliability and Performance Monitor
2	Laptop #2	Toshiba Tecra S10	CPU, RAM, HDD, LCD	Operations: BurnInTest
3	Laptop #1	Compaq Presario C762NR	CPU, RAM, HDD	Operations: BurnInTest Reliability: smartmontools
4	Laptop #2	Toshiba Tecra S10	CPU, RAM, HDD	Operations: BurnInTest Reliability: smartmontools
5, 7	Laptop #3	Toshiba Tecra S11	CPU, RAM, HDD	Operations: BurnInTest Reliability: smartmontools
6, 8	Laptop #4	Toshiba Portégé M780	CPU, RAM, HDD	Operations: BurnInTest Reliability: smartmontools
9-10	Laptop #5	Toshiba Portégé M780	CPU, RAM, HDD	Operations: BurnInTest Reliability: smartmontools
11-12	Laptop #6	Toshiba Portégé M780	CPU, RAM, HDD	Operations: BurnInTest Reliability: smartmontools
13-14	Laptop #7	Toshiba Portégé M780	CPU, RAM, HDD	Operations: BurnInTest Reliability: smartmontools
15-16	Laptop #8	Toshiba Portégé M780	CPU, RAM, HDD	Operations: BurnInTest Reliability: smartmontools
17	MNVG	General Starlight GS-14	Phosphor coatings, IR flashlight	CCD spectrometry

3.3.1.1 – Laptop Trial 1

A laptop computer (Compaq Presario C762NR, 'laptop #1') was selected to elicit the possible failure modes that could occur in operational decontamination conditions. The base of the laptop was enclosed in a 4-L polypropylene reactor which was instrumented with a digital thermometer (Fisher Scientific) and a digital multimeter (Fluke 8846), shown in Figure 9.

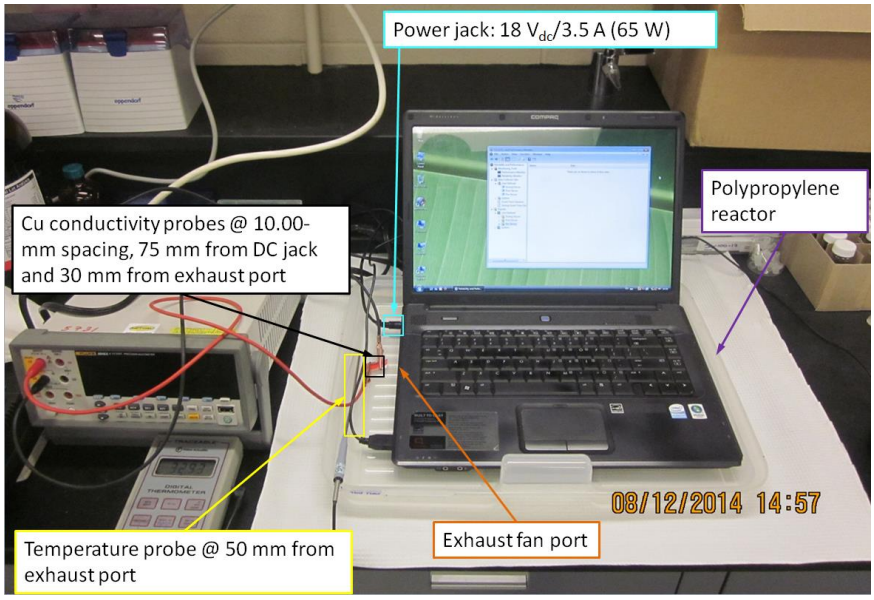

Figure 9: COTS Laptop Operational Trial Apparatus

System-wide performance data of the cache, memory, processors, and hard-drive were collected using pre-installed Microsoft Vista Reliability and Performance Monitor software. The Quality of Service (QoS) was measured as the time taken to burn 480 MB of data from the HDD to a blank recordable compact disc (CD-R). As a pre-decontamination test, the laptop was instructed to perform this CD recording task. Temperature within the reactor was logged manually.

To determine the effects of immersion decontamination, a mass of approximately 1728 g of FK-5-1-12 was poured into the reactor. The CD recording task was repeated with a blank CD-R to simulate operation during a decontamination procedure—an event designed to provoke possible failure modes. Conductivity within the reactor was also logged manually.

The system was left open for 18 hours for the FK-5-1-12 to evaporate. The task was again repeated with a blank CD-R as a post-decontamination test.

3.3.1.2 – Laptop Trial 2

A stress-test software package (BurnInTest v.7.1, PassMark Software) was used for commonality and comparison of results, independent of any

particular operating system. It was installed on a second laptop (Toshiba Tecra S10, 'laptop #2').

The processor, memory, and hard-disk drive of the laptop were subjected to 20-min stress tests using BurnInTest software. That is, each sub-system was instructed to operate at 50 % of its maximum throughput for 20 min, during which time its performance was logged automatically. The sub-systems were stress-tested in three phases: before decontamination, during decontamination (immersed in 1818 g of FK-5-1-12), and after decontamination, as in trial 1. Temperature and conductivity within the reactor were logged manually.

The laptop's video display (15.4-inch (391-mm) WSXGA+ Thin Film Transistor, High Brightness) was also tested for compatibility with FK-5-1-12 during this trial. It was immersed in a 770-g charge of FK-5-1-12 for 20 min and photographed. The laptop was then powered-down and the FK-5-1-12 allowed to evaporate. After 18 hours, it was powered-up and photographed again.

3.3.1.3 – Laptop Trials 3 and 4

The aim of laptop trials 3 and 4 was to evaluate the effects of 'second-pass' treatment, i.e. a second immersion in FK-5-1-12, on the operation of energised and functioning laptops. Laptops #1 and 2 were subjected to the same stress test using BurnInTest software in pre-, during-, and post-decontamination phases. For laptop #1, HDD reliability data were only collected post-decontamination using smartmontools v. 6.3 software (release 3976, authors B Allen and C Franke). For laptop #2, pre-, during-, and post-decontamination HDD reliability data were collected in trial 4 using smartmontools software. In the decontamination phase of trial 3, laptop #1 was immersed in a mass of 3561 g of FK-5-1-12. In the decontamination phase of trial 4, laptop #2 was immersed in a mass of 3250 g of FK-5-1-12.

3.3.1.4 – Laptop Trials 5 to 16

Six additional laptop computers were obtained at different stages of their life-cycle. All were from the same manufacturer (Toshiba), five were of the same model (Portégé M780), and four had identical specifications, including identical built-in operating systems (BIOS). Their hard-drive reliability metrics 'as obtained' were read from the SMART data set using smartmontools software. These laptops were then subjected to a common 20-min stress-test at pre-, during-, and post-decontamination phases.

For all test phases, performance metrics were recorded by BurnInTest software, and reliability metrics by smartmontools software. For the pre- and post-decontamination phases, no fluid was added to the reactor. For the during-decontamination phase of each trial, a charge of FK-5-1-12 was added to the reactor with a mean mass of 3512 g (standard deviation 743 g).

After the FK-5-1-12 had evaporated from the reactor (typically 18 hours), the inside of the reactor was swiped with a Kimwipe. Mass gains of the swipes were recorded. Hydrocarbon-soluble compounds in the swipes were extracted with 4.0 (± 0.5) mL of hexane isomers at ambient pressure. Samples of hexane and unknown compounds were drawn after 1 hour of extraction and injected into a gas chromatograph with flame ionisation detection (GC–FID). The fractions of carbon chain lengths in the samples were measured using a protocol for petroleum hydrocarbon determinations, with hexane responses subtracted.[167]

3.3.1.5 – Monocular Night-Vision Goggle Trial

A commercially available variant of the AN/PVS-14 monocular night vision device (GS-14, General Starlight) was obtained for a trial of immersion decontamination compatibility with electro-optical equipment. The device was used as delivered and according to the manufacturer's directions.

An optical table was set up with an incoherent arc lamp (Oriel/Newport), horizontal and vertical gratings, and a 6.4% transmission filter to simulate low visible-light conditions in the ambient. A focusing lens was used at a distance of 145 (± 1) mm from the MNVG ocular lens to simulate eye relief. All spectral data were captured via a charge-coupled device (CCD) spectrometer (BRC 111A-USB-VIS/NIR, Edmund Optics) and logged on a laptop computer (BWSpec 3.23 software, BWTek). The apparatus is shown, with the components from right to left, in Figure 10.

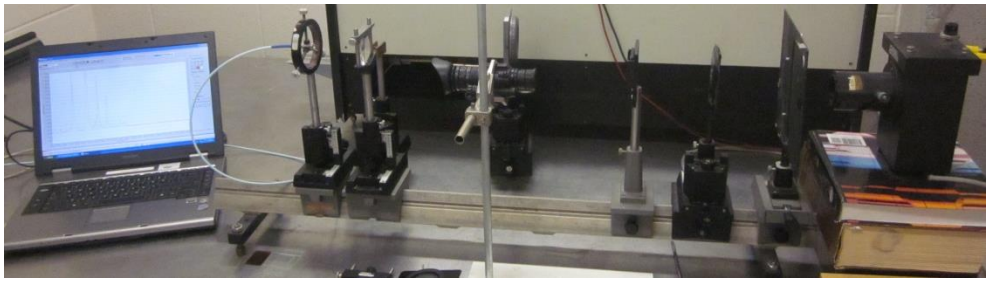

Figure 10: Optical Table Apparatus

With the room darkened, the transmittance of the arc lamp alone was recorded by the CCD spectrometer. The MNVG was energised and function-tested in the modes *ON*, *IR flashlight*, and *IR flashlight+*. The MNVG baseline, pre-decontamination transmittance spectrum in all modes was recorded.

The energised MNVG was subjected to a decontamination process. It was submerged in approximately 2670 g of as-delivered FK-5-1-12 for 20 min at a temperature of 19.3 (± 0.3) °C and relative humidity of 48.0 (± 0.5) % to simulate one pass of decontamination treatment in the field.

After 20 min had elapsed, the MNVG was withdrawn from the FK-5-1-12, drained, and function-tested. It was immediately returned to the optical table to record its post-decontamination transmittance spectrum.

3.3.1.6 – Fluid Recovery and Recycling

The rate of vaporisation of as-delivered FK-5-1-12 in a closed vessel, i.e. a reactor for field-expedient decontamination, was measured experimentally. 1.00 (± 0.05) kg of liquid FK-5-1-12 was weighed into a flask. The flask was stoppered, fitted with a digital thermometer, and its barb connected to an in-line float rotameter (Cole-Parmer) by flexible tubing. Starting at ambient laboratory temperature (typically 22 °C) and barometric pressure (1.00 bar), the FK-5-1-12 was gradually heated such that its rate of temperature increase was 1.2 $K \cdot min^{-1}$ (0.02 $K \cdot s^{-1}$). This rate was intended to approximate the maximum rate imposed by the boundary conditions of a NATO A1 climate condition, as determined through simulation. Given this rate of heat transferred into the system, the flow rate of saturated FK-5-1-12 vapour exiting the flask through the tubing was measured by the rotameter and readings were corrected for the density of the vapour.

The product of the vapour mass flow rate and the specific enthalpy of vaporisation gave a cooling load in units of power, i.e. the energy per unit time

required to condense the flow of FK-5-1-12 vapour for its re-use as a liquid. Tables and empirical equations of temperature-dependent FK-5-1-12 fluid and vapour properties were used in calculations. These are available from the manufacturer.[123]

4. Results and Discussion

4.1 – Properties of FK-5-1-12

The physical and chemical properties of any proposed decontaminant will govern (and perhaps limit) its fitness for the field-expedient decontamination of sensitive equipment. As discussed in the requirements for liquid decontaminants, properties such as high electrical conductivity, reactivity with contaminants and substrate materials, and volatility are all generally detrimental to this end. Some electrical and magnetic properties of FK-5-1-12, not previously published, were determined experimentally. The behaviour of FK-5-1-12 in heat transfer and chemical reaction was first estimated through numerical modelling and, to a limited extent, verified empirically. Finally, its tendency to deplete critical fluorinated lubricants from hard-disk drive coupons was tested through surface analytical methods.

4.1.1 – Hygroscopicity and Purity

The presence of free water in FK-5-1-12 could be a limiting consideration for its use in sensitive equipment decontamination, with risks of substrate material hydrolysis, dissolution of ionic species, and electrical conductivity. The manufacturer of FK-5-1-12 (3M Company) reports the extent of solubility of water in the fluid as 2×10^{-5} g·g^{-1}.[120] It was desired to take into account the possibility of hygroscopicity during transportation and storage. If impurities were found and attributable to storage and handling, then purification steps could be required to ensure that the fluid would perform in accordance with its published specifications. Determinations of possible hygroscopicity were made through potentiometric titration. All Fischer potentiometric titration determinations (n = 12) of FK-5-1-12 did not detect the presence of water above 5×10^{-4} g·g^{-1}, the limit of detection for the procedure. Unlike short-chain aliphatic ketones and hexafluoroacetone,[168] FK-5-1-12 did not appear to be hygroscopic. These results agree with previously published findings of its degradation to perfluoropropanoic acid within hours of contact with water.[128] If it were significantly hygroscopic, it would not be stable, but could continue to absorb moisture and degrade into acid. It would also exhibit behaviour, such as electrical conductivity, more typical of a Brønsted–Lowry acid than of a high dielectric strength fluid.

When testing the purity of the liquid, solids were collected by filtration. These solids were analyzed by INAA and EDAX. INAA, without quantitation, determined the presence of the elements Al, K, and F. Quantitation of solid

samples (n = 3) by EDAX (integration error ≤ 1.5 %) revealed the elemental abundances shown in Table 8.

Table 8: Elemental Abundances in Filtered Solids

Abundances (atom %)	C	F	K	O (Difference)
Mean (Standard Deviation)	14.73 (1.33)	30.59 (1.16)	6.61 (1.55)	48.07 (1.33)

Since Al was present in quantities > 10^{-8} mass fraction (i.e. above the limit of detection of Al by INAA) but ≪ 1 % atom fraction (not detected by EDAX), AlF_3 itself cannot be a major mineral constituent of the solids. Scanning electron micrographs of the solids are shown in Figure 11. The relatively high abundances of F and C with respect to K suggest that mineral KF is not the prime constituent, but that there is a significant organic fraction. Based on these elemental proportions, the solid structure in the micrograph is likely that of a fluorocarbon polymer.

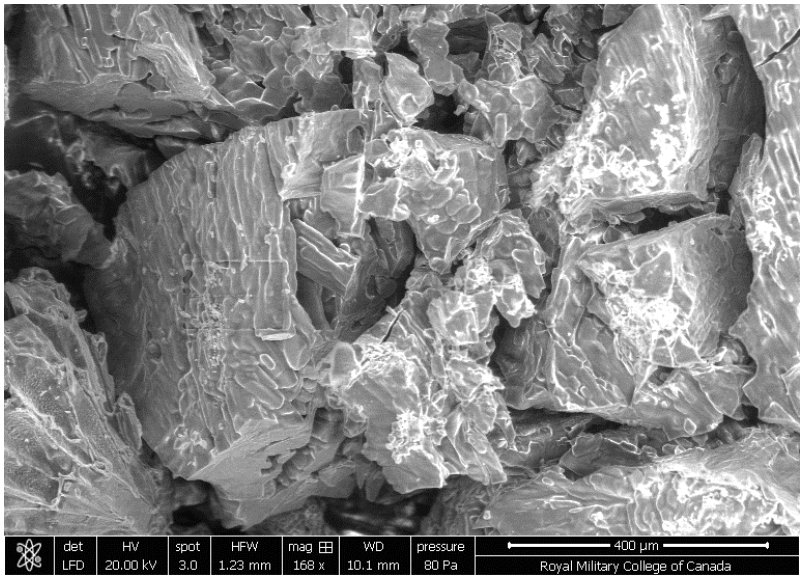

Figure 11: Scanning Electron Micrograph of Filtered Solid (400-µm Scale)

Review of the patent literature on FK-5-1-12 indicates that the presence of KF may be attributable to starting materials, which include anhydrous KF.[145] The mean C:F ratio in Table 8, after subtracting KF, is 1:1.6 (± 0.2). If KF is not subtracted stoichiometrically, the ratio of means is 1:2.1 (± 0.2). In either case, the ratio is approximately that of a polymer of hexafluoroprop-1-ene (C_3F_6), which is another starting material for FK-5-1-12. The overall oxygen

abundance is too large to be accounted for by oxygen-bearing starting materials and purification aids, including pentafluoropropanoyl fluoride, diglyme, acetone, acetic acid, and permanganate.[145] The oxygen abundance, as determined by difference in the EDAX procedure, may be spurious.

The presence of impurities in FK-5-1-12 of the order of 0.1 % by mass, multiplied by the quantities handled in the course of immersion decontamination, could result in several grams of impurities per kilogram of FK-5-1-12 used in the field. The presence of impurities in such quantities did not lead to a detectable decrease in resistivity, which was always measured to be $\gg 1$ GΩ·cm^{-1}. However, it would be prudent to filter FK-5-1-12 mechanically to minimise the possibility of depositing solid polymers within sensitive equipment. Additional trials could determine whether polymerisation is occurring in FK-5-1-12 and conclusions could be drawn as to its long-term stability in storage.

4.1.2 – Electrical and Magnetic Properties

The electrical and magnetic properties of a decontaminant have intrinsic importance as physical quantities. Knowing these quantities leads to more accurate predictions of interactions with photons and with other chemical species. Still, there are deeper motivations to study such properties in sensitive equipment decontamination. The foremost is that dielectric properties are crucial in modelling the attraction and resuspension of contaminant particles among surfaces and streams of fluids (air, water, or decontaminant).[169] Another motivation is that unwanted changes in electrical or magnetic behaviour could lead to diminished performance and reliability of sensitive equipment assemblies, including biasing, electrochemical corrosion, and loss of data in magnetic hard-disk drives, among many possible examples. Measuring the spectral properties (absorption, transmission, and refraction), relative permeability, and electrical resistance of FK-5-1-12 would allow improved predictions of its effects on the normal operations of such sensitive assemblies.

4.1.2.1 – Optical and Spectral Properties

4.1.2.1.1 – Index of Refraction

The real (n) and imaginary (jk) parts of the complex index of refraction $\tilde{n}$ of liquid-phase FK-5-1-12 were determined at 25 °C and 30 °C (± 0.5 °C) by methods suitable for the analysis of liquid films by variable-angle spectroscopic ellipsometry, including the rough-surface and prism minimum deviation methods.[151] The magnitude of uncertainty in the value of n was of

the order of 10^{-5}. Measurements from VASE were fitted to Cauchy and Sellmeier polynomial series (Equation 5 and Equation 6) and plotted across the [191, 1699] nm wavelength domain, corresponding to the far-UV, visible, and near-IR regions. The modelled real index of refraction as a function of wavelength, by analytical method, is presented in Figure 12.

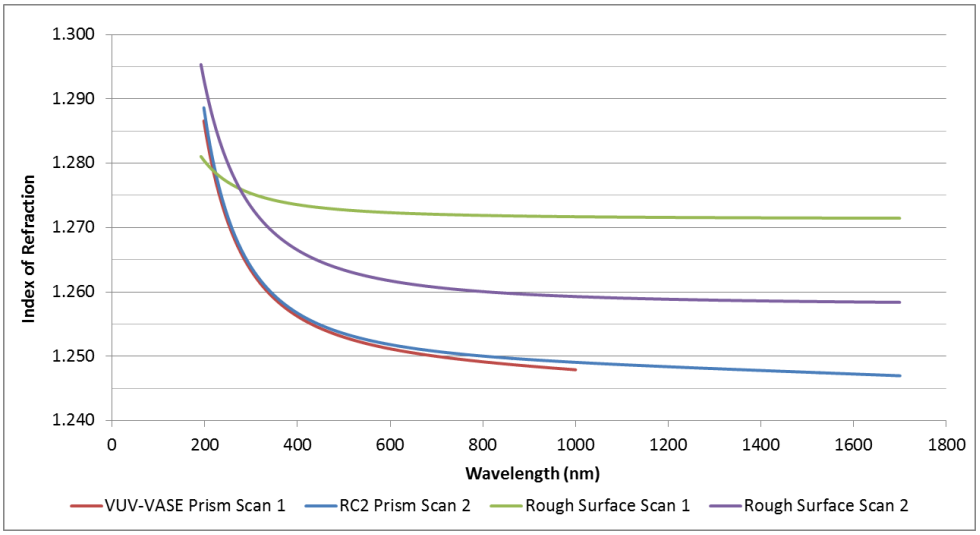

Figure 12: Index of Refraction of FK-5-1-12 in Near-Ultraviolet to Near-Infrared Regions

Corresponding data are summarised in Table 9, which shows the mean value of n calculated across the scanned spectrum, and in the visible region only, arranged by method, parameters, and ambient temperature.

Table 9: Real Index of Refraction of FK-5-1-12 by Multiple Methods

Method (Parameters)	Temperature (°C) (± 0.5 °C)	n (mean) (± 10^{-5})	n (mean, visible) (± 10^{-5})
Rough Surface (Scan 1), Cauchy Fit	25	1.273	1.273
Rough Surface (Scan 2), Cauchy Fit	25	1.263	1.263
Prism Minimum Deviation, RC2 Ellipsometer, Sellmeier Fit	25	1.252	1.253
Prism Minimum Deviation, VUV-VASE Ellipsometer, Sellmeier Fit	30	1.254	1.251

The prism minimum deviation method showed better reproducibility than the rough-surface method for FK-5-1-12. This was most likely because of the relatively low viscosity of FK-5-1-12 and its rapid evaporation when spread as a thin film, which would have led to deviations in film thickness during sampling to a greater extent than for other liquids. The real index of refraction of FK-5-1-12 in the visible region at ambient temperatures is closer to that of its perfluorocarbon analogue, C_6F_{14} (1.252),[124] than to its hydrogen-saturated ketone analogue, 2-methyl-pentan-3-one (1.396),[170] despite FK-5-1-12 having a 'polar' ketone carbonyl group. The index of refraction of a pure substance is a macroscopic measurement of the tendency of its molecules to disperse photons.[114] This is evidence that the FK-5-1-12 intermolecular interaction is minimally dispersive, in spite of its carbonyl group, but it is far from a complete representation.

The absorption (jk) part of the complex index of refraction was calculated through VASE measurements to be 2.8×10^{-6} for wavelengths shorter than 242 nm. Maximum absorption of FK-5-1-12 in the liquid phase was recorded in the UV region between 240 nm and 360 nm, which is consistent with previous determinations of its absorption as a vapour.[132] Other absorption modes were detected at wavelengths of 1890 nm (5291 cm^{-1}) and 2090 nm (4785 cm^{-1}). The former is likely a near-infrared harmonic ($3\bar{\nu}$) of the ketone carbonyl stretch (approximately 1760 cm^{-1}), and the latter a harmonic ($2\bar{\nu}$) from ambient carbon dioxide (approximately 2390 cm^{-1}). A comparison of the complex index of refraction and a Sellmeier polynomial series representation is shown in Figure 13. In the Sellmeier representation, the index of refraction is shown monotonically decreasing with wavelength. This representation evidently does not model behaviour outside the visible region. The imaginary (absorption) part shows a discontinuity rather than a maximum between 240 nm and 360 nm; thus, $k \gg 10^{-5}$.

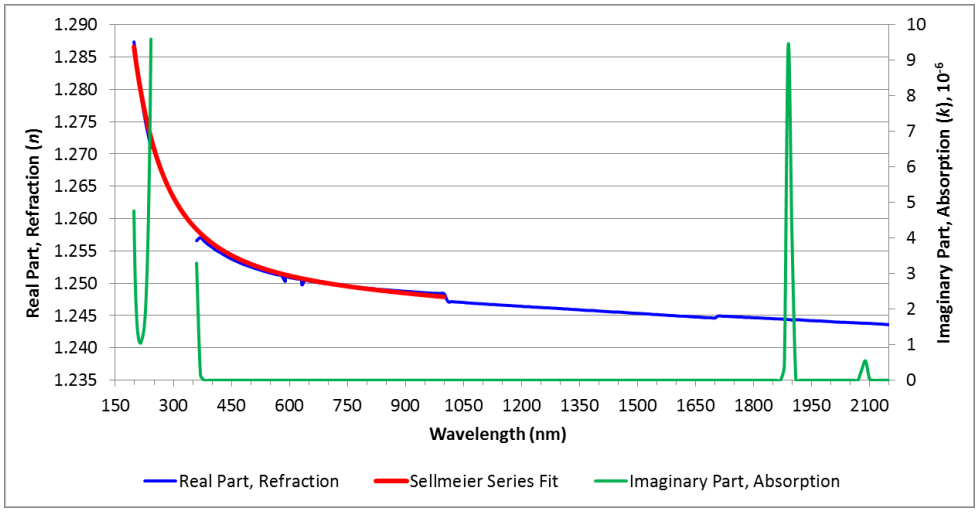

Figure 13: FK-5-1-12 Complex Index of Refraction and Sellmeier Fit v. Wavelength, 30 °C

The correspondence between photon absorption and electron oscillation or transition in a molecule spans frequencies up to the ultraviolet region, above which electrons do not merely oscillate or move to higher orbitals, but begin to become separated from the molecule through ionisation. The ultraviolet region, having wide spectral bandwidth and high-energy photons, is typically a major contributor to dispersion, but not necessarily the most significant—the absorption of water in the infrared and microwave regions being a familiar exception.[171] Increasingly accurate approximations of the interactions of a molecule are attainable by analysing dielectric data across the electromagnetic spectrum, particularly the infrared.[171]

By performing linear regression on the Sellmeier fit of the prism minimum deviation data in the visible region only, it was determined that FK-5-1-12 at 30 °C has a UV oscillator strength of 0.5554 at a relaxation frequency of 2.369×10^{16} rad·s^{-1} ($R^2 = 0.9999$). These values more closely resemble those of PTFE (approximately 0.841 and 2.647×10^{16} rad·s^{-1}, respectively) than of non-fluorinated liquids or polymers whose oscillator strengths and frequencies were determined by similar methods.[172] This result provides some corroboration, to a first approximation, of the 'repulsive' effect of FK-5-1-12 between liquid organic films and polymers in which dispersive interactions predominate. Hence, by introducing FK-5-1-12 between a contaminant and a polymer surface, it would be expected to be less attracted to both phases while providing steric bulk, and 'repel' the contaminant from the surface, just as a PTFE surface resists contamination by dispersive organic substances (oils and the like). FK-5-1-12 could act, at a minimum, as a

"release agent".[173] However, for a more thorough accounting of the long-range interactions of FK-5-1-12, it would be prudent to determine the magnitude of its oscillator strengths and frequencies in the infrared region, to assess the relative contributions of any such modes, and to determine its zero-frequency dielectric permittivity.[154]

4.1.2.1.2 – Near-Infrared Absorption Spectra

Absorption modes for FK-5-1-12 were detected in the near-infrared region using VASE. Tentative peak assignments, based upon integer harmonics from the mid-infrared region, are shown in Table 10.

Table 10: FK-5-1-12 Near-Infrared Spectral Peaks

Wavelength (nm) (± 0.5)	Wavenumber (cm^{-1})	Tentative Assignment
1019.0	9813	O–H stretch $3\bar{\nu}$
1384.0	7225	Fluorinated ketone C=O stretch $4\bar{\nu}$
1426.5	7010	*CO_2 C=O stretch $3\bar{\nu}$ (ambient air)*

A C=O stretch harmonic characteristic of carbon dioxide is readily explained by the presence of CO_2 in ambient air. An O–H stretch alone could signify the presence of water in the system or a hydroxyl functional group within FK-5-1-12, i.e. a fraction of the FK-5-1-12 having reacted to form a perfluorocarboxylic acid, which is a strong possibility, as discussed previously. However, given the absence of a C–O stretch harmonic, a complete set of carboxylic acid assignments is not possible with these data alone.

4.1.2.1.3 – Mid-Infrared Absorption Spectrum

The mid-IR spectrum of filtered FK-5-1-12, as determined by FTIR spectroscopy, exhibited peaks shown in Table 11. Tentative assignments are based upon the empirical IR and Raman spectra of both gas- and condensed-phase hexafluoroacetone,[174] and on the IR spectra of perfluorocarbons.[175]

Table 11: FK-5-1-12 Mid-Infrared Spectral Peaks

Wavenumber (cm^{-1})	Tentative Assignment
2360	*CO_2 C=O stretch (ambient air)*
1783	Fluorinated ketone C=O stretch
1360 – 1023	Fluoroalkyl C–F stretches
984 – 813	C–C stretches
759	*Methylene C–H_2 vibration (impurity)*
719	Trifluoromethyl C–F (dipole transition)
677	Trifluoromethyl C–F bend
620	Trifluoromethyl C–F bend
581	Trifluoromethyl C–F bend
525	Trifluoromethyl C–F bend

The wavelengths tentatively assigned to the carbonyl and CO_2 C=O stretches in the mid-IR vary from the near-IR harmonics tentatively assigned in Table 10 by 18 nm and 14 nm, respectively. This variation could be attributed to optical phenomena, such as different path lengths. There was no wide hydroxyl-like absorption band, which would have indicated the presence of water or carboxylic acid. However, the strengths of the fundamental mid-IR oscillations were not determined with the FTIR spectroscopy method. To do so would require control and measurement of parameters such as sample mass and photon path length for a Beer–Lambert law calculation. As previously discussed, these mid-IR oscillators would merit further quantitative investigation to form a more complete representation of the electronic dipole behaviour of FK-5-1-12.

4.1.2.2 – Magnetic Properties

The relative permeability of FK-5-1-12 was determined via its volume magnetic susceptibility using a magnetic susceptibility balance. From two determinations, the volume susceptibility of FK-5-1-12 was calculated to be $-3.82\ (\pm 0.09) \times 10^{-7}$ (Gaussian cgs base units). The relative permeability of FK-5-1-12 was, in turn, calculated to be 0.99 ± 0.02, which is consistent with the prediction of slight diamagnetism for organic liquids.[155] This small deviation from vacuum permeability should not affect the remanence of a ferromagnetic material within a hard-disk drive and the integrity of data encoded in its magnetic domains. Better precision in the value, given its small magnitude, could be obtained by subjecting the fluid to a larger applied magnetic field.

4.1.2.3 – Bulk Electrical Resistance

An IEC 60320-1 C13 appliance cable was immersed in FK-5-1-12 with an applied nominal rms potential of 120 V_{AC} and the leakage current was measured using a high-resistance electrometer to assess its electrical safety. The leakage current was measured to be 4.48×10^{-14} A (standard deviation 2×10^{-16} A), giving an instantaneous resistance value of 2.698×10^{18} Ω (standard deviation 5×10^{11} Ω). Actual rms voltage magnitude was 120.92 V_{AC} (standard deviation 0.42 V_{AC}), frequency 59.97 ± 0.01 Hz, and total harmonic distortion 3.3 % over a 5-min averaging time as determined by a power-quality meter. The magnitude of this leakage current with 120-V appliances is not a practical safety concern for appliances immersed in FK-5-1-12, even when they are operating.

4.1.3 – Thermodynamic Properties

4.1.3.1 – Heat-Transfer Simulation Results

Heat-transfer simulations were undertaken to evaluate the suitability of using FK-5-1-12 in a minimally insulated HDPE reactor at an ambient temperature close to its boiling point, as would be encountered in some operating environments. The results of a transient heat-transfer simulation by the Euler Method are shown in Figure 14.

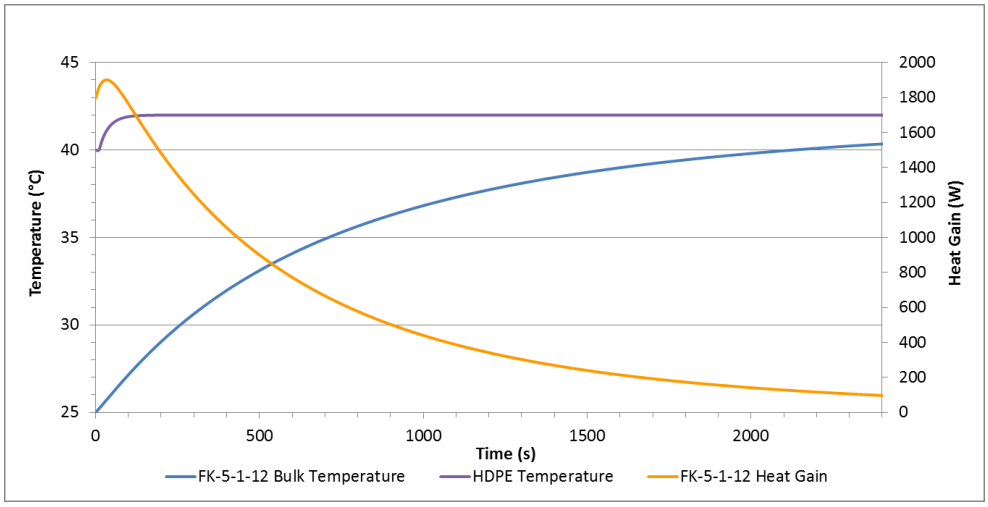

Figure 14: FK-5-1-12 Heat Transfer v. Time at 49°C in Insulated Reactor

As modelled, the insulation layer was effective in delaying heat transfer from the ambient. The solid HDPE layer, shown in Figure 14, offered the least thermal resistance, reaching a temperature > 41.9 °C after 100 s, which is explained by its smaller mass and thickness and relatively higher thermal conductivity than the other layers. The rate of temperature increase in the FK-5-1-12, initially at 25 °C and modelled as a single volume, began at 1.26 °C·min^{-1}.

A real system would likely have areas of reduced effective insulation, creating paths of lowered thermal resistance within the insulation layer and less-optimistic results as a consequence. The results in layers other than the insulation were found to be most sensitive to initial temperatures. With the rate of heat gain shown in Figure 14 and the initial temperature of the interior of the insulation at 42 °C, the bulk of the FK-5-1-12 would attain a temperature of 40 °C after 2130 s (35:30 min). In the limiting case of the initial temperature at the interior of the insulation equal to the ambient (49 °C), then the FK-5-1-12 would attain 40 °C after only 700 s (10:10 min). Indeed, neglecting insulation entirely, the model predicts that an HDPE container of FK-5-1-12 initially at 25 °C would attain 40 °C within one hour of exposure to any temperature greater than 40 °C in a NATO A1 climate. At temperatures greater than 40 °C, FK-5-1-12 vapour pressure would be greater than 0.746 atm, with increased volatility at sea level. At 2000 m altitude, FK-5-1-12 vapour pressure would be within 0.05 atm of barometric pressure. The likelihood of losing FK-5-1-12 to vaporisation in either environmental condition would increase.

If such sensible heat gain were to be avoided, cooling would be required. The magnitude of heat transfer modelled in the first case would impose a peak cooling load of 1.9 kW, or a specific cooling load of 24 $W \cdot kg^{-1}$ during the first 60 s. For the limiting case of no effective insulation, the peak cooling load would be 80 % higher, or 43 $W \cdot kg^{-1}$. Any peak cooling load could be lowered by ensuring persistent cold storage and more effective insulation of FK-5-1-12 were it to be used in ambient temperatures close to its boiling point. On account of its thermal conductivity, specific heat capacity, and viscosity, FK-5-1-12 would be amenable to refrigeration.

Because these calculations were numerical approximations, use of environmental chamber experiments would be prudent in reaching an optimal design of a deployable FK-5-1-12 refrigeration system. The rate of FK-5-1-12 evaporation from a reactor as a consequence of such boundary conditions was tested experimentally, but the modelled rate of temperature increase was reproduced by heating the FK-5-1-12 from a heat source, instead of imposing a 49 °C ambient temperature.

4.1.4 – Chemical Reactivity

4.1.4.1 – Structure

Calculations of the ground-state equilibrium geometry of the FK-5-1-12 molecule were made to estimate physical and chemical properties. Using Spartan '08 software[176] implementing B3LYP density functional theory and a 6-31G* basis set, the molecular geometries of FK-5-1-12 and some of its analogues were solved. Figure 5 is an electrostatic potential map of FK-5-1-12 showing coloured potential contours at an interval of −83.68 $kJ \cdot mol^{-1}$ and the orientation of the molecular dipole moment vector.

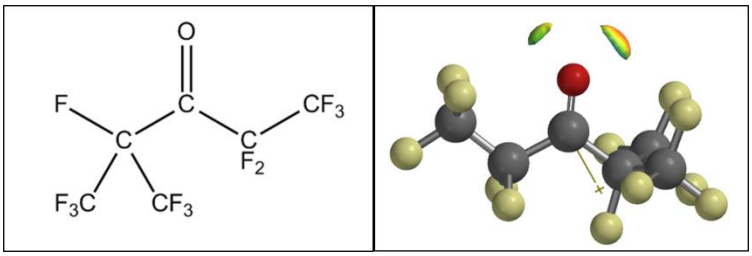

Figure 15: Electrostatic Potential Map of FK-5-1-12 by B3LYP DFT

The predicted magnitude of the FK-5-1-12 molecular electric dipole moment by this method was 0.50 D. This dipole moment is smaller than the one

predicted for non-fluorinated 2-methyl-pentan-3-one (2.52 D) by the same method, which is, in turn, smaller than the experimental value (3.11 D) for that molecule.[170] The polarity of FK-5-1-12 is less than would be expected from its carbonyl group alone, likely because of the electron-withdrawing effect of neighbouring fluorocarbon groups. The relatively small electrostatic potential about the carbonyl group and the orientation of the positive pole of the molecular dipole moment towards the electronegative HFC-227ea moiety support this conclusion.

A diagram of the lowest unoccupied molecular orbital (LUMO) of FK-5-1-12 from two perspectives is shown in Figure 16.

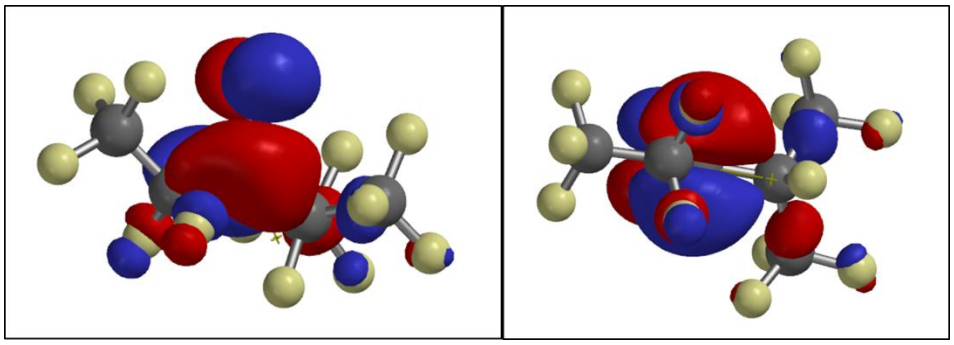

Figure 16: LUMO of FK-5-1-12 by B3LYP DFT

The LUMO is π-antibonding with respect to the carbonyl, with σ-antibonding contributions adjacent to the carbonyl carbon. The carbonyl group and its adjacent carbon–carbon bonds are the most accessible to electrons and hence are more likely to participate in reactions. Electrons occupying antibonding orbitals in turn tend to lower the stability of bonds by destructive interference, to the extent that a bond may be broken. Together, the computed frontier maps and dipole moment vectors generally support the mechanism of acyl substitution through attack on the positive charge density at the backside of the carbonyl carbon. These results are consistent with the photolytic/thermal homolytic and heterolytic decomposition reaction mechanisms observed in FK-5-1-12 to date.[128, 132, 138]

4.1.4.2 – Reactivity Determinations

On account of the magnitude and orientation of its molecular electric dipole (Figure 15), FK-5-1-12 has positive charge density about its carbonyl carbon and most likely reacts via a nucleophilic acyl substitution mechanism (as illustrated in Figure 6). Its reactions with nucleophiles such as water,

methanol, and ammonia have been shown by other researchers to yield a perfluorinated carboxylic acid, a fluorinated methyl ester,[128] and a perfluorinated 1° amide,[177] respectively. Other carboxylic acid derivatives—including 2° amide, thioester, and acid anhydride—were hypothesised to be formed if FK-5-1-12 were to react with a 1° amine, thiol, and carboxylic acid. Although 1° and 2° alcohols and amines would also be expected to react by the acyl substitution mechanism, 3° alcohols and amines would likely be too sterically hindered to do so. FK-5-1-12 is not symmetric about the carbonyl carbon, with a pentafluoroethyl moiety and a heptafluoroisopropyl moiety, and either of these moieities could serve as a 'good' electronegative leaving group. However, previous experiments have shown that fluorinated esters with the heptafluoroisopropyl moiety are unstable in the presence of fluoride ion above −78 °C.[178] Since the solid residual fraction of 'as-delivered' FK-5-1-12 was shown by EDAX to contain potassium at 5 % by atomic mass, likely from KF starting material, it would likely also contain residual fluoride as the counter-ion to maintain overall neutrality. It is more likely, then, that the linear pentafluoropropanoate ester would be stable enough to be detected at room temperature. However, the concentration of F^- itself, either in liquid-phase FK-5-1-12 or its solid residue, was not determined to confirm this identity.

Experiments were undertaken to determine if small quantities of nucleophiles (having alcohol, amine, and thiol functions), present as contaminants, would react with FK-5-1-12. A high likelihood of reaction could limit the safe application of FK-5-1-12 on a sensitive surface. For instance, if heat, corrosive species, particulates, or gases were evolved rapidly, these products could all induce forms of wear on sensitive substrate materials. Compounds with nucleophilic functions are in common industrial use and are found among the categories of industrial materials of concern to the CAF. Moreover, nucleophilic functions and their derivatives are common among the classical CW agents, with over 100 examples.[14] Typically, these are 3° amines or derivatives (amides or imides), as in Tabun (GA), the V-series, the Novichok agents, QL agent (*O*-ethyl 2-diisopropylaminoethyl methylphosphonite), the entire nitrogen mustard family, and many precursors and degradation products. Thioethers are found in the entire sulfur mustard family, its precursors, and degradation products. Alcohols and 1° thiols are also common precursors and products, and any of these may be assumed to be present in a suspected CW contamination situation.

4.1.4.2.1 – Typical Behaviour of FK with Nucleophiles

In most cases, FK-5-1-12 and the target reagent were apparently immiscible, forming two distinct phases. Yet, FK-5-1-12 was able to react with some nucleophiles at the interfacial boundary layer even in such cases. While FK-5-1-12 was observed to be insoluble in either $CHCl_3$ or DMSO below 25 °C, many of its reaction products with nucleophiles were observed to be more readily soluble in DMSO than in $CHCl_3$. Thus, DMSO-d6 was the preferred deuterated solvent for ^1H NMR spectroscopy.

4.1.4.2.2 – Reactivity of FK with Hydroxyl Groups

According to a previous study, FK-5-1-12 reacts with methanol to yield methyl pentafluoropropanoate by a mechanism such as that shown in Figure 17.[128] Hydroxyl nucleophiles may be alcohols (if protonated) or alkoxides (if deprotonated), depending upon the pH. It was hypothesised that 1° and 2° alcohols would follow the same mechanism, but that a 3° alcohol would not because of steric hindrance.

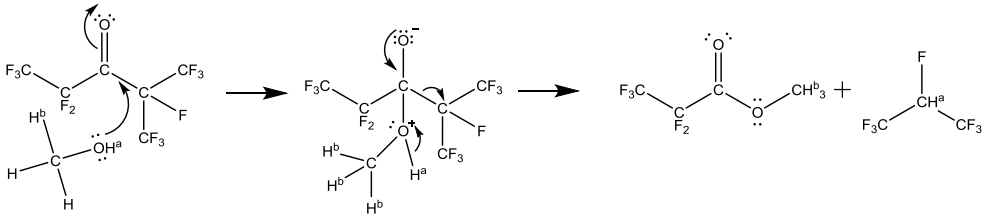

Figure 17: Attack of FK-5-1-12 by Methanol

Since the starting materials were observed to be mutually immiscible, two different flow conditions were studied: quiescent conditions dominated by diffusion, and turbulent conditions. In the quiescent case, refraction at the interfacial boundary was observed to diminish with time, although the index of refraction of neither phase was quantified. The less-dense, non-FK-5-1-12 phase was sampled with time in 100-µL aliquots. These were pipetted directly onto KBr discs for FTIR spectroscopy and pipetted into vials with 600 µL of DMSO-d6 for ^1H NMR spectroscopy.

A quiescent FK-5-1-12–methanol system was sampled after 8 days of contact time, at which point it resembled a single liquid phase. The FTIR spectrum of this phase showed prominent C–H (2952 cm^{-1}, 2839 cm^{-1}) and fluorinated ketone C=O (1782 cm^{-1}) stretches, as would be expected in the methyl

pentafluoropropanoate ester. In addition, it showed a wide O–H stretch (3342 cm^{-1}). The product may have been hygroscopic, but there was no secondary water band (ca. 1650 cm^{-1}). It is more likely that methyl esterification, if it occurred, did not go to completion in quiescent conditions even after 8 days, giving a strong free-hydroxyl O–H stretch.

^{1}H NMR spectra of the FK-5-1-12–methanol system showed a diminishing abundance of starting material methyl alcohol (H^b) protons and an increase in methyl ester protons (assigned to δ 4.00 ppm) with time. An example time series, for turbulent flow conditions, is shown in Figure 18.

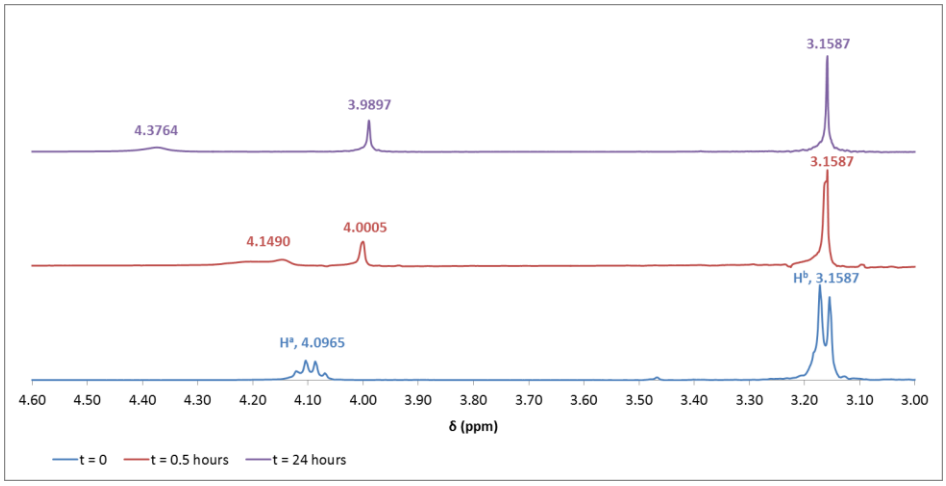

Figure 18: Time Series of Turbulent FK-5-1-12–Methanol System, ^{1}H NMR Spectra (300 MHz, 24 °C, DMSO-d6)

The bottom trace, neat methanol in DMSO-d6, shows an absence of proton exchange observable on the NMR timescale, since both the H^a quartet and H^b doublet are coupled at 4.98 Hz. With increasing time of contact between methanol and FK-5-1-12, this coupling apparently vanishes. This was more likely a consequence of the hygroscopicity of the DMSO itself.[180] A contribution of water from ambient moisture would have been sufficient to allow increased proton exchange, shown by the broadening hydroxyl (H^a) singlet (δ 4.149 to 4.376 ppm). Since DMSO was the preferred NMR solvent for FK-5-1-12 products, a drying step may be useful in future determinations. As the dispersion in the hydroxyl resonance frequency increases, there is further evidence of the increase in hydrogen bonding, but integration of the broad H^a singlet becomes less reliable. The methyl proton (H^b) peaks were integrated instead as an approximation of the rate of esterification. Pseudo-first order rate constants were estimated (by fitting ordered pairs of

integrated H^b peaks and time to a first-order decay equation) to be 1.6 $hour^{-1}$ for the turbulent case and 0.45 $hour^{-1}$ for the quiescent case. This difference in rate constants is consistent with the lower resistance to mass transfer in the turbulent case from the larger effective interfacial surface area between the immiscible phases.

The FK-5-1-12–ethanol system was maintained at constant agitation. After having withdrawn a vial from the platform shaker and allowing it to relax, the less dense (non-FK-5-1-12) phase was sampled. After 18 days, it showed an IR spectrum similar to that of the FK-5-1-12–methanol system, with both C–H and fluorinated ketone C=O stretches, suggesting esterification. Its ^1H NMR spectrum after 13 days (Figure 19) shows the presence of a new product and the starting material. The growth of an additional methyl triplet at δ 1.29 ppm from the starting material triplet at δ 1.05 ppm and a methylene quartet at δ 4.46 ppm from the starting triplet at δ 4.37 ppm support this conclusion.

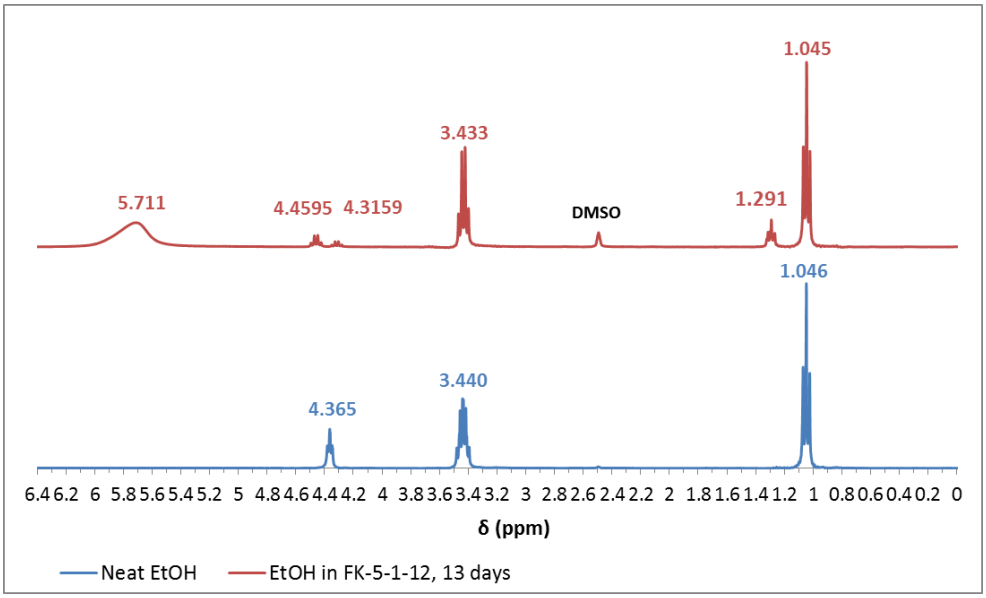

Figure 19: FK-5-1-12–Ethanol System, ^1H NMR Spectra (300 MHz, 24.2 °C, DMSO-d6)

The down-shifted signals are similar to those observed in the ethyl trifluoroethanoate ester (triplet at δ 1.37 ppm, quartet at δ 4.42 ppm),[178] providing evidence for esterification. The reaction was not complete, however, as seen by the continued presence of starting material. The apparently well-resolved quartet at δ 4.3159 ppm could correspond to a minor secondary substitution product, e.g. of ethanol with the

heptafluoroisopropanoyl moiety instead of the dominant pentafluoropropanoyl, but its signal is too weak to integrate and this hypothesis cannot be confirmed with these data.

The FK-5-1-12–2-propanol system also changed with time, with evidence of esterification similar to the methanol and ethanol cases. Its IR spectrum at 21 days was similar to that of the FK-5-1-12–ethanol system at 18 days. In the neat 2-propanol ^{1}H NMR spectrum, a doublet centred at δ 1.03 ppm represents the six methyl protons split by the lone vicinal isopropyl proton. A separate doublet at 1.31 ppm increased in abundance with time in the product between 40 hours and 7 days of contact and agitation (Figure 20).

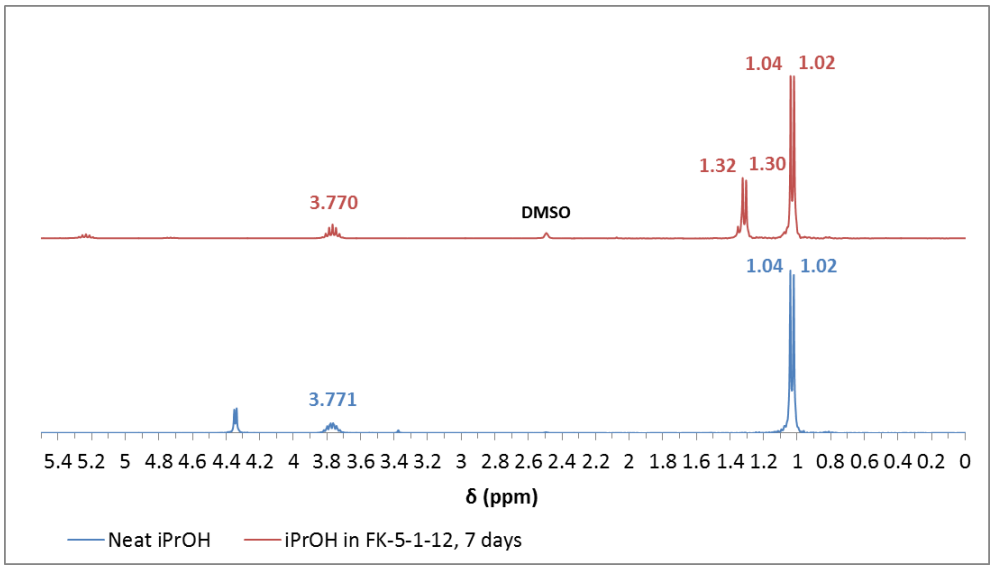

Figure 20: FK-5-1-12–2-Propanol System, ^{1}H NMR Spectra (300 MHz, 24.5 °C, DMSO-d6)

This second doublet is again assumed to represent the fraction of the population of methyl protons in esterified 2-propanol, both downshifted with respect to the starting material and retaining the homonuclear coupling with the vicinal proton.

2-Methyl-2-propanol (*tert*-butanol, *t*-BuOH) was included as a reagent to test the hypothesised acyl substitution reaction mechanism. *t*-BuOH, as a 3° alcohol, usually does not participate in such reactions because it is too sterically hindered. Indeed, the FK-5-1-12–*t*-BuOH system showed no significant changes in its FTIR or ^{1}H NMR spectra (92 % methyl abundance; 8 % hydroxyl abundance) over 7 days. If *t*-BuOH had esterified to any extent,

the hydroxyl oxygen would have lost its proton and the remaining, chemically identical methyl groups on the 3° carbon would have yielded a prominent singlet. There was no evidence of the presence of a new peak for this product.

FK-5-1-12 reacted rapidly with 2-aminoethanol; this reaction and its products are described in the following sub-section on amino groups. FK-5-1-12 reactions, if any, with ethane-1,2-diol and 2-thioethanol are less certain. When these latter two systems were removed from the platform shaker and allowed to relax, in both cases, the less-dense, non-FK-5-1-12 phase formed a toroidal shape. This phase showed a surface of negative curvature towards the FK-5-1-12 phase. The toroidal phase was sampled and analysed.

Given a 2:1 molar ratio of FK-5-1-12 to ethane-1,2-diol, the system could form a diester if reacted to completion (Figure 21), by analogy to the mono-substituted alcohols.

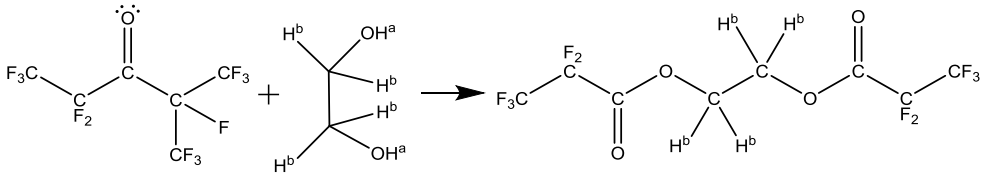

Figure 21: FK-5-1-12 Reaction with Ethane-1,2-diol

The FTIR spectrum of the toroidal phase of the FK-5-1-12–ethane-1,2-diol system showed a typical fluorinated carbonyl peak at 1779 cm^{-1} and four peaks not found in either starting reagent: two prominent peaks at 1285 cm^{-1} and 1209 cm^{-1} (likely C–F), and two at 2121.06 cm^{-1} and 1942 cm^{-1}, which have not been definitively assigned.

^{1}H NMR spectra of the FK-5-1-12–ethane-1,2-diol system in time are shown in Figure 22.

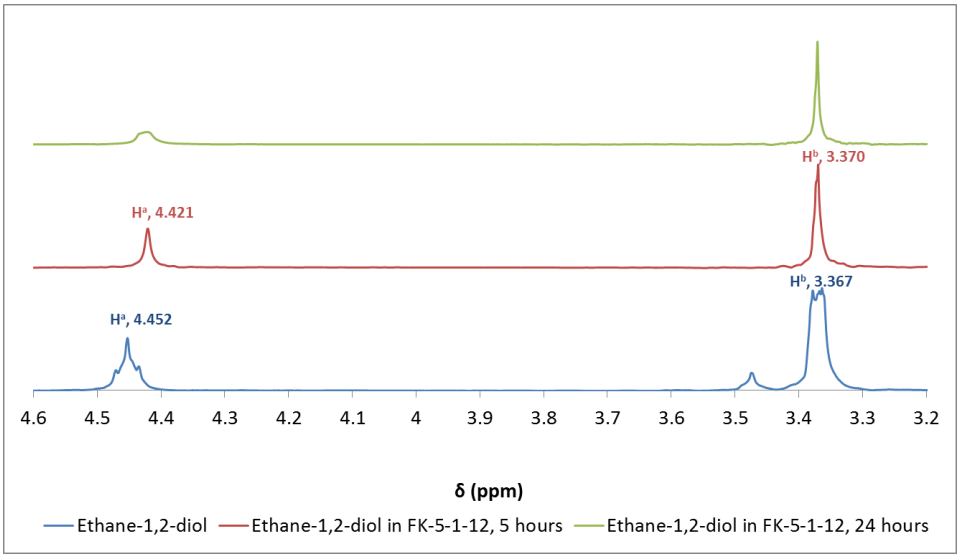

Figure 22: Ethane-1,2-diol ^{1}H NMR Spectra (300 MHz, 24.6 °C, DMSO-d6)

The singlet at δ 3.37 ppm, in the starting material at least, is suspected to include interference from water, given the hygroscopicity of ethane-1,2-diol. Hydrolysis of FK-5-1-12 from any available water to yield pentafluoropropanoic acid would not give a reliable proton signal on account of the low pK_a of PFPrA, as discussed in the environmental fate of FK-5-1-12.

Starting material, depicted on the bottom trace of Figure 22, exhibits first-order coupling consistent with chemically distinct proton–proton interactions. Coupling constants are less reliable in ethane-1,2-diol, however, because of conformational effects. In organic molecules with free axial rotation, including ethane-1,2-diol, the dihedral angle, i.e. the angle subtended by the vicinal protons when sighting down the axis, is free to vary. In turn, the potential energy of the conformation of the molecule and the coupling constants of the protons vary periodically like the dihedral angle. Local minima in energy are thermodynamically favourable. For ethane-1,2-diol, local minima occur in the *gauche* (dihedral angle of 60° or 300°) and *anti* (dihedral angle of 180°) conformations. These optimal separation angles generally result in the lowest coupling constants, sometimes tending to zero, because of the relatively longer distances between nuclei.[181] For ethane-1,2-diol, it has been determined that the *gauche* conformer (Figure 23) predominates in most solvents, including DMSO.[182]

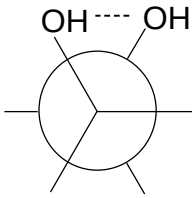

Figure 23 : *Gauche* Conformation of Ethane-1,2-diol (Newman Projection)

The *gauche* conformation also allows intramolecular O–H hydrogen bonding (dotted line) in addition to intermolecular hydrogen bonding. However, hydrogen bonding alone is insufficient in explaining relative reactivities in this case: as discussed in the preceding section, both water and ammonia were previously shown to react readily with FK-5-1-12, and as will be developed in the following section, primary amines and diamines are even more readily reactive. Hence, there must be some other property limiting the reactivity of diols.

Vanishing of the hydroxyl H^a coupling constant (5.4 Hz) observed in the starting material cannot be taken as evidence of reaction in this case, because of the possibility of rotation through different conformations. The magnitude of change in chemical shift between starting material and the 5-hour 'product', in tenths of ppm, is also insufficient evidence of reaction, but is attributable to changes in concentration of ethane-1,2-diol of the order of 10^{-2} to 10^{-3} mol, i.e. the approximate volume of EG (100 µL) in the aliquots used for NMR spectroscopy.[183] Although integration of the hydroxyl proton (H^a) singlet is not necessarily reliable, it did not change with time, with 30 % abundance of H^a and 70 % of H^b throughout, irrespective of line-shapes. In view of all these results, a reaction is unlikely to have occurred. Absence of reaction is explained by the fundamentally different character of the FK-5-1-12 carbonyl group to non-perfluorinated carbonyls. Ethane-1,2-diol usually reacts at the oxygen atom of the carbonyl in hydrocarbon aldehydes and ketones to form cyclic acetals or ketals, but on account of the much lower negative charge density about the oxygen atom in FK-5-1-12 (depicted in Figure 15), this reaction pathway is apparently less likely.

There are three possible products in the FK-5-1-12–2-thioethanol reaction (Figure 24): an ester with a terminal sulfhydryl group (Pathway 1), a thioester with a terminal hydroxyl group (Pathway 2), and a bifunctional product (Pathway 3).

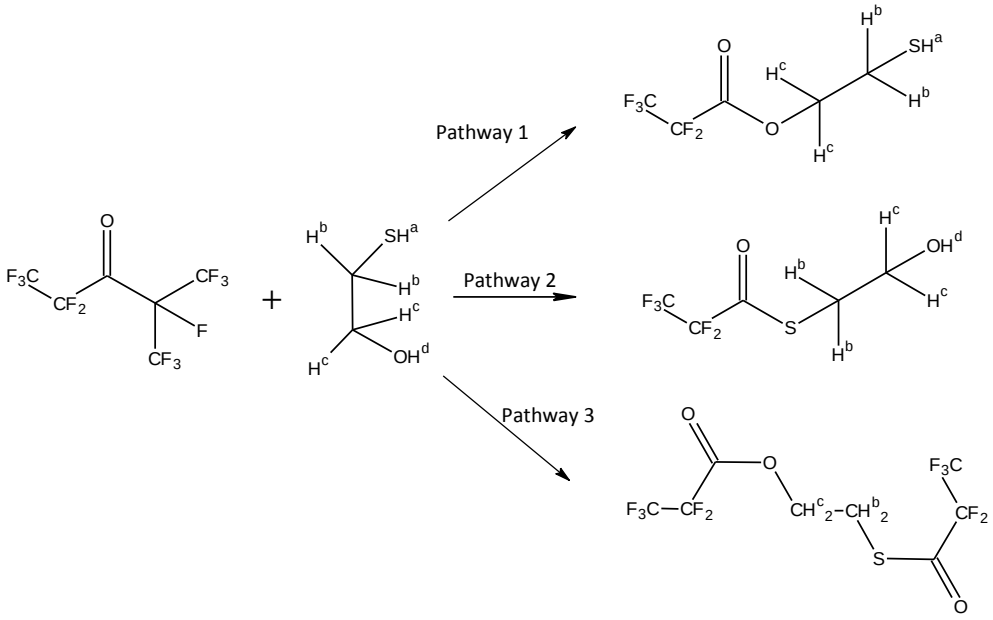

Figure 24: FK-5-1-12 Reactions with 2-Thioethanol

The FTIR spectrum of the non-FK-5-1-12 phase in the system after 8 days showed prominent O–H (3355 cm^{-1}) and S–H (2556 cm^{-1}) stretches, but, unexpectedly, no carbonyl stretch corresponding to either an oxygen ester or a thioester. 2-Mercaptoethyl pentafluoropropanoate, one product expected from acyl substitution of FK-5-1-12 by 2-thioethanol (Pathway 1) has been produced by other experimenters, but using perfluoropropanoyl fluoride as the starting material.[179] Fluoride alone (as found in the acyl fluoride) could be a better leaving group for substitution by 2-thioethanol than HFC-227ea (as found in FK-5-1-12), since fluoride alone is both highly electronegative and is more compact than the trifluoromethyl or pentafluoroethyl moieties.

The ^{1}H NMR spectra of the FK-5-1-12–2-thioethanol system are presented in Figure 25, with the strong singlet at δ 3.379 ppm in the starting material likely from water (as for ethane-1,2-diol).

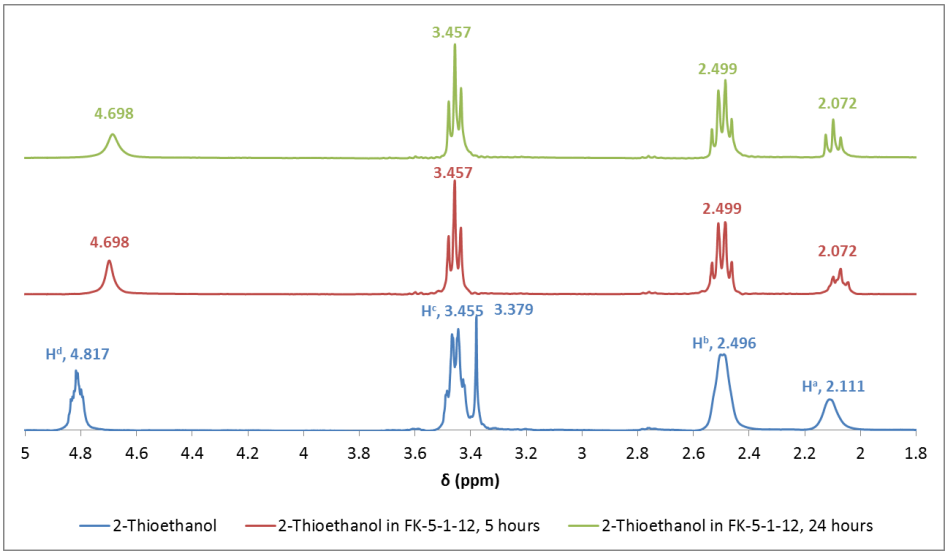

Figure 25: 2-Thioethanol ^{1}H NMR Spectra, (300 MHz, 24.6 °C, DMSO-d6)

As with 1,2-ethanediol, the peak at δ 4.8 ppm corresponding to the hydroxyl proton of the starting material coalesced into a singlet and shifted upfield with time, which is consistent with a hydroxyl concentration effect.[183] However, as neither of the distinct methylene protons H^b or H^c shifted in the 'product' traces, and neither the hydroxyl (H^d) nor sulfhydryl (H^a) protons disappeared, it is unlikely that a reaction actually occurred, e.g. to form an oxygen ester of 2-thioethanol, a decomposition product of that ester, such as thiirane, or a cyclic thioketal.[179] Indeed, the result that no carbonyl stretch was observed in the IR spectrum of the non-FK-5-1-12 phase further suggests that no acyl substitution reaction occurred by either the hydroxyl or sulfhydryl function, but this is consistent with the results obtained for ethane-1,2-diol. A linear sulfhydryl-substituted reagent was not available during the project as a basis for comparison. Hence, the relative reactivity of the sulfhydryl group alone with FK-5-1-12, compared to hydroxyl and amine groups, cannot be deduced from these experiments alone. This could be the object of future study.

4.1.4.2.3 – Amino Groups

The reactions of neat propan-1-amine, ethane-1,2-diamine, and 2-aminoethanol with FK-5-1-12 were all rapid and vigorous, proceeding in seconds at laboratory temperatures (22-25 °C). All reactions were exothermic and evolved gas, and the diamine yielded a white precipitate, while propan-1-amine and 2-aminoethanol yielded viscous yellow liquids.

The reaction of 1.25 mmol neat propan-1-amine with 22% molar excess of FK-5-1-12 (Figure 26) was carried out in a vial with a PTFE septum. It evolved a viscous, yellow liquid within seconds.

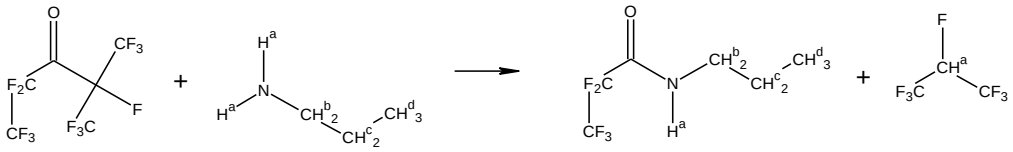

Figure 26: FK-5-1-12 Reaction with Propan-1-amine

From weighing by difference, 0.1532 (± 0.0001) g of gas, corresponding to 0.9010 mmol (72% of predicted yield) of HFC-227ea, were estimated to have been evolved immediately after mixing. The system was sealed for the following 45 hours. The product, sampled after 45 hours, was qualitatively soluble in DMSO. An IR spectrum of this phase was not obtained. Its ^{1}H NMR spectrum (Figure 27) showed evidence of impurities in the starting material, but a broad amide proton singlet at δ 6.0 ppm in the product.

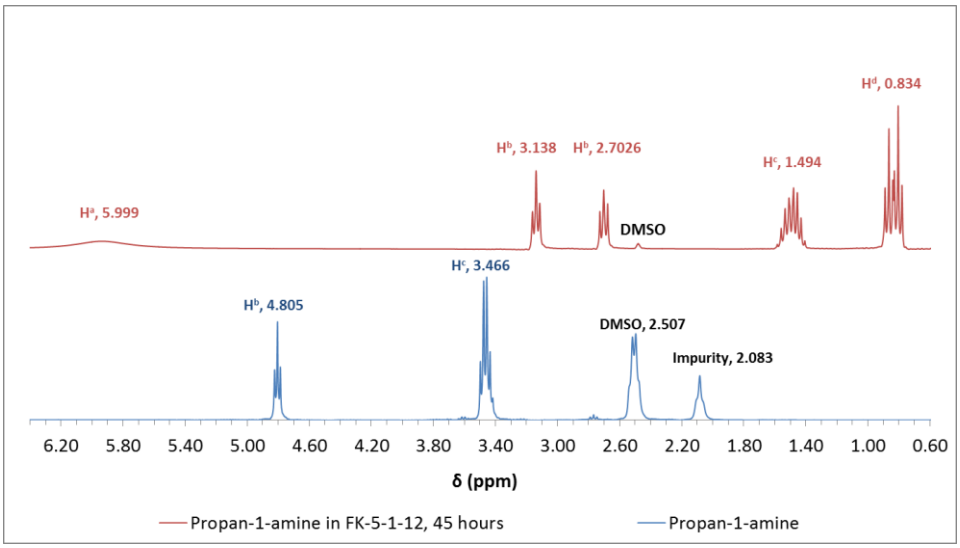

Figure 27: Propan-1-amine ^{1}H NMR Spectra (300 MHz, 23.5 °C, DMSO-d6)

Proton abundances in the product, determined by integration, were approximately 3:2 (H^d:H^c). If the observed H^b signals are considered a doublet of a triplet, they would account for the remaining non-exchangeable protons in an amide product at a 3:2:2 (H^d:H^c:H^b) ratio, as expected from the

mechanism in Figure 26. Coupling constants for H^b and H^c increased from approximately 5.5 Hz in the starting material to > 7 Hz in the product, and H^a (a nitrogen-bonded proton) appeared in the product only. The additional splitting in H^d (doublet of a triplet in the terminal methyl protons) ought also to be attributed to reaction: the result of stronger coupling between the amide proton and adjacent protons than was the case in the starting amine. The 1° amine propan-1-amine appeared to obey the same reaction mechanism as would nucleophilic NH_3 with FK-5-1-12, with the difference that it formed a 2° amide, propyl perfluoropropanamide, as opposed to a 1° amide.

With increasing dilution of aqueous propan-1-amine, the reaction with FK-5-1-12 became much less vigorous, particularly for unit percentages by volume of amine. The immiscible FK-5-1-12 phase tended to settle as dense bubbles. As the reaction progressed, the increasing volume of HFC-227ea vapour within a bubble eventually caused it to rise to the surface by buoyancy. Bubbles were observed to break and release the vapour. A smaller volume of dense, hydrophobic phase, presumed to be the propyl perfluoropropanamide product, was observed to settle.

The reaction of ethane-1,2-diamine (ED) was first carried out in an open beaker with a 100-fold volumetric excess of FK-5-1-12. The proposed reaction scheme (Figure 28) assumes that each amine group would attack an FK-5-1-12 molecule to yield a larger product.

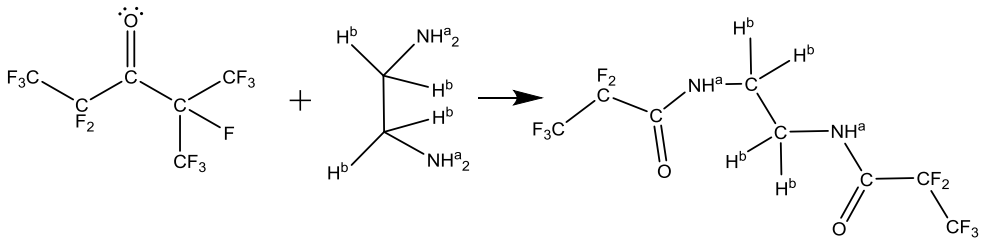

Figure 28: FK-5-1-12 Reaction with Ethane-1,2-diamine

After 24 hours had elapsed, the excess FK-5-1-12 had evaporated and the resulting white precipitate was analysed. It was qualitatively soluble in acetone and DMSO, but insoluble in several non-polar and polar protic solvents, including hexane, dichloromethane, chloroform, and water. Indeed, it appeared to be hydrophobic. The solid FK-5-1-12–ED product was milled in a mortar and pestle and pressed into a KBr disc at 1 % by mass for infrared spectroscopy. Its IR spectrum showed an N–H stretch at 3323 cm^{-1} and an N–H bend at 1561 cm^{-1}. It showed a C=O stretch at 1697 cm^{-1}, which could be

adjacent to N (i.e. a 2° amide) as it differs significantly from the FK-5-1-12 carbonyl, which was typically observed at 1780 cm^{-1}. Since there was no carbonyl in the diamine starting material, and no fluorinated ketone carbonyl, this is most likely evidence of amide formation.

The FK-5-1-12–ED product ^{1}H NMR spectrum is shown in Figure 29. A spectrum of neat ethane-1,2-diamine in DMSO-d6 for direct comparison of chemical shifts was not obtained. It is likely that the sample mixture was too viscous to relax at room temperature and give reliable ^{1}H NMR signals.

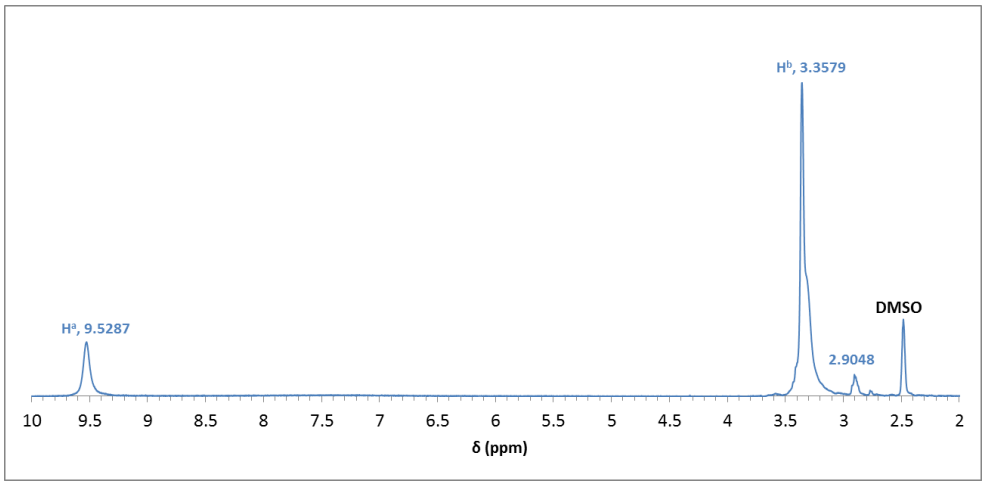

Figure 29: FK-5-1-12–Ethane-1,2-diamine Product ^{1}H NMR Spectrum (300 MHz, 23.0 °C, DMSO-d6)

The H^{a} singlet is readily assigned to an amide proton. The H^{b} signal is not a well-resolved singlet and it overlaps with the shift associated with water in DMSO, making integration unreliable. The poorly resolved doublets at δ 2.90 and 2.77 ppm are likely from a consequence of inhomogeneity, a minor product, or residual starting material, and have not been assigned. Their total proton abundance is approximately 5 %. Other lines of evidence proved more useful. For instance, the actual precipitate yield at 24 hours was 0.5140 (± 0.0001) g, which corresponds to 97.72 (± 0.03) % of the theoretical yield of the proposed diamine–perfluorocarboxylic acid product, 1,2-bis(perfluoropropanamido)ethane. This major product is, in turn, supported by the FTIR spectrum, and to a lesser extent, the ^{1}H NMR spectrum, but the identity of the minor product or abundance of residual starting material has not been determined.

There are three possible acyl substitution products in a reaction of FK-5-1-12 with 2-aminoethanol, shown in Figure 30: an ester with terminal amino group (Pathway 1), an amide with terminal hydroxyl group (Pathway 2), and a bifunctional product (Pathway 3).

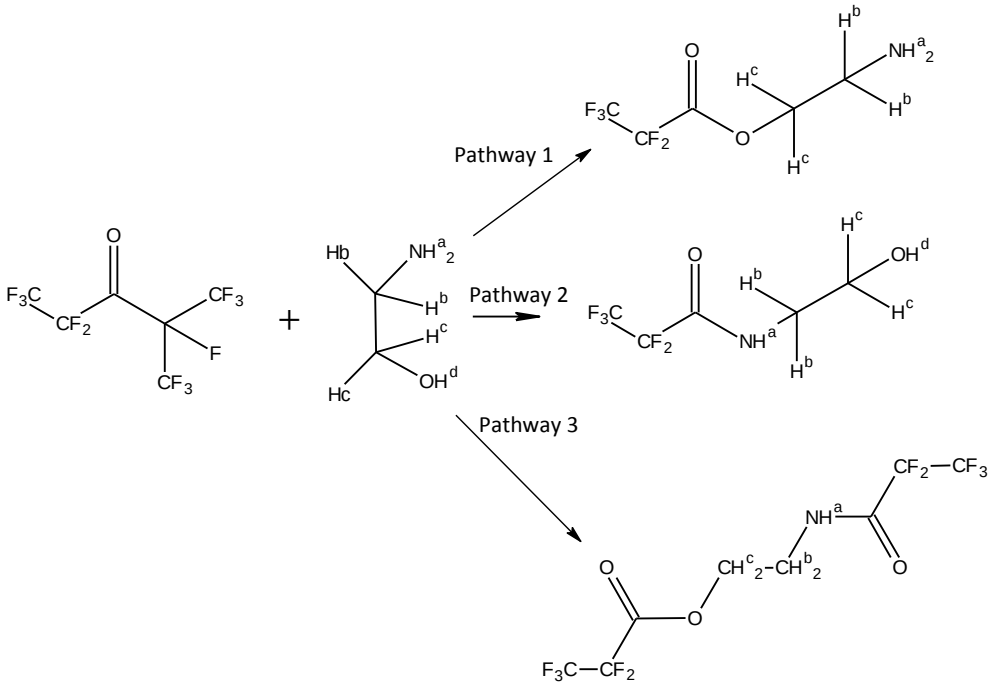

Figure 30: FK-5-1-12 Reaction with 2-Aminoethanol

The IR spectrum of the FK-5-1-12–2-aminoethanol product at 24 hours showed N–H stretching peaks at 3286 cm^{-1} and 3084 cm^{-1}. Prominent C–F peaks at 1216 cm^{-1} and 1163 cm^{-1} provided evidence of a perfluoroalkyl group. A 2° amide-linked C=O stretch peak at 1708 cm^{-1} and an N–H bend peak at 1554 cm^{-1} provided additional evidence for a 2° amide. The [3500, 2500] cm^{-1} domain was broad, likely from extensive H-bonding with hydroxyl, which qualitatively identifies Pathway 2 or starting material. If an ester (Pathway 1) or bifunctional product (Pathway 3) had been significantly favoured over the amide, there would likely not have been such a broad hydroxyl-like peak.

The ^{1}H NMR spectra of the FK-5-1-12–2-aminoethanol product are shown in Figure 31.

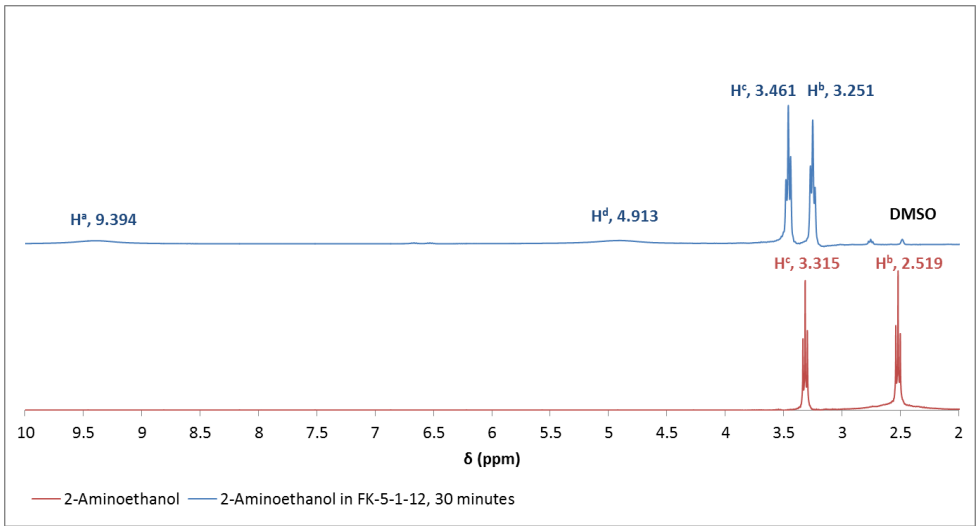

Figure 31: 2-Aminoethanol ^{1}H NMR Spectra (300 MHz, 24.3 °C, DMSO-d6)

H^b and H^c are shifted downfield in the product and exhibit higher proton–proton coupling at 5.9 Hz than in the starting material (5.5 Hz). The chemical shifts of H^a and H^d do not appear in the starting material, as is typical for exchangeable protons, but are visible in the product. The presence of H-bonding at H^d, the terminal hydroxyl proton, is consistent with a reaction at the amine function of 2-aminoethanol (Pathway 2). In a 2° amide, H^a could still show a singlet, as it did in this case. However, both the H^a and H^d singlets are broad and they cannot be practically separated from the noise floor for quantitation.

The apparently rapid reactions of neat 1° amines—whether present as the sole nucleophile or with other nucleophilic functions—could be problematic if these species were to be removed by FK-5-1-12. On the other hand, the rates of reaction of dilute aqueous solutions of propan-1-amine were qualitatively lower.

4.1.4.2.4 – Phosphoryl Groups

On mixing, FK-5-1-12 and all of the phosphoric acid esters (OMPA, DIMP, and DMMP) appeared to form two distinct phases, with neither gas nor precipitate evolved. The systems were sealed for 7 days and sampled. There was no evidence of reaction in any mixture by either NMR or FTIR spectroscopy.

4.1.4.3 – Reactivity Summary

FK-5-1-12 was observed to react vigorously with 1° amines, likely by nucleophilic acyl substitution. The nucleophilic character of the hydroxyl and thiol functions, however, could not be quantitatively compared to amines in this project.

The reactivity of FK-5-1-12 may be seen either to diminish its utility as a primarily 'physical' decontaminant, or to confirm its suitability with respect to environmental concerns. Unlike CFC-113 and the liquid perfluorocarbons, there are many mechanisms by which FK-5-1-12 may be degraded in the environment. Its most rapid reactions were with pure and generally reactive species, such as ethane-1,2-diamine, but it was also found to react with 1° and 2° alcohols. In contrast, it did not apparently react with, or solvate, three organophosphorus compounds. Qualitatively, it was not observed to react vigorously even with amines when they were diluted in aqueous solution. Rather, it tended to displace and repel these species.

In most cases, reactions seem to have been confined to the FK–reagent interface because FK-5-1-12 did not dissolve the reagents. To limit undesired consequences of reactions, i.e. evolution of heat or vapour, near a sensitive surface would be to achieve contaminant detachment more rapidly than the rate of reaction. In this way, the immiscible reagent would evolve heat or vapour in the bulk of the FK-5-1-12 phase rather than upon the sensitive surface. Conversely, if this is not practicable, the tendency of FK-5-1-12 to react rapidly with contaminants containing amino groups may be unacceptable in view of the operational requirement to preserve substrate integrity. As examples, the priority #32 TIM of greatest operational concern, *o*-anisidine, has an amino group, and aqueous solutions of ammonia (priority #4) may not be feasibly decontaminated by FK-5-1-12.

4.1.5 – Fluorinated Lubricant Depletion

Among the predicted drawbacks of a fluorinated solvent- or surfactant-based decontamination method was the likelihood of lubricant depletion, and fluorinated lubricant depletion in particular. Effective lubrication is a common requirement for mechanical reliability, and fluorinated lubricants have been employed expressly for their tolerances to challenging operating environments, such as those in hard-disk drives. Since hydrofluoroethers and fluorinated ketones have been used to dissolve fluorinated lubricants, it was hypothesised that HFEs and FKs could cause such lubricants to be depleted from manufactured parts during a decontamination procedure. Auger

electron spectroscopy (AES), secondary ion molecular spectroscopy (SIMS), and X-ray photoelectron spectroscopy (XPS) surface analytical methods were available to test this hypothesis. HDD coupons were obtained from disassembled parts and were subjected either to decontamination by immersion in quiescent HFE-7200 or FK-5-1-12 (test specimens), or to no decontamination at all (controls).

For a given HDD coupon, AES provided elemental profiling with time to a maximum depth of 3 nm. SIMS provided the abundance of secondary ion fragments which could be interpreted structurally, in a manner similar to GC–MS. XPS could not determine characteristic ion fragments as can SIMS, but was more sensitive to elemental composition at the nanometric scale relevant for HDD platters, and was capable of the deepest elemental profiling (e.g. 10 nm compared to 2-3 nm for AES). The strength of this approach was in subjecting genuine computer parts to the decontamination procedure and analysing them directly. The shortcoming of this series of surface determinations was the small sample size.

Auger and SIMS spectroscopic analyses of HDD platter coupons did not reveal any definite tendencies. XPS analysis of HDD platter coupons (Figure 32) yielded elemental profiles starting from the surface of each platter and progressing into the ferromagnetic recording layer, as shown by the small, but detectable, elemental abundances of cobalt, chromium, and platinum. The intermediate layers profiled, which are depicted schematically in Figure 3, evidently included the carbonaceous–nitrogenous layer and a layer of perfluoropolyether, shown by relatively larger abundances of carbon, fluorine, and oxygen, as expected. These data were more useful: the HDD coupon immersed for 20 min in FK-5-1-12 showed lower fluorine abundance than its unimmersed control counterpart. In contrast, both the coupon immersed in HFE-7200 and its counterpart had similar abundances of fluorine.

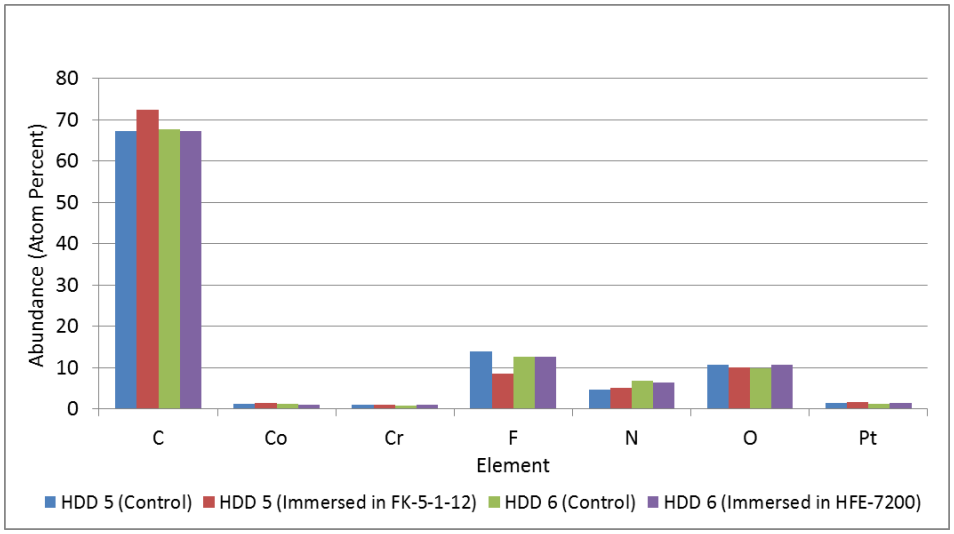

Figure 32: Elemental Abundances in HDD Platters to 10-nm Probe Depth by XPS

This difference in fluorine content could suggest marginally less PFPE lubricant on the surface of the FK-5-1-12-immersed platter, but fluorine-containing species—which would include the PFPE lubricant—were still present. It is unlikely that lubricant was fully dewetted from the platter's carbonaceous overcoat.[184] Given 20-min immersion time in HFE or FK in ambient conditions, delubrication of PFPEs from HDD platters may not be a limiting consideration in a future sensitive equipment decontamination system, in contrast to the delubrication predicted from a review of the literature. A larger sample of genuine, representative computer parts would be required to increase the level of confidence in the results.

4.2 – Decontamination with FK-5-1-12

4.2.1 – Proof-of-Concept—OP Pesticide and HDPE Substrate

BrPMe (shown in Figure 33) was selected as the challenge contaminant for the proof-of-concept decontamination study because its phosphorothioate group is structurally similar to the pesticides posing the most severe acute health hazards (e.g. OMPA), which are all phosphoric acid esters.

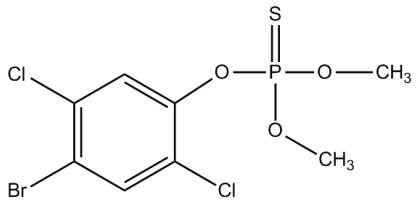

Figure 33: Bromophos-methyl Structure

BrPMe has low acute mammalian toxicity, as well as low chronic toxicity in humans, resulting in less-burdensome safety requirements for storage and manipulation.[185] Its halogenations provide ease of detection at low quantities by INAA. The bromination of the 2,5-dichlorophenol ring is particularly useful, because bromine as a tracer element is both amenable to analysis by neutron activation ($^{80}_{35}$Br emits a characteristic γ-ray at 616 keV), and much less environmentally abundant, typically by 2-3 orders of magnitude, than is chlorine.[51, 186]

HDPE coupons were contaminated with a BrPMe solution, aged for ≥ 10 min, and then immersed in glass vials containing nominally 10 mL of FK-5-1-12, where they were held for different time intervals. At the end of an interval, the coupon was withdrawn and its bulk Br content measured by an INAA method for hydrocarbon matrices. The initial surface loading of BrPMe was 14 μg·cm^{-2}.

For the first determination of decontamination effectiveness, the residual amount of Br in HDPE coupons, as detected by INAA, is shown normalised with respect to the amount of Br measured from control spikes. Values are reported as a function of time over 24 hours and presented in Figure 34. Individual bounds of relative uncertainty are within ± 10 % of the normalised concentration of Br in the control spike.

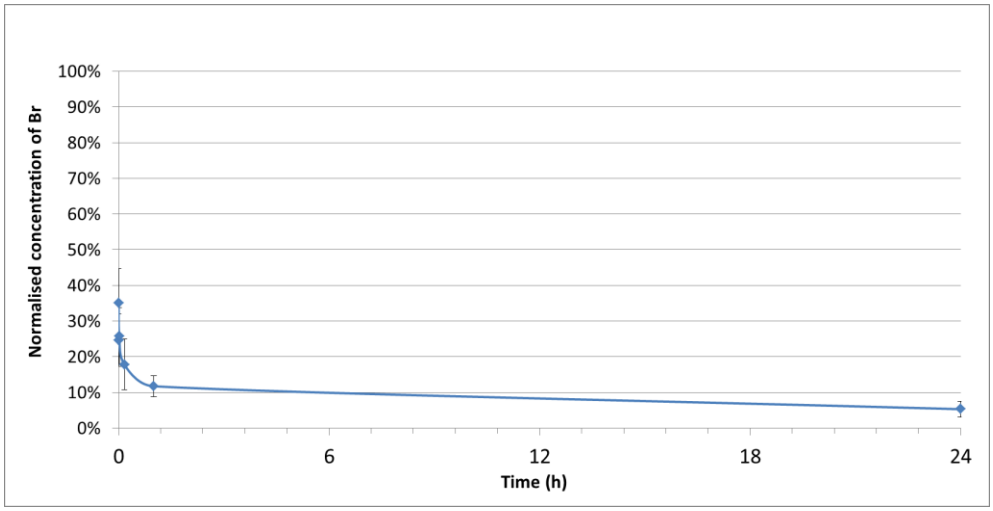

Figure 34: Bromine Residual in HDPE Coupons v. Immersion Time with FK-5-1-12 Decontamination, 14 µg BrPMe·cm^{-2} Coupon Loading Density

Although it is not strictly monotonic, the function depicts progressive removal of Br from the coupon in time, with most mass transfer occurring within the first hour of immersion. From a loading density of 14 µg·cm^{-2} of BrPMe, nearly one order of magnitude of removal—the first design goal of the project—was achieved in the first hour of immersion.

Figure 35 shows the residual Br in HDPE coupons that were subjected to increased loading densities of 70 µg·cm^{-2} and 140 µg·cm^{-2} of BrPMe and the same decontamination procedure.

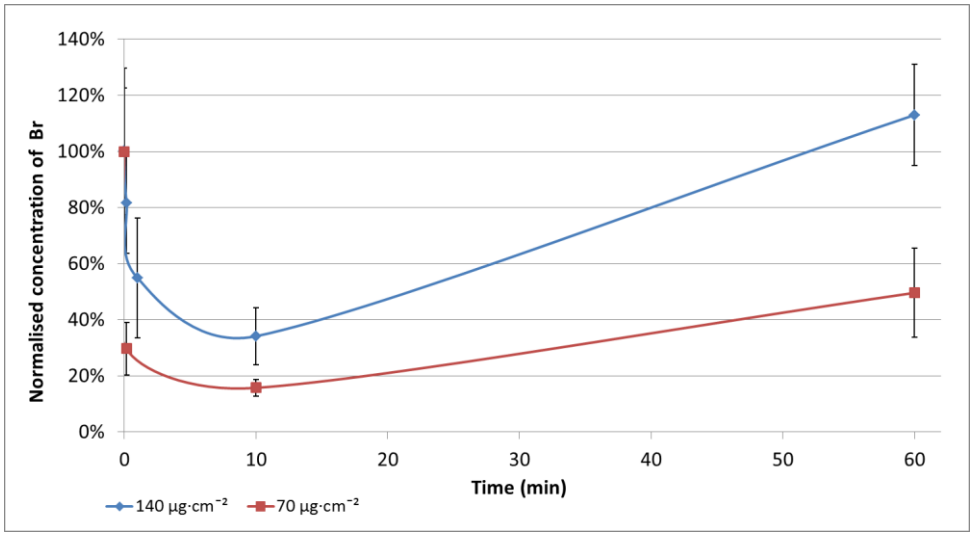

Figure 35: Bromine Residual on HDPE Coupon Surfaces v. Immersion Time (Higher Loading Densities)

These functions are less promising because they suggest that contaminant was re-sorbing onto the coupon surfaces after the initial dispersion or removal process (approximately 10 min). They suggest that the 10-mL volume of FK-5-1-12 alone was unable to maintain the coupons in a decontaminated condition. Although the FK-5-1-12 phase itself was sampled and analysed in these cases, contaminant mass balance as Br was not obtained. This was likely a consequence of the lack of homogeneity of the BrPMe dispersion in the FK-5-1-12 phase (a form of sampling error).

To test the hypothesis that FK-5-1-12 may achieve decontamination by repelling weakly sorbed contaminants from affected surfaces, a separation process was incorporated in parallel with immersion. It was again desired, in the first place, to minimise mechanical power input by maintaining a quiescent régime, so that mass flux would occur only through natural convection, dispersion, and diffusion. If the hypothesis were true, then contaminant removed from surfaces and dispersed into the FK-5-1-12 phase could, in principle, be captured in absorbent media having a higher affinity for it than the surface on which it was originally deposited. Contaminants so captured would not pose the same enduring risk to a human receptor by re-sorbing onto previously decontaminated surfaces. This, in turn, would increase the confidence in the safety of the decontamination process. Sorption would also be a feasible way to demonstrate contaminant mass balance across the process with greater certainty.

4.2.2 – Contaminant Mass Balance

In an effort to obtain contaminant mass balance through the parts of the bench-scale decontamination system, HDPE coupons were used as substrate material, TPhAs as the challenge contaminant, and cellulose and GAC as sorptive media. The temperature of the decontamination system was typically 22 °C and there was no mechanical power input apart from the actions of immersing and withdrawing contaminated coupons. Initial TPhAs loading on coupon surfaces was 12 $\mu g \cdot cm^{-2}$. Once the aforementioned parts of the system were sampled, residues on the interiors of empty decontamination vials were extracted with hexane isomers, and the extract was also sampled. The FK-5-1-12 phase was allowed to evaporate and was not sampled because of the results of the preceding experiment, which suggested that a contaminant would have been dispersed inhomogeneously in it.

Results are presented in Figure 36, showing the mean As recovery of duplicate or triplicate determinations in the different parts of the decontamination system as a function of immersion time. Recovery in every part is normalised with respect to the amount of As detected in the control spike, with background masses of As subtracted.

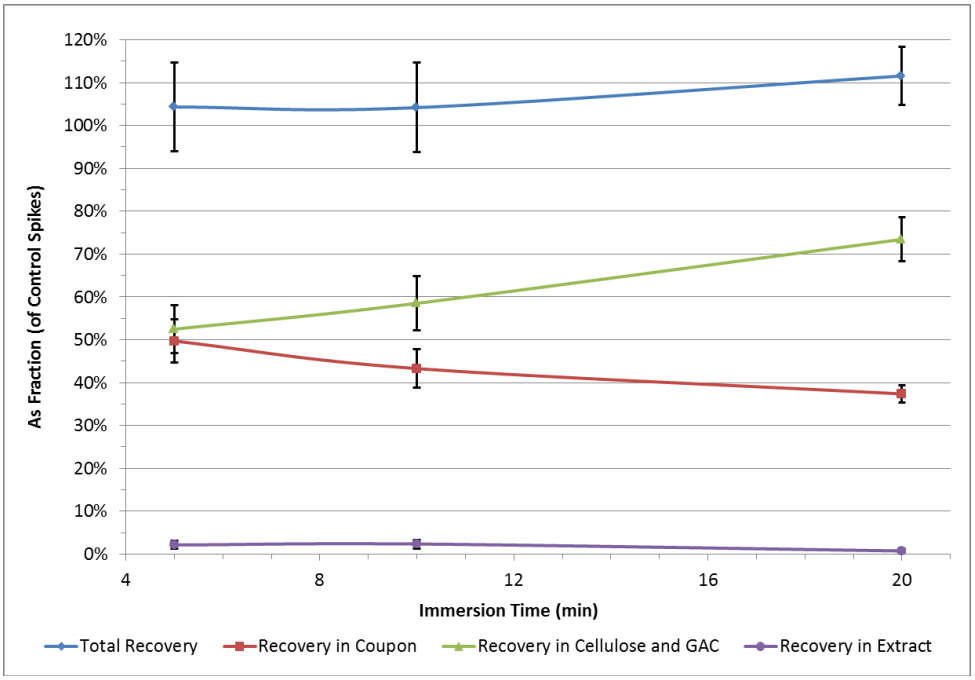

Figure 36: Arsenic Recovery Mass Balance v. Immersion Time in Quiescent FK-5-1-12

The decreasing recovery of As in coupons and increasing recovery in the sorptive media with time demonstrate that As removed from the coupon surface was entrapped in the sorptive media within the bounds of experimental uncertainty. There was no significant amount of residue extractable by the hexane solvent: the quantity of As recovered in hexanes was approximately equal to the LOQ for As by the INAA method used. Thus, contaminant that was removed from the substrate material was present in the sorptive media, and was not found elsewhere in the system.

Provided the contaminant's interaction with the surface is relatively weak, as for HDPE, the presence of FK-5-1-12 appears to hasten contaminant removal through mass transfer. On the other hand, if the overall interaction with a surface is stronger, as for cellulose and GAC, then the FK-5-1-12 apparently does not cause it to be removed from such surfaces. These results suggest a process in which contaminated substrate materials may be decontaminated passively (through natural convection, dispersion, and diffusion), with contaminant retained in sorptive media.

Although removal was rapid in this case, the process also required testing against a broader range of representative sensitive materials. In addition, it

would be worthwhile to re-evaluate the tradeoff between power input and removal efficiency, so as to shorten the length of time required for a desired extent of removal.

4.2.3 – Factorial Contaminant–Substrate Studies

In order to evaluate the decontamination capability of FK-5-1-12 more generally, different contaminant–surface material pairs were tested. Substrate materials typically used in sensitive equipment were obtained and testing coupons were fabricated from them. The surfaces of these materials of different composition were characterised by common metrics of surface roughness, with the expectation that a smoother surface would be more amenable to decontamination. A summary of the surface roughness parameters obtained through profilometry is presented in Table 12.

Table 12: Summary of Surface Roughness Parameters

Coupon/Face	Roughness Parameters, Mean (one Standard Deviation), [μm]			
	R_a	R_z	R_q	R_t
PC-ABS, FR3008, Exterior	2.135 (0.313)	6.039 (0.885)	2.340 (0.605)	6.144 (0.950)
PC-ABS, FR3008, Interior (Sputtered)	2.534 (0.266)	7.168 (0.753)	2.521 (0.266)	7.239 (0.760)
Fibreglass-Reinforced Epoxy, G-10/FR-4, 'Bottom'	0.961 (0.035)	2.718 (0.098)	0.956 (0.037)	2.745 (0.099)
Paper-Clad Phenolic, XXX, 'Bottom'	0.804 (0.019)	2.275 (0.054)	0.799 (0.019)	2.297 (0.054)
HDPE, 'Bottom'	0.916 (0.005)	2.592 (0.015)	0.909 (0.005)	2.618 (0.015)

Roughnesses were of comparable orders of magnitude, with recovered materials showing generally higher values than virgin ones. HDPE most closely resembled the virgin circuit board materials in terms of its roughness values. From reading the scale of SEM images (Figure 37), the projected diameter of individual strands of Nylon-6,6 in MIL-W-4088K specification webbing coupons was estimated to be 30 (± 1) μm.

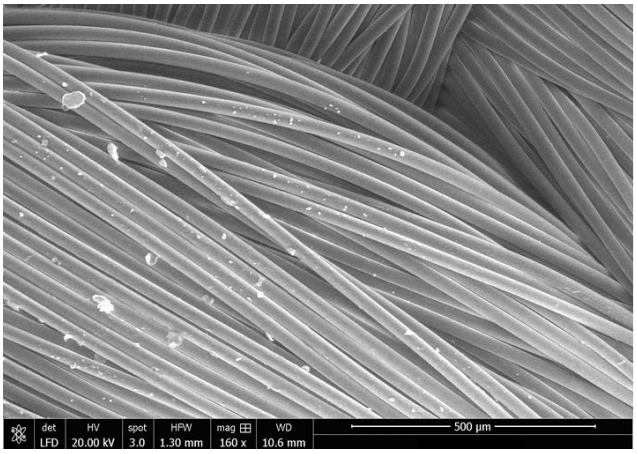

Figure 37: Nylon-6,6 SEM Image

The extents of decontamination of samples of these substrate materials were tested with BrPMe and TPhAs challenge contaminants with cellulose and GAC sorptive media together in quiescent FK-5-1-12. Mean contaminant tracer atom recoveries from FR3021 PC–ABS, Nylon-6,6, and FR-4 fibreglass epoxy coupons were normalised with respect to control spikes directly into sorptive media. The background abundances of Br and As in the materials were subtracted to give values of recovery indicative of the extent of decontamination. These recoveries in sorptive media are plotted against immersion time in FK-5-1-12 in Figure 38 (bromine) and Figure 39 (arsenic). Points are connected with curvilinear lines as a visual aid. Although samples describe a time-course, they were all independent of one another. Unlike the results in preceding sections, which showed the measured contaminant residual in coupons, these results show contaminant recovery in sorptive media. Hence, higher values represent more effective decontamination.

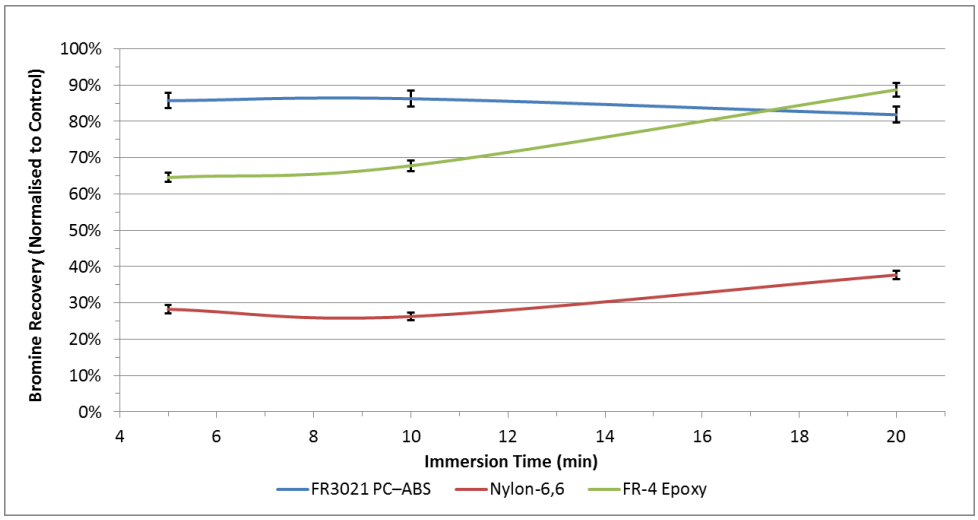

Figure 38: Bromine Recovery v. Immersion Time in Quiescent FK-5-1-12 by Substrate Material

Bromine recovery in quiescent conditions was most rapid from PC–ABS (keyboard and case material) coupons, followed by FR-4 printed circuit board coupons. Contaminant was removed at rates of 80-90 % after 20 min from those coupons, but removal was comparatively lower (< 50 % for all times) from Nylon-6,6 coupons. The higher affinity for the Nylon-6,6 than the other substrates by BrPMe could be explained by chemical composition, with BrPMe more attracted to the polar amide functions of the Nylon than non-polar TPhAs. The lower extent of contaminant removal in general from Nylon-6,6 is likely a consequence of its weave, which would serve to intercept contaminant particles. Hence, a more efficient decontamination technique would be required to achieve at least an order of magnitude of removal from Nylon-6,6 webbing within this time budget.

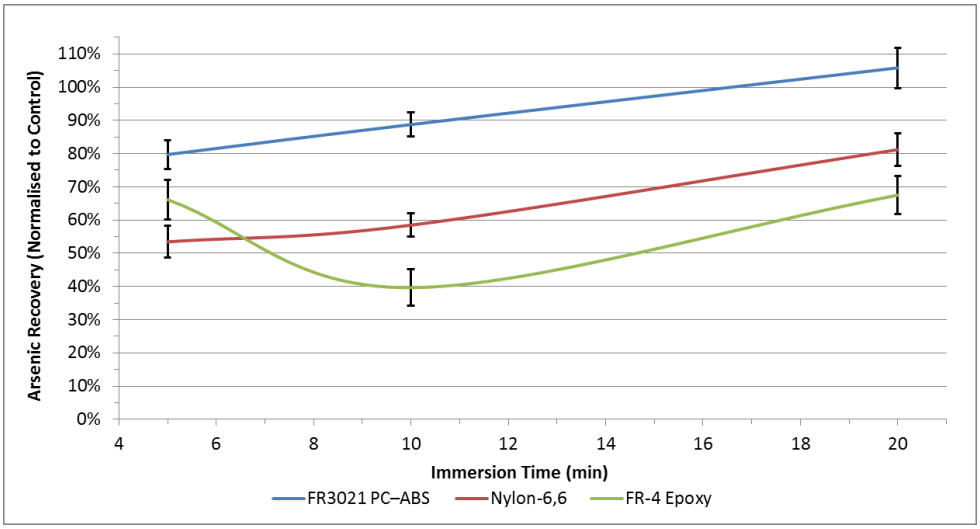

Figure 39: Arsenic Recovery v. Immersion Time in Quiescent FK-5-1-12 by Substrate Material

Arsenic recovery from all coupons was higher than that of bromine. Indeed, arsenic recovery was complete, within the bounds of uncertainty, from PC–ABS coupons, but its recovery from Nylon-6,6 and FR-4 did not exceed 80 % within 20 min of treatment time.

As shown by the rates of recovery, both contaminants were removed from coupon surfaces, even in quiescent fluid conditions. The contaminants evidently had higher affinity for the sorptive media than the surfaces, with the exception of Nylon-6,6. In general, recovery from Nylon-6,6 was lower than from PC–ABS and FR-4 epoxy coupons, indicative of the relatively higher affinity of the contaminants for Nylon-6,6. The tendencies for removal between and among contaminant tracers and substrates were neither consistent, nor consistently monotonic in time, and there was no correlation to surface roughness. However, tracer atom removal, even of low loadings and in quiescent FK-5-1-12, occurred on a scale rapid enough to be operationally relevant. The non-monotonic behaviour of the rates of removal is a possible consequence of individual, independent determinations, and would be averaged by multiple independent determinations.

The predictive strength of INAA in this case is that it is a bulk analytical method, not confined to the surfaces, and requiring no intermediate extraction steps. From this perspective, the results are conservative. However, the major drawbacks of INAA as used in this case are twofold: the lack of

structural information of the contaminants, and the unknown depth of migration of contaminant tracer atoms into the substrates. Surface techniques, as applied to the problem of HDD platter delubrication, could answer the latter question. To cope with the lack of structural knowledge, there is knowledge of the common degradation products of the contaminants. All degradation products that could have been formed (e.g. through oxidation) are less toxic than the original species, with the exception of the oxon-activated form of BrPMe, in which case the Br atom remains on the dichlorophenol ring, and the presence of bromine is still indicative of contamination.[185]

Although removal of contaminants from coupon surfaces was achieved in all cases, not every system achieved the desired ≥ 90 % decontamination efficiency over an operationally relevant 20-min interval, i.e. within the time budget deduced as a requirement. Hence, in keeping with the aim of achieving at least one order of magnitude of removal within this time budget, the model decontamination process required optimisation.

4.2.4 – Process Optimisation

Having demonstrated that contaminant removal by FK-5-1-12 in an entirely passive system was feasible, but not optimal for operational use, flow was introduced into the decontamination system. A flowing liquid would be expected, from theories of mass transfer, to increase removal, albeit at the cost of power input. This is analogous to the increased rate of heat transfer through convection of a moving fluid compared to conduction alone. At the bench scale, flow was imparted to FK-5-1-12 inside decontamination vials by using a rotating platform shaker. For some selective removal techniques on larger scales, e.g. washing of textiles, it may be acceptable to subject the substrate and the fluid to uniform circular motion.[187] For full-scale vibration- and impact-sensitive equipment, however, it would be more prudent to impart motion to the fluid only, through the use of paddles, impellers, or jets. There are additional constraints on achievable liquid flow, including, as previously discussed, the tendency of a liquid to cavitate when its velocity is sufficiently high.

Flow conditions at the bench scale have been non-dimensionalised with respect to fluid properties and system geometry in terms of the Reynolds number, Re, at the centreline of a cylinder (Equation 15). Tangential velocity is the product of radius of rotation $r_{rotation}$ and angular velocity ω. The characteristic length is the hydraulic diameter $\emptyset_{hydraulic}$, and kinematic viscosity υ accounts for fluid density and kinetic viscosity. This convention

corresponds to a forced vortex, i.e. that which is imposed on the liquid by the angular velocity and radius of rotation of the shaker table.

$$\mathrm{Re} = \frac{r_{rotation} \cdot \omega \cdot \emptyset_{hydraulic}}{\nu}$$

Equation 15: Reynolds Number in Tube

The extent of decontamination efficiency as a function of flow condition is depicted in terms of residual As detected within the HDPE coupons in Figure 40. The residual As has been normalised with respect to the total amount of As detected in controls, with blank As responses subtracted, as in all previous depictions of decontamination.

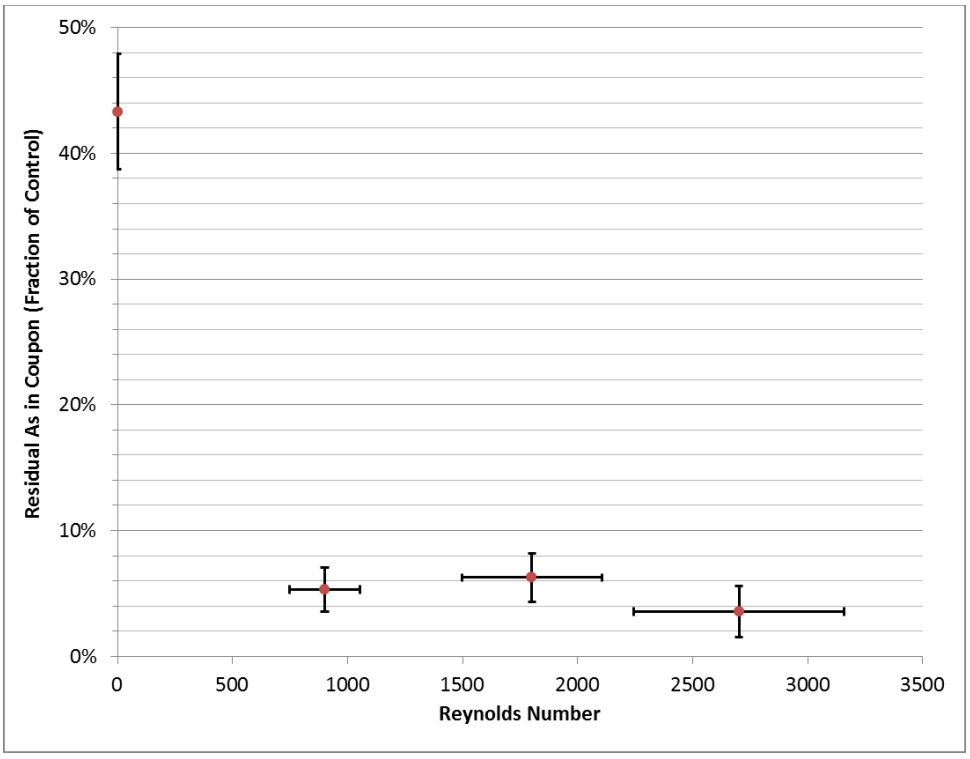

Figure 40: Residual As in Coupons v. Flow Régime

The residual As abundances in laminar (Re < 2300) and transitional (2300 < Re < 4000) conditions, at 3-6 %, are all lower by an order of magnitude than the residual in quiescent conditions (Re = 0), at 43 %, after only 10 min of immersion. Hence, when rapid treatment is essential, power input yields a

return in decontamination efficiency, as expected from theories of mass transfer. An increase in velocity to fully developed, turbulent flow, subject to the velocity constraint at the onset of cavitation, would be expected to result in even more efficient removal.

Having demonstrated the feasibility of a physical decontamination process, that is, removing and entrapping at least one order of magnitude of mass concentration, it was necessary to confirm the suitability of an FK-5-1-12-driven process on representative, functioning equipment, and not simply on material coupons of such equipment.

4.3 – Suitability of FK-5-1-12

The aim of the final stage of experiments was to reconcile the two preceding parts of the research plan. The capabilities of FK-5-1-12 to achieve sensitive equipment decontamination were to be tested against the constraints on its suitability.

4.3.1 – Operational Trials of COTS Equipment

A feasible decontamination procedure will, in principle, be both effective in terms of contaminant removal and well-tolerated by representative items of sensitive equipment. Operational trials of sensitive equipment—laptop computers and night-vision goggles—were therefore complementary to analytical determinations of decontamination effectiveness on individual substrate materials. The trial plan is summarised in Table 7. By considering and testing for likely failure mechanisms at both component and device levels, the overall tolerance of sensitive equipment to the operating conditions brought about by decontamination may be described statistically.

4.3.1.1 – Laptop Trial 1

The first laptop trial was intended to explore possible failure modes, and for this reason, its test procedure differed from the consistent approach used in subsequent trials. Built-in software (Windows Vista Performance and Reliability Monitor) was used to record performance and reliability data automatically. The Quality of Service was measured by the time taken to complete the task of recording 480 MB of data from the hard-disk drive to a recordable compact disc. The decontamination system consisted of a polypropylene reactor in which the base or the screen of the laptop could be immersed in FK-5-1-12. The temperature and electrical continuity of the decontamination system were measured with probes and recorded manually.

The trial was divided into pre-, during-, and post-decontamination phases, with no immersion in the pre- and post- phases.

The results of all operating phases are summarised in Table 13.

Table 13: Laptop Trial 1 Summary

Operating Phase	Burn Time (mm:ss)
Pre-Decontamination	06:42
During Decontamination	06:45
Post-Decontamination	06:12

In the pre-decontamination phase, 480 MB of data were burnt to a recordable compact disc (CD-R) in 6 min 42 s. During the decontamination phase, while the laptop was immersed in FK-5-1-12, the CPU displayed activity for 6 min 45 s, corresponding to the sequence of the previous burn, but the CD-R was ejected automatically with no information having been written, presumably as a result of the mismatch in optical indices of refraction between air and FK-5-1-12. This mismatch would have skewed the propagation of laser pulses from the emitter on the optical drive to the surface of the disc. The multimeter measured electrical discontinuity within the meter's threshold of detection of 1 GΩ·cm, which is consistent with the reported bulk resistivity of FK-5-1-12 of 10^4 GΩ·cm.[188] In the post-decontamination phase, the 480 MB of data were burnt successfully in 6 min 12 s. The orders of magnitude of the average number of HDD bytes transferred were unchanged between the *during* and *post* phases, and the disk's behaviour while attempting to burn data to the CD-R was consistent in both phases. However, the disk transfer rate during decontamination peaked at only 903 transfers·s^{-1}, while it peaked at 3635 transfers·s^{-1} after decontamination.

This trial was intended to explore possible failure modes and evaluate some performance metrics. Although burn time in Table 13 is indicative of the overall QoS, the value for the *during decontamination* phase applies only to HDD operations, since no data were actually burnt to the immersed disc. Indeed, it showed that it was not possible to use an optical drive during immersion in FK-5-1-12 (an expected result), but other laptop sub-systems, including processing, cache, memory, and HDD, continued to operate. However, this trial provided only one datum with which to report device-level reliability in a decontamination process with FK-5-1-12. More trials on untreated equipment were needed to increase the confidence level of statistics for first-pass treatment. Thus, additional trials of the same and similar

equipment were undertaken to determine if equipment failure, and what kind, would be more likely to occur as a result of decontamination.

4.3.1.2 – Laptop Trial 2

In laptop trial 2, a stress-test programme (BurnInTest software) was used for greater commonality of testing and reporting performance metrics. A summary of the incremental pre-, during-, and post-decontamination performance metrics of the second laptop trial, as determined by BurnInTest software, are presented in Table 14.

Table 14: Burn-In Test Results of Laptop Trial 2

Pre-Decontamination			
Sub-system	**Cycles**	**Operations (×10⁹)**	**Errors**
CPU	71	386	0
Hard Disk	3	10.888	0
RAM	18	67.078	0
During Decontamination			
Sub-system	**Cycles**	**Operations (×10⁹)**	**Errors**
CPU	71	390	0
Hard Disk	3	11.028	0
RAM	18	56.922	0
Post-Decontamination			
Sub-system	**Cycles**	**Operations (×10⁹)**	**Errors**
CPU	71	391	0
Hard Disk	3	13.104	0
RAM	18	63.000	0

Evidence for the equipment's apparent tolerance of the decontamination procedure is seen in the zero-count of errors both during and after treatment, the consistent number of cycles, and small variations in the number of hard disk drive and RAM operations.

Following the stress test, the liquid-crystal display only was immersed in FK-5-1-12. Qualitative changes were noted in transmittance of lamp light. Evidently, the FK-5-1-12 was able to penetrate and become entrained in some of the layers of the display to cause such visible changes. However, no visible aberrations were observed 18 hours after removal from the fluid, during which the FK-5-1-12 was able to evaporate, as shown in Figure 41.

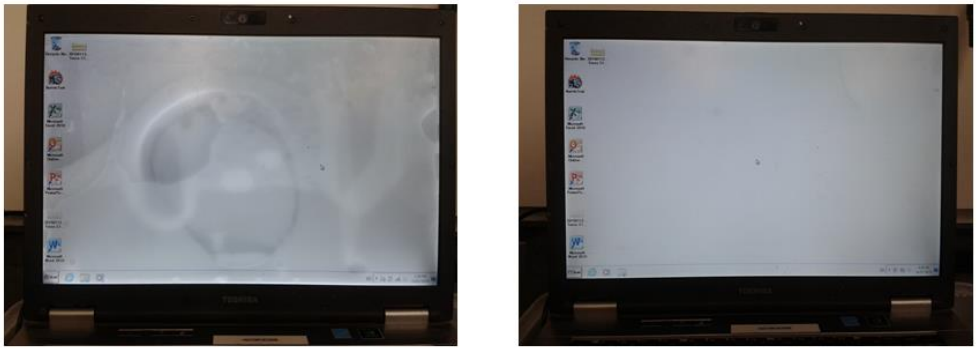

Left: Thin-Film Transistor screen 13 min after immersion in FK-5-1-12

Right: Thin-Film Transistor screen 18 hrs 23 min after immersion in FK-5-1-12

Figure 41: Thin-Film Transistor Screen after Immersion in FK-5-1-12

The presence of optical aberrations in the former case but not the latter is similar to the performance of the CD-R in Trial 1. That is, the presence of FK-5-1-12 in the light path caused a transient change in operation, but once the liquid evaporated, there was no discernible change in operation. These observations are qualitative, however, and do not relate to the quantitative reliability of liquid-crystal displays immersed in FK-5-1-12.

4.3.1.3 – Laptop Trials 3 and 4

Laptop trials 3 and 4 used the same laptops as in the preceding trials; these were subjected to a second decontamination treatment. Before presenting the results of the stress test, it is important to note the behaviour of laptop 1 during this procedure. During trial 3, immediately after the decontamination phase, one of the three rotating mechanisms in the laptop produced audible noise. After 5 min, the laptop ceased to 'echo' keyboard and mouse inputs to the screen. After another 2 min, the system clock did not display an increment in minutes. Finally, 1 min later, the operating system initiated a crash dump. The laptop was removed from the FK-5-1-12, drained, and rebooted. During the boot-up cycle, the built-in operating system (BIOS) did not recognise the presence of a bootable device (i.e. the HDD). The laptop was left in a fume-hood for 18 hours to allow entrained FK-5-1-12 to evaporate.

With the FK-5-1-12 evaporated, solid particulate matter in the upper right-hand part of the reactor was observed. Elemental analysis of the solid particulate by INAA determined the presence of Br, As, Mn, Na, and Cl, though these could not be quantitated. The presence of Na and Cl in the particulate may be attributable to ions in the ambient or to displaced skin secretions in

contact with the laptop case and keys. The other elements are less likely to have originated from ambient particulate matter. However, the presence of these substances did not change the measured resistance of the FK-5-1-12 fluid.

The laptop was cycled off and on three times in the next 50 min. After the third cycle, the BIOS booted successfully, the Windows OS attempted to initialise, and the user was prompted for Startup Repair, which was unable to correct the fault. System Restore was attempted next but was unable to find the OS loader files. A BIOS start-up test indicated no faults with CPU or RAM, but revealed HDD failure with a 21 % loss of HDD data volume. A 4-hour, 9-min BIOS-level HDD reformatting operation was attempted, and this successfully restored the factory HDD image.

Subsequent stress-testing of the CPU, HDD, and RAM of laptop #1 at a 50 % duty cycle resulted in deviations in performance with respect to pre- and during-decontamination phases. The laptop did not echo keyboard and mouse inputs at 9 min 36 s into this stress test. Restarting the laptop in Safe Mode and repeating the stress test yielded a fourth set of performance results. These sets are compared in Figure 42 and Figure 43.

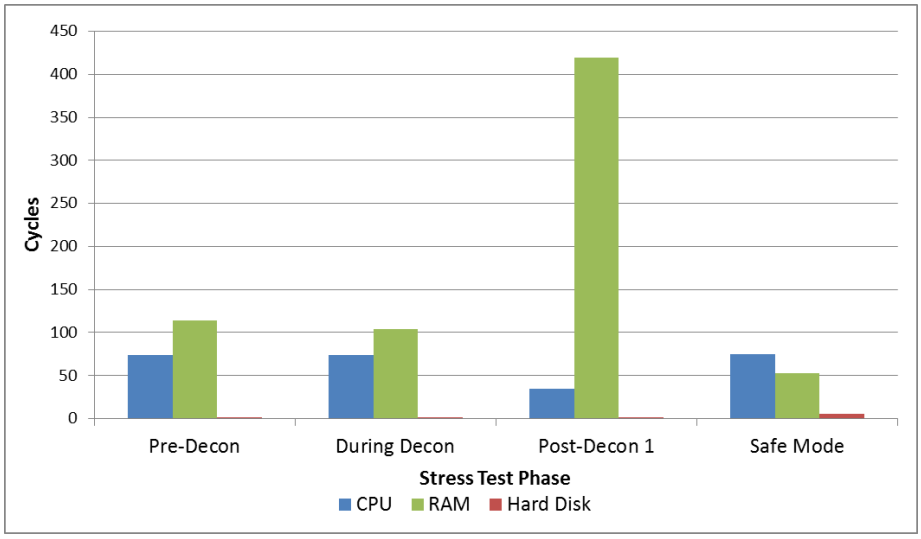

Figure 42: Trial 3 – Laptop #1, 2nd Pass Stress Test Cycles

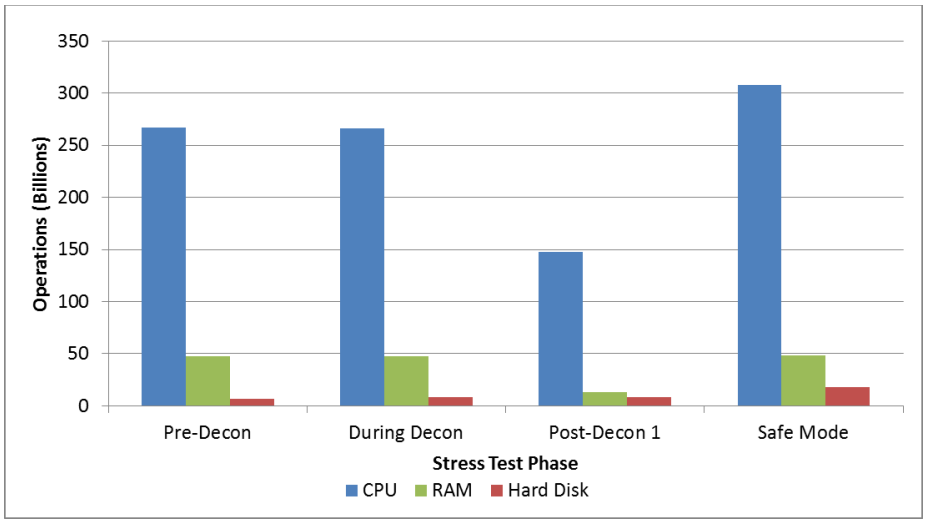

Figure 43: Trial 3 – Laptop #1, 2nd Pass Stress Test Operations

The physical integrity of the HDD, as it turned out, was not catastrophically compromised, and the factory-set HDD partition, along with basic functionality, was restored. Indeed, the number of memory and HDD operations completed during the 20-min stress test in Safe Mode was larger than before decontamination. However, subsequent BIOS-level self-tests revealed a permanent (post-reformatting) loss of 3 % HDD volume. This

permanent failure was likely a consequence of decontamination treatment, but it was beyond the analytical scope of the project to attribute a mechanism to it.

The results of trial 4 with laptop #2 are depicted in Figure 44 and Figure 45.

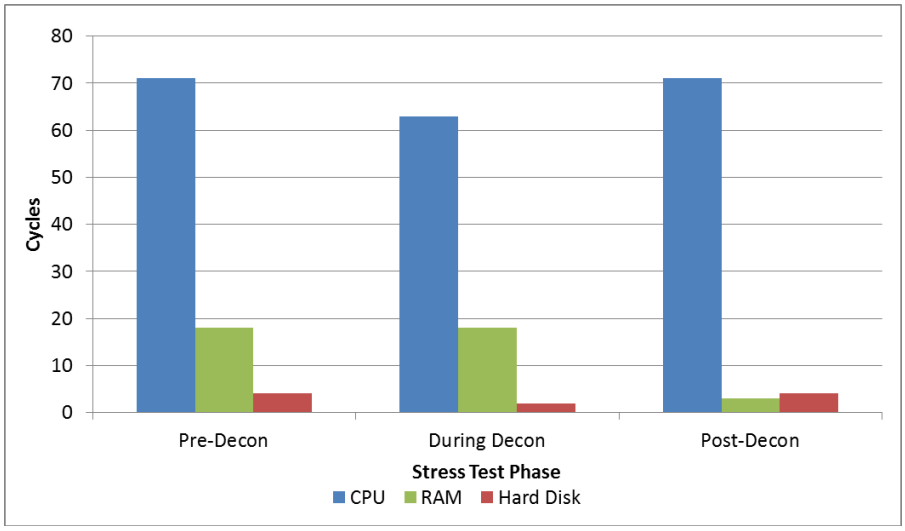

Figure 44: Trial 4 – Laptop #2, 2nd Pass Stress Test Cycles

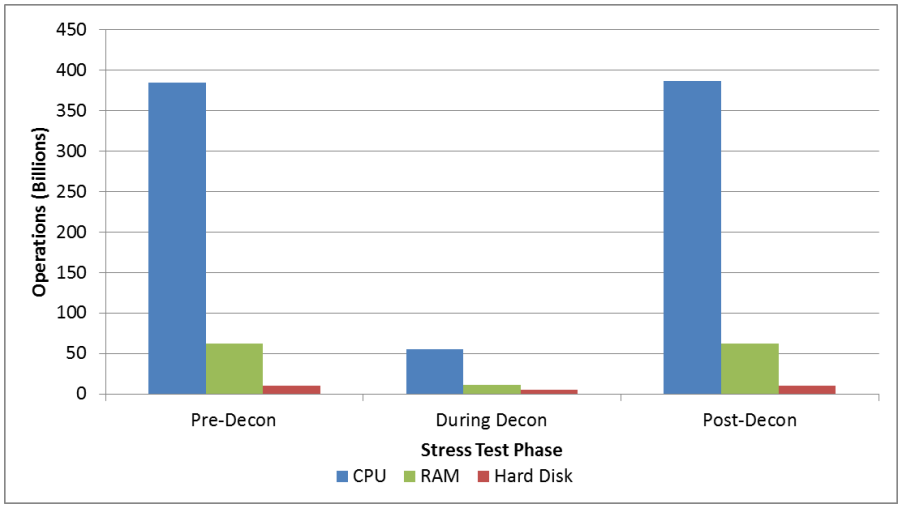

Figure 45: Trial 4 – Laptop #2, 2nd Pass Stress Test Operations

There was a reduction in QoS as seen in the lower number of CPU, RAM, and hard-drive cycles and operations completed in 20 min during decontamination. Unlike trial 3, no post-decontamination failures were detected, and its performance in terms of number of operations post-decontamination varied ≤ 1.3 % compared to the pre-decontamination case.

For more rigorous evaluation of possible effects on reliability, SMART metrics were also available in this trial, the results of which are shown in Figure 46. SMART metrics have been normalised with respect to their readings after the successful first-pass immersion decontamination.

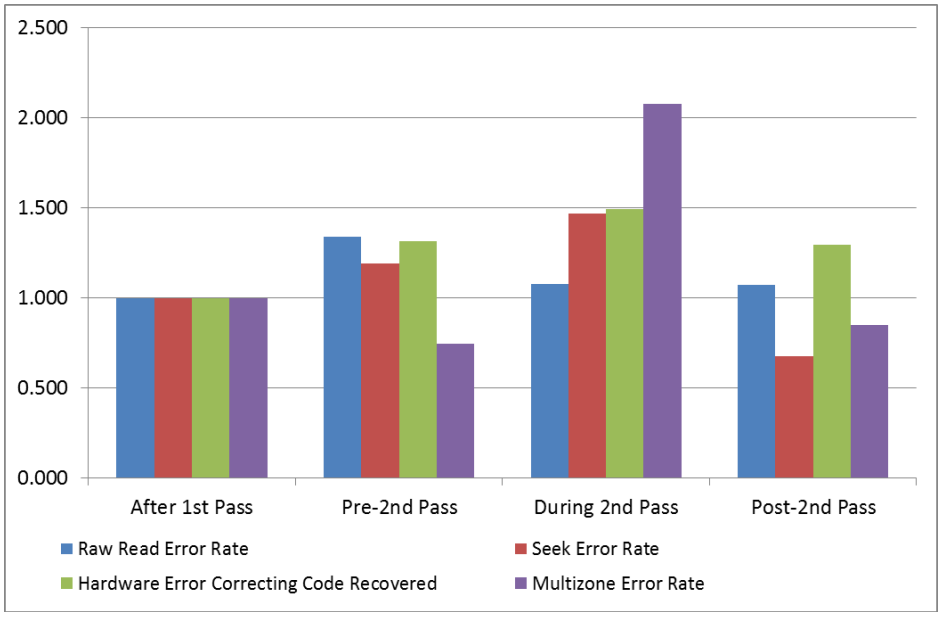

Figure 46: Trial 4 – Laptop #2, 2nd Pass Normalised Reliability Metrics

Figure 46 suggests that, on a trial phase-to-phase basis, there would be a greater likelihood of transient HDD hardware errors occurring during immersion in FK-5-1-12, since the multizone error rate increased twofold during the second-pass immersion compared to its reading after the first pass.

Such early results were informative only to the extent that they allowed a 'test to failure, design for success' trial plan. Additional replications of this common trial plan were needed to increase the statistical power of observations.

4.3.1.4 – Laptop Trials 5 to 16

The next objective was to test the null hypothesis that there would be no significant differences between the mean performance and reliability of devices subjected to decontamination and those not subjected. Further replications of the standard trial method developed for trial 4 would also serve to increase statistical power and decrease the likelihood of attributing effects to any kind of treatment (i.e. Type II statistical errors).

Among laptops #3 to 8, there were no CPU, HDD, or RAM errors recorded after first- and second-pass treatments. There were also no increments recorded in

the SMART reliability identities most closely associated with early failure (5, 7, 196, 198, or 199) during the twelve subsequent trials.

4.3.1.5 – Laptop Trial Summary

With a sample of n = 7 laptops, a post-decontamination reliability rate of 90 % was demonstrated at a confidence level of 50 %, according to Equation 1. The failure of laptop #1, rather than setting the rule, proved to be the exception. In the entire population (n = 8, 16 trials), no failures occurred in first-pass treatment. After second-pass treatment, one permanent failure was noted in the reduction in available HDD volume of laptop #1. Although no catastrophic failures occurred, timely replacement of laptop #1 or its HDD following second-pass treatment would have been necessary in the field.

Twenty paired, two-tailed *t*-tests were conducted to test for hypothetical changes in performance and reliability that could be attributed to the decontamination process. The discrete numbers of operations of the key sub-systems (CPU, HDD, and RAM, as determined through stress-testing) were used to quantify performance effects, including errors, if any, and QoS. The increments in raw values of SMART data were used to quantify reliability effects. For n = 6 laptops of the same make, the only significant (at α = 0.01) effects of any kind were observed reductions in CPU and RAM operations at both first- and second-pass treatments (Table 15). The sample means of both *CPU Ops* and *RAM Ops* declined by factors of 0.33 and 0.44 during first-pass treatment. Sample standard deviations increased by factors of 12.5 and 29.3. Hence, there were system-level reductions in throughput QoS as well as higher variation in throughput.

Table 15: Selected Performance Metrics of Laptops #3-8

			Before First-Pass Treatment		During First-Pass Treatment	
Laptop #	**Make**	**Model**	**CPU Ops ($\times 10^9$)**	**RAM Ops ($\times 10^9$)**	**CPU Ops ($\times 10^9$)**	**RAM Ops ($\times 10^9$)**
3	Toshiba	Tecra S11	829	49.321	449	17.092
4	Toshiba	Portégé M780	863	48.539	641	38.811
5	Toshiba	Portégé M780	833	49.594	439	20.259
6	Toshiba	Portégé M780	833	49.274	457	18.505
7	Toshiba	Portégé M780	831	49.568	839	43.535
8	Toshiba	Portégé M780	832	49.653	453	18.266
		Mean:	838	49.259	565	27.640
		Standard Deviation:	14	0.427	175	12.516

These reductions in QoS could have occurred for many reasons. A likely explanation is that built-in thermal management systems (Intel SpeedStep software) automatically 'throttled-down' CPU and memory performance once the laptop was immersed.[189] Upon immersion, laptops #4-8 displayed a dialogue box, "Warning: Problem with Cooling System Detected" in all but two cases: the first-pass treatment of laptop #7 (in Table 15, above) and the second-pass treatment of laptop #8. Both of these cases also showed the least differences in performance compared to their respective pre-decontamination phases. The warning dialogue box was likely the result of low fan speed measurement rather than a true lack of heat dissipation.[190] Video of the laptop fan pushing FK-5-1-12 liquid showed cyclic operation: movement for 3 (± 0.5) s, stopping, then a 5-s delay, after which movement resumed. The temperature in the bulk of the FK-5-1-12 fluid during decontamination, as recorded by laptops' built-in temperature sensors and by temperature probes, was only 1-2 °C above the laboratory temperature, and was 20-30 °C lower than the typical fan exhaust air temperature. No temperature measurement was correlated with a "Problem with Cooling System Detected" warning. Although it displaced convective cooling air, FK-5-1-12 itself would have acted as a conductive heat-transfer fluid. The fan, in attempting to impart momentum to the FK-5-1-12, experienced higher drag than if it had been moving air, and drew more than its allocated power budget when trying to reach its operating point. This power draw would have been curtailed by

Operating System-directed Power Management (OSPM).[190] Therefore, the fan never reached its operating point. It seems most likely that the OSPM instructions issued a low Fan Speed Level notification, causing the fan to attempt to reach its operating point again and again, only to exceed its power budget and be stopped cyclically.

Only at a threshold of $\alpha = 0.05$ was there a significant effect that could be attributed to any of the measured reliability metrics. This effect was observed in the increments of raw values of load cycle count between the 'before-first pass treatment' and 'during-first pass treatment' phases. The observed increments represented, if anything, an improvement in reliability, i.e. a lower incidence of the HDD head moving into a standby position and therefore steadier performance (Table 16).

Table 16: Reliability Metrics of Laptops #3-8

			Before First-Pass Treatment	**During First-Pass Treatment**
Laptop #	**Make**	**Model**	**ΔLoad Cycle Count**	**ΔLoad Cycle Count**
3	Toshiba	Tecra S11	4	9
4	Toshiba	Portégé M780	6	4
5	Toshiba	Portégé M780	135	21
6	Toshiba	Portégé M780	179	24
7	Toshiba	Portégé M780	98	21
8	Toshiba	Portégé M780	85	32
		Mean:	85	19
		Standard Deviation:	70	10

When the load cycle count was normalised with respect to the number of *CPU Ops*, higher performance throughput per load cycle count was also found to have occurred during treatment. The *before* and *during* increments in load cycle count were tested for normality by linear regression on quantile–quantile plots.[191] The transformed increments were both determined to have correlation coefficients of 0.94 with respect to a theoretical normal distribution—marginally less than 95 %, but not a gross violation of the assumption of normality. Even so, it would be prudent not to attribute a positive effect on HDD reliability to immersion in FK-5-1-12 because of the

small number of items tested and other risks, to be discussed in the following section.

Apart from the permanent and transient failures in laptop #1 after second-pass treatment, no errors in performance testing, and no increments in failure-indicative reliability data, were accrued in the other devices.

4.3.1.6 – Process Residue and Possible Delubrication

The mass of residue recovered from the reactor after laptop trials was ≤ 1 mg as determined by weighing swipes. Typically, two phases were observed: solid particulate matter at the back, and a thin layer of viscous liquid film in the centre.

The particulate matter was suspected to have included ambient airborne contaminants, desorbed from the laptop shell and components after their immersion in FK-5-1-12. The liquid phase was suspected to include lubricants from laptop mechanical components and human sebum from contact with the laptop shell and keys. Displacement of lubricants from laptop mechanisms could prove detrimental to reliability, and so this possibility was tested.

On five occasions after decontamination, the liquid film residue was sampled, extracted with hexane, and analysed by gas chromatography with flame ionisation detection. Among the aliquots (n = 12) of extractable liquid, hydrocarbon chain lengths of C_{16} to C_{34} were found to be most abundant. These are shown in Table 17, with the hexane responses subtracted.

Table 17: Relative Abundances of Extractable Hydrocarbons in Film Residue

Chain Length	Mean Abundance	Standard Deviation
C_{10} to C_{15}	4.79%	3.23%
C_{16} to C_{34}	82.30%	3.71%
≥ C_{35}	12.92%	1.27%

Shorter-chain hydrocarbons may also have been present immediately after decontamination, but these would have evaporated more rapidly than longer-chain fractions. The readings are likely to have originated either from non-fluorinated, hydrocarbon base-oil esters, e.g. a C_{23} diester commonly used in synthetic lubricants,[192] or from squalene, free fatty acids, wax and cholesterol esters of comparable backbone length in deposited sebum.[193] Further identification of the film residue was not feasible during these trials, but would merit further investigation for effects on the long-term reliability of decontaminated computers. In particular, it would be instructive to

determine with greater certainty the identity and origin of the constituents of the process residue. Removal of true contaminants from the ambient and from deposited sebum would be beneficial, but depletion of critical fluorinated and non-fluorinated lubricants would be detrimental.

4.3.1.7 – Monocular Night-Vision Goggle Trials

The final test item was a civilian-pattern monocular night-vision goggle (MNVG). The MNVG required different test methods than laptop computers because of its different construction and operating principles. Spectrometric analysis was used to quantify any changes in its performance that may have resulted from decontamination using FK-5-1-12.

The baseline (pre-decontamination) performance of the MNVG is shown as the transmittance spectrum through its electro-optics assembly (Figure 47).

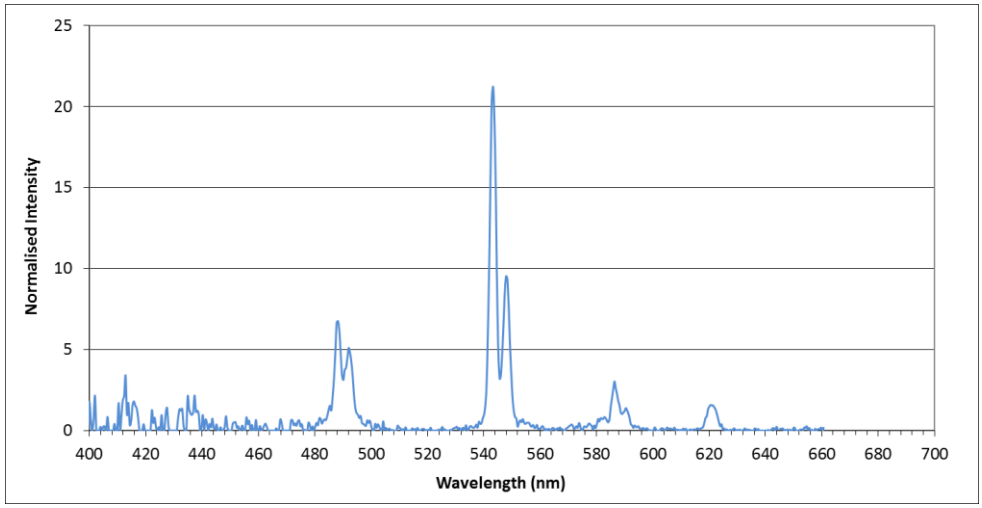

Figure 47: Pre-Decontamination Normalised Transmittance Spectrum through MNVG – Visible Region

The trace is normalised with respect to the peaks of the arc lamp discharge. Peak heights depict the amplification of available light and bandwidths correspond to those characteristic of emissions of Tb(III) as the dopant in the phosphor (Table 18).[194]

Table 18: Characteristic Wavelength Emissions of Tb(III)

Wavelength (nm)	Electronic Transition
488, 492	$^5D_4 \rightarrow {}^7F_6$
543, 548	$^5D_4 \rightarrow {}^7F_5$
586, 591	$^5D_4 \rightarrow {}^7F_4$
620	$^5D_4 \rightarrow {}^7F_3$

The operation of the built-in infrared flashlight in normal and high-intensity modes was also confirmed at the pre-decontamination phase.

The MNVG continued to operate throughout the simulated decontamination phase (while immersed) but its transmittance spectrum was only analysed after it was withdrawn. Normalised transmittance spectra, including the absolute difference between pre- and post-decontamination phases, are summarised in Figure 48. The arc lamp transmission spectrum is included to show the quantisation of incident light achieved by the MNVG in all trial phases.

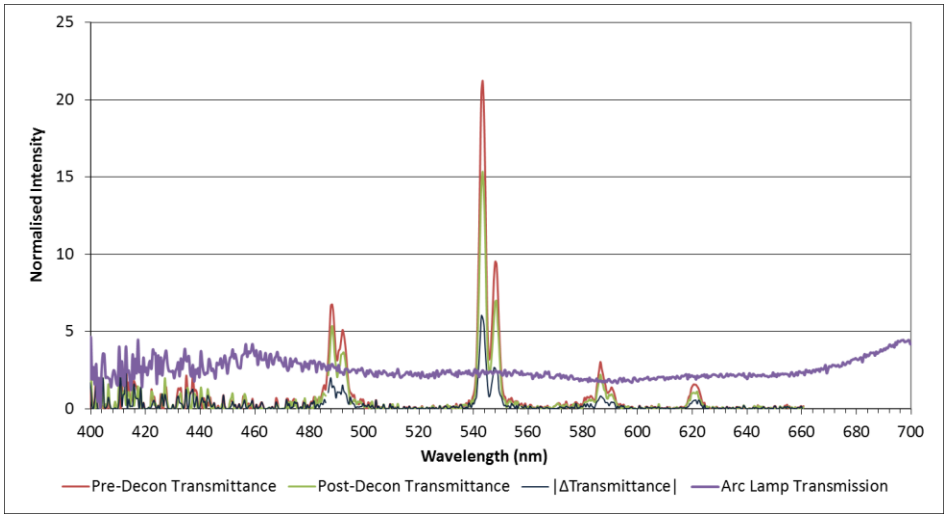

Figure 48: Comparison of Normalised Transmittance Spectra through MNVG – Visible Region

The traces do not show an absence of a particular wavelength in the post-decontamination case, which would be evidence of phosphor depletion. Traces cannot be integrated for direct comparisons of intensity because of the fluctuations within each spectrum and geometric uncertainties in the centreline of the apparatus. Fluctuations are also apparent in the normalised transmittance spectra with the IR flashlight activated, which are shown in

Figure 49. Peak intensities post-decontamination, captured twice as *Post-Decon Transmittance* and *Post-Decon Transmittance 2*, appear to exceed those of the baseline trial, but this is also a consequence of fluctuations.

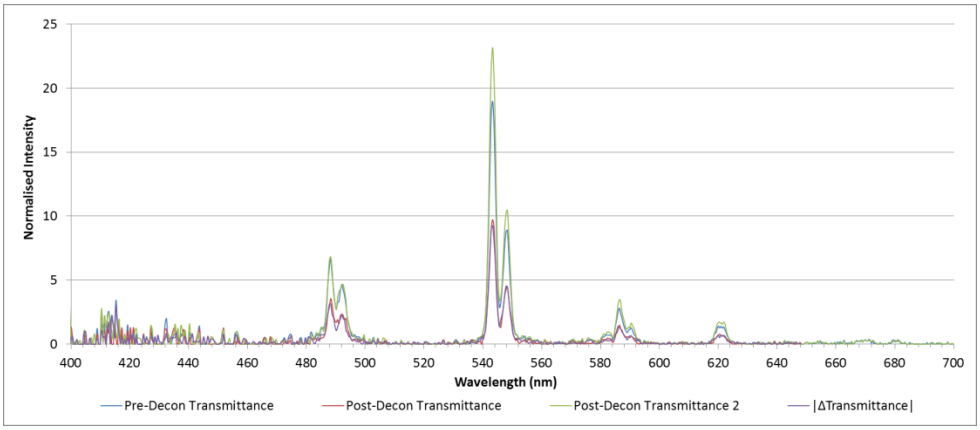

Figure 49: Comparison of Normalised Transmittance Spectra through MNVG with IR Flashlight On – Visible Region

The coincidence of peaks at the relevant wavelengths appears to show a lack of permanent chromatic aberration and a lack of phosphor depletion, as detectable at the aperture of the CCD, after 20 min of immersion in FK-5-1-12. If the phosphor had been depleted, then there would have been no emission at those wavelengths for either *Post-Decon Transmittance* trace. Most important, the device continued to function during and after immersion. When the device was de-energised and the gasketed battery compartment was opened 50 min after withdrawal from the liquid, residual FK-5-1-12 wept out from inside the compartment. The maximum extent of penetration within the assembly was not known during this trial.

Many improvements to this trial method are possible, including a larger sample size and quantitative comparisons of the MNVG electronic circuits before and after decontamination. The sample size was small on account of financial and procurement constraints, but it could be expanded by testing representative coupons or sub-assemblies (e.g. individual coated lenses), in keeping with the logic of testing printed circuit board and hard-disk drive material coupons instead of entire hardware assemblies.

4.3.2 – Fluid Retention and Recovery

The rates of evaporation of FK-5-1-12 fluid elements were measured at a rate of heat gain (obtained through numerical simulation) that could be expected in operational conditions in which the ambient temperature could approach 49 °C: in particular, NATO climate conditions A1 and A2.

Starting at a laboratory temperature of 23 °C and barometric pressure of 0.997 bar, FK-5-1-12 was gradually brought to boil. Visible convection currents and nucleation were observed at 31.0 (± 0.1) °C. At the onset of observable boiling, system temperature was 49.4 °C and the flow rate of vapour exiting the system was measured to be 8.6 (± 0.6) $g \cdot s^{-1}$. Under these conditions, and with an enthalpy of vaporisation of approximately 88 $kJ \cdot kg^{-1}$, the resultant cooling load to condense the vapour was estimated to be 0.78 (± 0.07) $kW \cdot kg^{-1}$ of fluid.

The experiment was repeated at a laboratory temperature of 21 °C and barometric pressure of 1.005 bar. Convection currents and nucleation were observed at 24.0 °C. At this higher ambient pressure, the fluid did not boil until 49.7 (± 0.1) °C, however, and the cooling load at this temperature was estimated to be 0.60 (± 0.05) $kW \cdot kg^{-1}$ of fluid.

The logistical burdens of removing 0.6 to 0.8 kW of latent enthalpy per kg of vapour (approximately 1 $kW \cdot L^{-1}$ of fluid near the boiling point), in addition to removing vapour superheat at altitude, could prove significant to a field-deployed task force relying on diesel-powered generators. It would be preferable to avoid evaporative phase change and superheating, and mitigate the power requirement associated with condensing FK-5-1-12 vapour, through the judicious use of cold storage, passive insulation, and refrigeration. The order of magnitude of the cooling load associated with refrigeration (0.025 $kW \cdot kg^{-1}$) is lower and more practicable in austere, deployed conditions than the load for condensation. With effective insulation, this load could be decreased even further. Alternatively, a molecule having similar chemical and dielectric properties as FK-5-1-12, but a higher boiling point, could be procured in order to satisfy the environmental operating requirement of NATO climate A1 without powered cooling. Although the patent for FK-5-1-12 includes formulae for such molecules,[145] none is currently available on the market.

5. Summary

FK-5-1-12, a commercially available perfluorinated ketone, was evaluated for its fitness as part of a deployable sensitive equipment decontamination system. It was tested with analytical chemical methods to determine its physical properties and reactivity with select nucleophiles, as well as its effectiveness in removing contaminants, such as organic compounds and biocides, from sensitive materials. It was also tested according to the methods of reliability engineering so as to evaluate its compatibility with representative full-scale Commercial-off-the-Shelf equipment, including laptop computers and night optics.

Based upon previous research by others, FK-5-1-12 was suspected to react as would an acyl halide, through nucleophilic acyl substitution, with elimination of its electronegative HFC-227ea moiety as a leaving group. The possible reaction mechanisms of FK-5-1-12 with nucleophiles including alcohols, thiols, and amines were studied using Fourier-transform infrared and nuclear magnetic resonance spectroscopy. Short-chain 1° and 2° alcohols reacted with it to yield fluorinated esters, but 3° alcohols were too sterically hindered to react in the conditions studied. The presence of a 1° amine function, either alone or with other nucleophilic functions in a reagent, was determined to produce the most rapid reactions with FK-5-1-12. It generated amide products, likely through a nucleophilic acyl substitution mechanism. The reaction between FK-5-1-12 and neat amines, unlike water, alcohols, or diluted amines, was observed to evolve heat and gases rapidly, which could damage the integrity of the substrate material and lead to their failure. FK-5-1-12 reactivity with 1° thiols was not satisfactorily ascertained in this project.

Immersion of contaminated sensitive substrate materials in quiescent FK-5-1-12 was shown to repel the contaminants from surfaces within minutes, although there were definite differences attributable to substrate material affinities for contaminants. Such performance is consistent with the time and efficiency requirements deduced for a deployable decontamination system, but would require optimisation before being scaled-up. Subsequent trials showed that it was feasible to recover contaminants in commonly available sorptive media—granular activated carbon and cellulose—through a parallel sorption process. Contaminant mass balance of the components of the bench-scale decontamination process revealed that contaminant removed from surfaces was entrapped in sorptive media, where it tended to remain. This result increases the confidence of FK-5-1-12-based decontamination as a risk-reduction measure.

The trade-off between decontamination efficiency and power input was quantified, with the demonstration that a transitional flow régime achieved an order of magnitude higher decontamination than did quiescent conditions over the same time interval, as expected from theories of mass transfer. Since an upper limit of achievable velocity before the onset of cavitation is known through other studies, there is further room to optimise contaminant mass transfer by FK-5-1-12, e.g. by developing fully turbulent flow.

Equipment reliability trials on energised laptop computers with stress-testing programmes were intended to provoke the most likely transient and permanent failure modes and establish meaningful reliability metrics. No failures of any kind occurred during first-pass immersion of any laptop, and only one permanent failure (loss of 3 % of hard-disk drive volume) occurred in one laptop after successful second-pass treatment, over sixteen trials in all. It is likely that FK-5-1-12 can displace desired surface treatments, such as lubricants, from sensitive equipment, which is assessed to be a common risk for many decontamination schemes.

Transient failures in reading and writing optical media were observed. These failures confirmed the hypothesis that digital optical communications are fundamentally incompatible with immersion in FK-5-1-12 as a consequence of mismatch of indices of refraction. On the other hand, an analogue electro-optical device did not exhibit signs of failure—corrosion, wear, or phosphor depletion—as a result of a single immersion in FK-5-1-12. Liquid crystal displays also appeared, qualitatively, to tolerate short-duration immersion.

FK-5-1-12 had previously shown no deleterious effect to the operation of solid-state memory devices. For laptop computers, immersion in FK-5-1-12 sometimes caused 'down-throttling' of performance of solid-state systems, likely because of increased resistance to fan motion in liquid as opposed to air. Otherwise, short-duration immersion in FK-5-1-12 did not appear to harm the performance or reliability of solid-state electronic equipment.

By virtue of its physico-chemical properties, FK-5-1-12 is apparently capable of immersion-cleaning sensitive substrate materials of some surface-deposited contaminants, and hence may be useful as a physical decontaminant on deployed military operations. However, its use may be constrained in very hot climatic conditions, in which engineered controls—either pressurisation or refrigeration—would be required to avoid superheating and unwanted evaporative losses. Alternatively, a similar but longer-chain molecule could be procured that would be expected to achieve similar results in terms of decontamination but would have a higher boiling point. FK-5-1-12 should in

any case be protected from ultraviolet radiation and moisture to avoid premature degradation.

In summary, FK-5-1-12 may satisfy some of the effectiveness, efficiency, and environmental requirements of a physical decontaminant for a field-deployable sensitive equipment decontamination system. Owing to its observed chemical reactivity and physical properties, it may not be suitable for deployment against all contaminants and in all climatic conditions.

6. Future Direction

The course of this project has suggested further research in four areas. First, additional compatibility trials between FK-5-1-12 and sensitive equipment would increase the confidence in its inclusion in a decontamination system. Were incompatibilities to be found, these would evidently diminish its fitness for decontamination. One example of possible incompatibility that merits further investigation is of lubricant depletion, which could be tested further on representative material coupons (e.g. hard-disk platters) through surface techniques.

Second, in a similar vein, further study is warranted into the mechanisms, kinetics, and thermodynamics of possible FK-5-1-12 reactions, particularly with species containing hydroxyl, amine, and thiol functions. The results of such studies could be margins of safety—both to equipment and to personnel—in the deployment of FK-5-1-12 as a decontaminant.

A third topic would be to find an optimal balance between decontamination effectiveness and suitability, comparing FK-5-1-12 to established technologies. There may be no currently available technologies that, alone or in combination, will adequately satisfy performance and logistical requirements. As suggested in the review of the literature and patents, a system based upon air, vacuum, or inert fluid may be the most generally effective against a range of contaminants, and yet minimally detrimental to the widest variety of sensitive substrate materials and equipment. Full life-cycle costs and environmental impacts, including of power systems and waste management, would also figure into such an optimisation calculation.

Furthermore, there may be policy alternatives to resolve the capability gap of sensitive equipment decontamination. It may be more attractive to dispose of COTS equipment than to adhere to hard requirements for decontamination of all deployable equipment to a Thorough standard. It was accepted in the terms of this project that mass disposal of contaminated equipment was not a feasible option, but such a policy may prove acceptable as limited-lifetime COTS equipment becomes increasingly prevalent. Together, these lines of research could lead to a full-scale capability as envisioned for the decontamination of deployed forces.

References

1. Medina VF, Brandon DL, Hay KJ, Khona DS, Smith HK, Morrow AB. Environmental Assessment during Intelligence Preparation of the Battlefield (IPB) – Evaluation of the TIC-Master Computer Program (Report ERDC TR-12-5). Washington, DC: United States Army Corps of Engineers Engineer Research and Development Center Environmental Laboratory; 2012.

2. Marrs TC, Maynard RL, Sidell FR. Chemical Warfare Agents: Toxicology and Treatment. 2nd Edition. Chichester, West Sussex: John Wiley & Sons; 2007.

3. Sutto TE. Prioritisation and Sensitivity Analysis of the Inhalation/Ocular Hazard of Industrial Chemicals (Report NRL/FR/6364--11-10,211). Washington, DC: Department of the Navy; 2011.

4. Bubbico R, Mazzarotta B. Accidental Release of Toxic Chemicals: Influence of the Main Input Parameters on Consequence Calculation. Journal of Hazardous Materials 2008;151:394-406.

5. Scheringer M, Strempel S, Hukari S, Ng CA, Blepp M, Hungerbuhler K. How Many Persistent Organic Pollutants should we Expect? Atmospheric Pollution Research 2012;3:383-91.

6. de Nevers N. Air Pollution Control Engineering. New York, New York: McGraw-Hill; 1995.

7. Massolo L, Rehwagen M, Porta A, Ronco A, Herbarth O, Mueller A. Indoor–Outdoor Distribution and Risk Assessment of Volatile Organic Compounds in the Atmosphere of Industrial and Urban Areas. Environmental Toxicology 2010;25(4):339-49.

8. Atkinson R. Atmospheric Chemistry of VOCs and NO_x. Atmospheric Environment 2000;34:2063-101.

9. Jørgensen RB, Bjørseth O, Malvik B. Chamber Testing of Adsorption of Volatile Organic Compounds (VOCs) on Material Surfaces. Indoor Air 1999;9:2-9.

10. Chemical, Biological, Radiological and Nuclear Defence Operating Concept. Ottawa, Ontario: Department of National Defence; 2012.

11. Winkler RL. Uncertainty in Probabilistic Risk Assessment. Reliability Engineering and System Safety 1996;54:127-32.

12. Technical Guidance for Assessing Cumulative Environmental Effects Under the Canadian Environmental Assessment Act, 2012; 2015. https://www.ceaa-acee.gc.ca/default.asp?lang=En&n=B82352FF-1&offset=11&toc=show

13. Klaassen CD. Casarett and Doull's Toxicology: The Basic Science of Poisons. 5th Edition. New York, New York: McGraw-Hill; 1996.

14. Ellison DH. Handbook of Chemical and Biological Warfare Agents. 2nd Edition. Boca Raton, Florida: CRC Press; 2008.

15. Boone CM. Present State of CBRN Decontamination Methodologies (Report TNO-DV 2007 A028). Rijswijk, the Netherlands: Nederlandse Organisatie voor Toegepast Natuurwetenschappelijk Onderzoek; 2007.

16. Canadian Forces Joint Publication 3-8: Chemical, Biological, Radiological, and Nuclear Defence. Ottawa, Ontario: Department of National Defence; 2012.

17. Girard S, Martel A, Berger J, Boukhtouta A, Chouinard M, Ghanmi A, Guitouni A. Canadian Forces Overseas Supply Network: Strategic Need and Design Methodology (Report CIRRELT-2008-34). Montréal/Québec, Québec: Centre interuniversitaire de recherche sur les réseaux d'entreprise, la logistique et le transport; 2008.

18. Buckley DH. Tribology Series 5 - Surface Effects in Adhesion, Friction, Wear, and Lubrication. New York, New York: Elsevier Scientific Publishing Company; 1981.

19. Elimelech M, Gregory J, Jia X, Williams RA. Particle Deposition and Aggregation: Measurement, Modelling, and Simulation. Woburn, Massachusetts: Butterworth-Heinemann; 1995.

20. Rowe AW, Counce RM, Morton III SA, Hu MZ-, DePaoli DW. Oil Detachment from Solid Surfaces in Aqueous Surfactant Solutions as a Function of pH. Industrial and Engineering Chemistry Research 2002;41:1787-95.

21. Unal H, Mimaroglu A, Kadıoglu U, Ekiz H. Sliding Friction and Wear Behaviour of Polytetrafluoroethylene and its Composites Under Dry Conditions. Materials and Design 2004;25:239-45.

22. Israelachvili JN. Intermolecular and Surface Forces. 3rd Edition. Waltham, Massachusetts: Academic Press; 2011.

23. Freire MG, Carvalho PJ, Queimada AJ, Marrucho IM, Coutinho JAP. Surface Tension of Liquid Fluorocompounds. Journal of Chemical Engineering Data 2006;51:1820-4.

24. Sirimaharaj M, Balachandran C, Chan WC, Hunyor AP, Chang AA, Gregory-Roberts J, Hunyor AB, Playfair TJ. Vitrectomy with Short Term Postoperative Tamponade using Perfluorocarbon Liquid for Giant Retinal Tears. British Journal of Opthamology 2005;89(9):1176-9.

25. Basu S, Nandakumar K, Masliyah JH. A Model for Detachment of a Partially Wetting Drop from a Solid Surface by Shear Flow. Journal of Colloid and Interface Science 1997;190:253-7.

26. Feng H, Barbosa-Cánovas GV, Weiss J. Ultrasound Technologies for Food and Bioprocessing. New York, New York: Springer Science+Business Media; 2011.

27. Franklin RW, Miedema JG, Robbins JN. The Decontamination of Sensitive Electronic Equipment - Applied Military Science Project Report. Kingston, Ontario: Royal Military College of Canada; 2013.

28. Fowler DE, Duque R, Anoikin T, Zhou J. Protecting the Head/Disk Interface from the Chemical Environment with Disk Drive Filtration. IEEE Trans Magn 2003;39(2):769-74.

29. Statement of Operational Requirement 00002253: Canadian Forces CBRN Decontamination System (Revision AL5). Ottawa, Ontario: Chief of Force Development, Department of National Defence; 2011.

30. North Atlantic Treaty Organisation Allied Environmental Conditions and Test Publication AECTP-200. Edition 3; 2006.

31. Alexander M. Biodegradation and Bioremediation. 2nd Edition. San Diego, California: Academic Press; 1999.

32. Baboian R. Corrosion Tests and Standards: Application and Interpretation. 2nd Edition. Baltimore, Maryland: ASTM International; 2005.

33. Rampling A, Wiseman S, Davis L, Hyett AP, Walbridge AN, Payne GC, Cornaby AJ. Evidence that Hospital Hygiene is Important in the Control of Methicillin-resistant *Staphylococcus Aureus*. Journal of Hospital Infection 2001;49(2):109-16.

34. White FM. Fluid Mechanics. 2nd Edition. New York, New York: McGraw-Hill; 1986.

35. Review of the Optimised CB Vacuum Decontamination Technologies; 2015. http://www.foi.se/Global/V%C3%A5ra%20tj%C3%A4nster/Konferenser%20och%20seminarier/CBW%20symposium/Proceedings/Toepfer.pdf

36. Miorotti S. Innovative Decontamination for Sensitive Surfaces and Large Volumes (Unclassified Presentation to NATO CBRN Centre of Excellence, 2015). Rivoli Veronese, Italy: Cristanini CBRN Decontamination Systems; 2015.

37. STERIS Corporation - Hot-Air Decontamination; 2015. http://www.steris.com/products/viewDef.cfm?id=5090

38. Park SH, Peltz L, Dytioco RT, Van Camp CJ (inventors). High temperature decontamination of aircraft compartments. US 20140271347 A1. 2014.

39. Prokop EJ, Crigler JR, Wells CM, Young AA, Buhr TL. Response Surface Modeling for Hot, Humid Air Decontamination of Materials Contaminated with *Bacillus Anthracis* ΔSterne and *Bacillus Thuringiensis* Al Hakam Spores. AMB Express 2014;4(21):2-15.

40. Mundis C, Judd A, Sickle G, MacIver B, Weimaster J, Mueller M. Hot Air Decontamination of the C-141 Aircraft Technology Development Program (ECBC-TR-379). Aberdeen, Maryland: Edgewood Chemical Biological Centre; 2004.

41. McHugh M, Krukonis V. Supercritical Fluid Extraction. 2nd Edition. Stoneham, Massachusetts: Butterworth-Heinemann; 1994.

42. Perrut M. Supercritical Fluid Applications: Industrial Developments and Economic Issues. Industrial and Engineering Chemistry Research 2000;39:4531-5.

43. Dun S, Wood J, Martin B. Workshop on Decontamination, Cleanup, and Associated Issues for Sites Contaminated with Chemical, Biological, Or Radiological Materials (Report EPA/600/R-05/083). Cincinnati, Ohio: United States Environmental Protection Agency; 2005.

44. Smith CW, Rosio LR, Shore SH, Karle JA (inventors). Precision cleaning system. US 5377705 A. 1995.

45. Turner JR, West KN (inventors). Extraction process utilzing [*sic*] liquified carbon dioxide. US 7915379 B2. 2011.

46. Charoenchaitrakool M, Tungkasatan S, Vatanatham T, Limtrakul S. Cleaning of Lubricant-Oil-Contaminated Plastic using Liquid Carbon Dioxide. Journal of Industrial and Engineering Chemistry 2016;34:313-20.

47. Kohli R, Mittal KL. Developments in Surface Contamination and Cleaning: Fundamentals and Applied Aspects. Norwich, New York: William Andrew; 2008.

48. ASTM Standard D5127-2013: Standard Guide for Ultra-Pure Water used in the Semiconductor and Electronics Industries. West Conshohocken, Pennsylvania: ASTM International; 2013.

49. Pocius AV. Adhesion and Adhesives Technology: An Introduction. 3rd Edition. Cincinnati, Ohio: Hanser Publications; 2012.

50. Owens DK, Wendt RC. Estimation of the Surface Free Energy of Polymers. J Appl Polym Sci 1969;13(8):1741-7.

51. Lide DR. CRC Handbook of Chemistry and Physics. Internet Edition. Boca Raton, Florida: CRC Press; 2005.

52. Kanegsberg B, Kanegsberg E. Handbook for Critical Cleaning: Cleaning Systems and Agents. 2nd Edition. Boca Raton, Florida: CRC Press; 2011.

53. Ohtani H. Experimental Study on Flammability Characteristics of Perfluorocarbons. Fire Safety Science 1990:245-54.

54. Chang CC, Lo GG, Tsai CH, Wang JL. Concentration Variability of Halocarbons Over an Electronics Industrial Park and its Implication in Compliance with the Montreal Protocol. Environmental Science and Technology 2001;35(16):3273-9.

55. Prather MJ, Watson RT. Stratospheric Ozone Depletion and Future Levels of Atmospheric Chlorine and Bromine. Nature 1990;344:729-34.

56. Andersen SO, Bonnelycke N, Sparks J, Zatz M. Aqueous and Semi-Aqueous Alternatives for CFC-113 and Methyl Chloroform Cleaning of Printed Circuit Board Assemblies. Washington, DC: United States Environmental Protection Agency; 1994.

57. Oborny MC, Lopez EP, Peebles DE, Sorensen NR. Solvent Substitution for Electronic Assembly Cleaning, in Proceedings of the International Conference on Pollution Prevention, Clean Technologies and Clean Products. Washington, DC: United States Environmental Protection Agency Risk Reduction Laboratory; 1990.

58. Missick P. Health and Safety Impacts of Citrus-Based Terpenes in Printed Circuit Board Cleaning. Lowell, Massachusetts: University of Massachusetts, Lowell; 1993.

59. Chen J, Cranton W, Finn M. Handbook of Visual Display Technology. Berlin/Heidelberg, Germany: Springer-Verlag; 2012.

60. Smart BE. Fluorine Substituent Effects (on Bioactivity). Journal of Fluorine Chemistry 2001;109:3-11.

61. E.I. Du Pont De Nemours and Company - DuPont Vertrel X-P10 Specialty Fluid; 2013. https://www.chemours.com/Vertrel/en_US/assets/downloads/pdf/k16682.pdf

62. 3M Novec 7200 Engineered Fluid; 2009. http://multimedia.3m.com/mws/media/1998190/3mtm-novectm-7200-engineered-fluid.pdf

63. Andrle M, Opluštil F, Čáslavský J. Effects of Ultrasound Power, Temperature and Flow Rate of Solvent on Decontamination of Sensitive Equipment by Extraction. Defence Science Journal 2014;64:168-72.

64. MacIver B, Spafford R, Kaiser R, Kulczyk A, Smadbeck J. Development of a Portable Sensitive Equipment Decontamination System, Volume 2: Activated Carbon Fibre Wipe (Technical Report TR-766). Aberdeen Proving Ground, Maryland: Edgewood Chemical Biological Centre; 2010.

65. Klabunde KJ. Nanoscale Materials in Chemistry. New York, New York: Wiley Interscience; 2001.

66. Štengl V, Grygar TM, Opluštil F, Olšanska M. Decontamination of Sulfur Mustard from Printed Circuit Board using Zr-Doped Titania Suspension. Industrial and Engineering Chemistry Research 2013;52:3436-40.

67. Saxena A, Sharma A, Srivastava AK, Singh B, Gutch PK, Semwal RP. Kinetics of Adsorption of Sulfur Mustard on Al_2O_3 Nanoparticles with and without Impregnants. Journal of Chemical Technology and Biotechnology 2009;84:1860-72.

68. Mahato TH, Prasad GK, Singh B, Acharya J, Srivastava AR, Vijayaraghavan R. Nanocrystalline Zinc Oxide for the Decontamination of Sarin. Journal of Hazardous Materials 2009;165:928-32.

69. Waysbort D, McGarvey DJ, Creasy WR, Morrissey KM, Hendrickson DM, Durst HD. A Decontamination System for Chemical Weapons Agents using a Liquid Solution on a Solid Sorbent. Journal of Hazardous Materials 2009;161:1114-21.

70. Kim K, Tsay OG, Atwood DA, Churchill DG. Destruction and Detection of Chemical Warfare Agents. Chemical Reviews 2011;111:5345-403.

71. Wagner GW, Yang YC. Rapid Nucleophilic/Oxidative Decontamination of Chemical Warfare Agents. Industrial and Engineering Chemistry Research 2002;41:1925-8.

72. Fitch JP, Raber E, Imbro DR. Technology Challenges in Responding to Biological Or Chemical Attacks in the Civilian Sector. Science 2003;302(21):1350-4.

73. Rastogi VK, Ryan SP, Wallace L, Smith LS, Shah SS, Martin GB. Systematic Evaluation of the Efficacy of Chlorine Dioxide in Decontamination of Building Interior Surfaces Contaminated with Anthrax Spores. Applied and Environmental Microbiology 2010;76(10):3343-51.

74. McAnoy AM, Sait M, Pantelidis S. Establishment of a Vaporous Hydrogen Peroxide Bio-Decontamination Capability (Report DSTO-TR-1994). Fishermans Bend, Victoria, Australia: Defence Science and Technology Organisation; 2007.

75. Chou SF, Sk MH, Sofyan NI, Overfelt RA, Gale WF, Gale HS, Shannon CG, Fergus JW. Report DOT/FAA/AM-09/23: Evaluation of the Effects of Hydrogen Peroxide on Common Aviation Structural Materials. Washington, DC: Federal Aviation Administration; 2009.

76. O'Connor PDT, Kleyner A. Practical Reliability Engineering. 5th Edition. Chichester, West Sussex: John Wiley & Sons; 2012.

77. Melnychuk S, Neverov A, Brown RS. Catalytic Decomposition of Simulants for Chemical Warfare V Agents: Highly Efficient Catalysis of the Methanolysis of Phosphonothioate Esters. Angewandte Chemie International Edition 2006;45:1767-70.

78. Blinov V, Volchek K, Kuang W, Brown CE, Bhalerao A. Two-Stage Decontamination of Organophosphorus Compounds on Sensitive Equipment Materials. Industrial and Engineering Chemistry Research 2012;52:1405-13.

79. Bigley AN, Raushel FM. Catalytic Mechanisms for Phosphotriesterases. Biochimica Et Biophysica Acta 2012;1834(1):443-53.

80. Genencor DEFENZ Decon Enzymes; 2007. http://www.genencor.cn/uploads/tx_tcdaniscofiles/GENC-7877_DEFENZ_Bkgdr_Update_fnl3_07.pdf

81. Oudejans L, Wyrzykowska-Ceradini B, Williams C, Tabor D, Martinez J. Impact of Environmental Conditions on the Enzymatic Decontamination

of a Material Surface Contaminated with Chemical Warfare Agent Simulants. Industrial and Engineering Chemistry Research 2013;52:10072-9.

82. Linden KG, Shin GA, Faubert G, Cairns W, Sobsey MD. UV Disinfection of *Giardia Lamblia* Cysts in Water. Environmental Science and Technology 2002;36(11):2519-22.

83. Song K, Mohseni M, Taghipour F. Application of Ultraviolet Light-Emitting Diodes (UV-LEDs) for Water Disinfection: A Review. Water Research 2016;94:341-9.

84. Östin A. Review of Analytical Methods for the Analysis of Agents Related to Dumped Chemical Weapons for the CHEMSEA Project. Umeå, Sweden: European CBRNE Centre; 2012.

85. Mesilaakso M. Chemical Weapons Convention Chemicals Analysis: Sample Collection, Preparation, and Analytical Methods. Chichester, United Kingdom: John Wiley & Sons Ltd; 2005.

86. Gross JH. Mass Spectrometry. Heidelberg, Germany: Springer-Verlag; 2004.

87. Griffiths PR, de Haseth JA. Fourier Transform Infrared Spectroscopy. 2nd Edition. Hoboken, New Jersey: John Wiley & Sons; 2007.

88. Harris RK, Becker ED, Cabral de Menezes SM, Goodfellow R, Granger P. NMR Nomenclature: Nuclear Spin Properties and Conventions for Chemical Shifts. Pure and Applied Chemistry 2001;73:1795-818.

89. Witkowska E, Szczepaniak K, Biziuk M. Some Applications of Neutron Activation Analysis: A Review. Journal of Radioanalytical and Nuclear Chemistry 2005;265(1):141-50.

90. Neutron Activation Analysis. http://mnrc.ucdavis.edu/neutronactivation.html

91. Řanda Z, Kučera J, Mizera J, Frána J. Comparison of the Role of Photon and Neutron Activation Analyses for Elemental Characterization of Geological, Biological and Environmental Materials. Journal of Radioanalytical and Nuclear Chemistry 2007;271(3):589-96.

92. Wu ML. Assessing the Impact of Uncertainty in Physics-of-Failure Analysis of Microelectronics Damage. Materials Science and Engineering A 2012;558:259-64.

93. Kececioglu D. Reliability Engineering Handbook, Volume 1. Englewood Cliffs, New Jersey: Prentice Hall; 1991.

94. International Organisation for Standardisation/International Electrotechnical Commission Standard 7498-1. Geneva, Switzerland: International Organisation for Standardisation; 1996.

95. Ohring M, Kasprzak L. Reliability and Failure of Electronic Devices and Materials. 2nd Edition. Amsterdam, The Netherlands: Academic Press; 2015.

96. ASTM Standard D4308: Standard Test Method for Electrical Conductivity of Liquid Hydrocarbons by Precision Meter. West Conshohocken, Pennsylvania: ASTM International; 2013.

97. Çengel YA. Heat Transfer: A Practical Approach. Boston, Massachusetts: WCB-McGraw-Hill; 1998.

98. Hamburgen WR. Optimal Finned Heat Sinks (Report WRL-86/4). Palo Alto, California: Digital Equipment Corporation Western Research Laboratory; 1986.

99. Jin X, Azarian MH, Lau C, Cheng LL, Pecht M. Physics-of-Failure Analysis of Cooling Fans. Proceedings of the 2011 Prognostics & System Health Management Conference 2011

100. Karis TE, Miller JL, Hunziker HE, de Vries MS, Hopper DA, Nagaraj HS. Oxidation Chemistry of a Pentaerythritol Tetraester Oil. Tribol Trans 1999;42(3):431-42.

101. Williams J. Engineering Tribology. New York, New York: Cambridge University Press; 2005.

102. Gohar R, Rahnejat H. Fundamentals of Tribology. 2nd Edition. London, United Kingdom: Imperial College Press; 2012.

103. Brunner R. Properties of Carbon Overcoats and Perfluoro-Polyether Lubricants in Hard Disk Drives. San Diego, California: University of California at San Diego; 2009.

104. Ambekar RP, Bogy DB, Bhatia CS. Lubricant Depletion and Disk-to-Head Lubricant Transfer at the Head-Disk Interface in Hard Disk Drives. Journal of Tribology 2009;131:1-8.

105. Scheirs J. Modern Fluoropolymers: High Performance Polymers for Diverse Applications. Chichester, West Sussex: John Wiley & Sons Ltd; 1997.

106. Karis TE, Marchon B, Hopper DA, Siemens RL. Perfluoropolyether Characterization by Nuclear Magnetic Resonance Spectroscopy and Gel Permeation Chromatography. Journal of Fluorine Chemistry 2002;5814:1-14.

107. Kasai PH. Carbon Overcoat: Structure and Bonding of Z-DOL. Tribology Letters 2002;13(3):155-66.

108. Parent MJ, Kehren JM, Minday RM (inventors). Fluorinated ketones as lubricant deposition solvents for magnetic media applications. US 6403149. 2002.

109. He Z, Yang H, She M. Statistical Modelling of Hard Disk Drives (HDDs) Failure. Proceedings of the 2012 Asia-Pacific Magnetic Recording Conference; 2012.

110. Hughes GF, Murray JF, Kreutz-Delgado K, Elkan C. Improved Disk-Drive Failure Warnings. IEEE Trans Reliab 2002;51(3):350-7.

111. Hughes GF, Murray JF, Kreutz-Delgado K. Machine Learning Methods for Predicting Failures in Hard Drives: A Multiple-Instance Application. Journal of Machine Learning Research 2005;6:783-816.

112. Pinheiro E, Weber WD, Barroso LA. Failure Trends in a Large Disk Drive Population. Proceedings of the 5th USENIX Conference on File and Storage Technologies (FAST '07) 2007:1-13.

113. Asthana P, Finkelstein BI, Fennema AA. Rewritable Optical Disk Drive Technology. IBM Journal of Research and Development 1996;40(5):534-58.

114. Joos G, Freeman IM. Theoretical Physics. 3rd Edition. New York, New York: Dover; 1986.

115. Vicari L. Optical Applications of Liquid Crystals. Bristol, United Kingdom: Institute of Physics Publishing; 2003.

116. Task HL. Night Vision Devices and Characteristics. Neuilly-sur-Seine, France: Proceedings of NATO Advisory Group for Aerospace Research & Development; 1992.

117. Iosue MJ (inventor). Night vision device and method. US 6198090 B1. 2011.

118. LaDou J. Printed Circuit Board Industry. International Journal of Hygiene and Environmental Health 2006;209:211-9.

119. Popiel S, Nawała J, Dziedzic D, Söderström M, Vanninen P. Determination of Mustard Gas Hydrolysis Products Thiodiglycol and Thiodiglycol Sulfoxide by Gas Chromatography-Tandem Mass Spectrometry After Trifluoroacetylation. Analytical Chemistry 2014;86:5865-72.

120. 3M Novec 649 Engineered Fluid; 2009. http://multimedia.3m.com/mws/media/569865O/3mtm-novectm-649-engineered-fluid.pdf?fn=Novec649_6003926.pdf

121. 3M Novec 1230 Engineered Fluid; 2009. http://multimedia.3m.com/mws/media/1246880/3mtm-novectm-1230-fire-protection-fluid.pdf?fn=prodinfo_novec1230.pdf

122. Graziano G. On the Superhydrophobicity of Tetrafluoromethane. Chemical Physics Letters 2008;460:470-3.

123. Pietracupa J. FK-5-1-12 Thermodynamic Data (Personal Correspondence). St. Paul, Minnesota: 3M Company; 2015.

124. Baasner B, Hagemann H, Tatlow JC. Organo-Fluorine Compounds. Workbook Edition E10a. Stuttgart, Germany: Georg Thieme Verlag; 2000.

125. Sandford G. Perfluoroalkanes. Tetrahedron 2003;59:437-54.

126. Gambaryan NP, Rokhlin EM, Zeifman YV, Ching-Yun C, Knunyants IL. Reactions of the Carbonyl Group in Fluorinated Ketones. Angewandte Chemie International Edition 1966;5(11):947-56.

127. Jackson DA. Hydrolysis and Atmospheric Oxidation Reactions of Perfluorinated Carboxylic Acid Precursors. Toronto, Ontario: University of Toronto; 2013.

128. Jackson DA, Young CJ, Hurley MD, Wallington TJ, Mabury SA. Atmospheric Degradation of Perfluoro-2-Methyl-3-Pentanone. Environmental Science and Technology 2011;45:8030-6.

129. Wade LG. Organic Chemistry. 6th Edition. Upper Saddle River, New Jersey: Prentice Hall; 2005.

130. Wang Y, Niu J, Zhang L, Shi J. Toxicity Assessment of Perfluorinated Carboxylic Acids (PFCAs) Towards the Rotifer *Brachionus Calyciflorus*. Science of the Total Environment 2014;491-492:266-70.

131. Snell TW, Moffat BD, Janssen C, Persoone G. Acute Toxicity Tests using Rotifers: IV Effects of Cyst, Age, Temperature, and Salinity on the Sensitivity of *Brachionus Calyciflorus*. Ecotoxicology and Environmental Safety 1991;21:308-17.

132. Taniguchi N, Wallington TJ, Hurley MD, Guschin AG, Molina LT, Molina MJ. Atmospheric Chemistry of $C_2F_5C(O)CF(CF_3)_2$: Photolysis and Reaction with Cl Atoms, OH Radicals, and Ozone. Journal of Physical Chemistry 2003;107:2674-9.

133. Scott BF, MacDonald RW, Kannan K, Fisk A, Witter A, Yamashita N, Durham L, Spencer FC, Muir DCG. Trifluoroacetate Profiles in the Arctic, Atlantic, and Pacific Oceans. Environmental Science and Technology 2005;39:6555-60.

134. Møgelberg TE, Nielsen OJ, Sehested J, Wallington TJ, Hurley MD. Atmospheric Chemistry of CF_3COOH. Kinetics of the Reaction with OH Radicals. Chemical Physics Letters 1994;226(1-2):171-7.

135. Solomon K, Velders G, Wilson S, Madronich S, Longstreth J, Aucamp P, Bornman J. Sources, Fates, Toxicity, and Risks of Trifluoroacetic Acid and its Salts: Relevance to Substances Regulated Under the Montreal and Kyoto Protocols. Journal of Toxicology and Environmental Health, Part B: Critical Reviews 2016;Jun 28(1):1-16.

136. O'Hagan D, Harper DB. Fluorine-Containing Natural Products. Journal of Fluorine Chemistry 1999;100:127-33.

137. McCulloch A. Fluorocarbons in the Global Environment: A Review of the Important Interactions with Atmospheric Chemistry and Physics. Journal of Fluorine Chemistry 2003;123:21-9.

138. Linteris GT, Babushok VI, Sunderland PB, Takahashi F, Katta VR, Meier O. Unwanted Combustion Enhancement by $C_6F_{12}O$ Fire Suppressant. Proceedings of the Combustion Institute 2013;34(2):2683-90.

139. Malow M, Krause U. The overall Activation Energy of the Exothermic Reactions of Thermally Unstable Materials. Journal of Loss Prevention in the Process Industries 2004;17:51-8.

140. Ozone-Depleting Substances Regulations, 1998 (SOR/99-7).

141. Federal Halocarbon Regulations, 2003 (SOR/2003-289).

142. List of National Pollutant Release Inventory (NPRI) Substances for 2014 and 2015; 2015. https://www.ec.gc.ca/inrp-npri/default.asp?lang=En&n=9617CEC8-1

143. Canadian Environmental Protection Act, 1999 (S.C. 1999, c. 33).

144. 3M Novec 1230 Fire Protection Fluid, FK-5-1-12 Safety Data Sheet. Version 27.07. St. Paul, Minnesota: 3M Company; 2014.

145. Behr FE, Vitcak DR, Flynn RM, Costello MG, Parent MJ, Zhang Z (inventors). Use of fluorinated ketones in fire extinguishing compositions. US 6630075 B2. 2003.

146. McLinden MO, Perkins RA, Lemmon EW, Fortin TJ. Thermodynamic Properties of 1,1,1,2,2,4,5,5,5-Nonafluoro-4-(Trifluoromethyl)-3-Pentanone: Vapour Pressure, (p, ρ, T) Behaviour, and Speed of Sound

Measurements, and an Equation of State. Journal of Chemical & Engineering Data 2015;60:3646-59.

147. Almy EG, Griffin WC, Wilcox CS. Fischer Volumetric Determination of Water: Application to Technical Substances. Industrial and Engineering Chemistry, Analytical Edition 1940;12(7):392-6.

148. Low-Level Detection of Elements by Neutron Activation Analysis, Method ASG 084, Issue 1.1. Kingston, Ontario: Analytical Sciences Group; 2015.

149. MPA120 EZ-Melt Automated Melting Point Apparatus; 2014. http://www.thinksrs.com/downloads/PDFs/Manuals/MPA120m.pdf

150. Bergström L. Hamaker Constants of Inorganic Materials. Advances in Colloid and Interface Science 1997;70:125-69.

151. Synowicki RA, Pribil GK, Cooney G, Herzinger CM, Green SE, French RH, Yang MK, Burnett JH, Kaplan S. Fluid Refractive Index Measurements using Rough Surface and Prism Minimum Deviation Techniques. Journal of Vacuum Science and Technology B 2004;22(6):3450-3.

152. Hinrichs K, Eichhorn KJ. Ellipsometry of Functional Organic Surfaces and Films. Heidelberg, Germany: Springer-Verlag; 2014.

153. Tompkins HG, Irene EA. Handbook of Ellipsometry. Norwich, New York: William Andrew Publishing; 2005.

154. Hough DB, White LR. The Calculation of Hamaker Constants from Lifshitz Theory with Applications to Wetting Phenomena. Advances in Colloid and Interface Science 1980;14:3-41.

155. Broersma S. Magnetic Measurements on Organic Compounds. Zaltbommel, The Netherlands: N.V. van de Garde & Co's Drukkerij; 1947.

156. Evans DF. A New Type of Magnetic Balance. Journal of Physics E - Scientific Instruments 1974;7:247-9.

157. Johnson Matthey Magnetic Susceptibility Balance Instruction MSB Mk 1 Instruction Manual; 2004. https://www.unf.edu/~michael.lufaso/chem3610L/JM_MSB_Mk1.pdf

158. Davis RS. Equation for the Volume Magnetic Susceptibility of Moist Air. Metrologia 1998;35(1):49-55.

159. Putz MV, Mingos DMP. Applications of Density Functional Theory to Chemical Reactivity. Berlin/Heidelberg, Germany: Springer-Verlag; 2012.

160. Fiolhais C, Nogueira F, Marques M (editors). A Primer in Density Functional Theory. 1st Edition. Berlin/Heidelberg, Germany: Springer-Verlag; 2003.

161. Binkley JS, Pople JA, Hehre WJ. Self-Consistent Molecular Orbital Methods 21. Small Split-Valence Basis Sets for First-Row Elements. Journal of the American Chemical Society 1980;102(3):939-47.

162. Hoffman RE. Standardisation of Chemical Shifts of TMS and Solvent Signals in NMR Solvents. Magnetic Resonance in Chemistry 2006;44:606-16.

163. Hoffman RE, Becker ED. Temperature Dependence of the ^{1}H Chemical Shift of Tetramethylsilane in Chloroform, Methanol, and Dimethylsulfoxide. Journal of Magnetic Resonance 2005;176:87-98.

164. Nageswara Rao BD. Nuclear Magnetic Resonance Line-Shape Analysis and Determination of Exchange Rates. Methods in Enzymology 1989;176:279-311.

165. Military Specification: Webbing, Textile, Woven Nylon, MIL-W-4088K. Natick, Massachusetts: US Army Natick Research & Development Laboratories; 1988.

166. Clark MM. Transport Modelling for Environmental Engineers and Scientists. 2nd Edition. Hoboken, New Jersey: John Wiley & Sons; 2009.

167. Petroleum Hydrocarbons (PHC) in Soil Determined by Gas Chromatography–Flame Ionisation Detector (FID), Method ASG 053,Issue 2.4. Kingston, Ontario: Analytical Sciences Group; 2010.

168. Murphy KP. The Vapour Pressure of Hexafluoro and Pentafluorochloroacetone. Journal of Chemical & Engineering Data 1964;9(2):259-60.

169. Priye A, Marlow WH. Computations of Lifshitz–van Der Waals Interaction Energies between Irregular Particles and Surfaces at all Separations for Resuspension Modelling. Journal of Physics D - Applied Physics 2013;46(42):1-13.

170. Yaws CL. Yaws' Thermophysical Properties of Chemicals and Hydrocarbons. Norwich, New York: Knovel; 2009.

171. Ninham BW, Parsegian VA. Van Der Waals Forces: Special Characteristics in Lipid–Water Systems and a General Method of Calculation Based on the Lifshitz Theory. Biophysical Journal 1970;10:646-63.

172. Drummond CJ, Chan DYC. Van Der Waals Interaction, Surface Free Energies, and Contact Angles: Dispersive Polymers and Liquids. Langmuir 1997;13:3890-5.

173. Banerjee S, Sutanto S, Kleijn JM, van Roosmalen MJE, Witkamp G, Cohen Stuart MA. Colloidal Interactions in Liquid CO_2 — A Dry-Cleaning Perspective. Advances in Colloid and Interface Science 2012;175:11-24.

174. Berney CV. Infrared, Raman and Near-Ultraviolet Spectra of CF_3CO_Z compounds—Hexafluoroacetone. Spectrochimica Acta 1951;21(10):1809-23.

175. Zoellner RW, Latham CD, Goss JP, Golden WG, Jones R, Briddon PR. The Structures and Properties of Tetrafluoromethane, Hexafluoroethane, and Octafluoropropane using the AIMPRO Density Functional Program. Journal of Fluorine Chemistry 2003;121:193-9.

176. Wavefunction I. Spartan '08 [computer program]. Irvine, California: Wavefunction, Inc.; 2008.

177. Vilenchik YM, Soshin VA, Novoselitskaya LM, Lekontseva GI, Neifeld PG. Synthesis of Perfluorinated Ethyl Ketones (Abstract Only). Zhurnal Vsesoyuznogo Khimicheskogo Obshchestva Im. D.I. Mendeleeva 1978;23

178. Majid A, Shreeve JM. Fluorinated Esters Stable to Fluoride Ion. Journal of Organic Chemistry 1973;38(23):4028-31.

179. Kawa H, Ishikawa N. Formation of C–S Bond by Elimination of Perfluorocarboxylic Acid. Bulletin of the Chemical Society of Japan 1980;53:2097-8.

180. Waybright TJ, Britt JR, McCloud TG. Overcoming Problems of Compound Storage in DMSO: Solvent and Process Alternatives. Journal of Biomolecular Screening 2009;14(6):708-15.

181. Shoolery JN. A Basic Guide to NMR. 3rd Edition. Castano Primo, Italy: Extra Byte; 2008.

182. Petterson KA, Stein RS, Drake MD, Roberts JD. An NMR Investigation of the Importance of Intramolecular Hydrogen Bonding in Determining the Conformational Equilibrium of Ethylene Glycol in Solution. Magnetic Resonance in Chemistry 2005;43:225-30.

183. Pearce CM, Sanders JKM. Improving the use of Hydroxyl Proton Resonances in Structure Determination and NMR Spectral Assignment: Inhibition of Exchange by Dilution. Journal of the Chemical Society, Perkins Transactions 1 1994;1(9):1119-24.

184. Waltman RJ. The Stability of Ultra-Thin Perfluoropolyether Mixture Films on the Amorphous Nitrogenated Carbon Surface. Journal of Colloid and Interface Science 2007;313:608-11.

185. Snelson JT. Grain Protectants. Melbourne, Australia: Ruskin Press; 1987.

186. Flury M, Papritz A. Bromide in the Natural Environment: Occurrence and Toxicity. Journal of Environmental Quality 1993;22:747-58.

187. Van Oorspronk J, Bostoen AJA, Van Haasteren C, Warmoeskerken MMCG (inventors). Method and device for industrial washing of textile. EP 2496751 A1. 2011.

188. Tuma PE. Fluoroketone $C_2F_5C(O)CF(CF_3)_2$ as a Heat Transfer Fluid for Passive and Pumped 2-Phase Applications. Proceedings of 24th Annual IEEE/CPMT Semiconductor Thermal Measurement, Modeling & Management Symposium (SEMI-THERM) 2008:173-9.

189. Intel - Enhanced Intel SpeedStep Technology for the Intel Pentium M Processor; 2004. ftp://download.intel.com/design/network/papers/30117401.pdf

190. Advanced Configuration and Power Interface Specification (Revision 5.0 Errata A); 2013. http://www.acpi.info/DOWNLOADS/ACPI_5_Errata%20A.pdf

191. Montgomery DC. Design and Analysis of Experiments. 8th Edition. Hoboken, New Jersey: John Wiley & Sons; 2009.

192. Toujou F, Tsukamoto K, Matsuoka K. Characterisation of Lubricants for Fluid Dynamic Bearing by TOF-SIMS. Applied Surface Science 2003;203-204:590-5.

193. Camera E, Ludovici M, Galante M, Sinagra JL, Picardo M. Comprehensive Analysis of the Major Lipid Classes in Sebum by Rapid-Resolution High-Performance Liquid Chromatography and Electrospray Mass Spectrometry. J Lipid Res 2010;51(11):3377-88.

194. Zmojda J, Kochanowicz M, Miluski P, Dorosz D. Side-Detecting Optical Fiber Doped with Tb^{3+} for Ultraviolet Sensor Application. Fibers 2015;2(2):150-7.

Appendix A

2012-13 Decontamination Project

A.1 – Experiments

Experiments in the 2012-13 decontamination project proceeded in three phases. The first was to assess the solubility of CW agent simulants in two candidate decontaminants, HFE-7200 and FK-5-1-12, which resulted in down-selection to FK-5-1-12. The second was to study the kinetics of simulant and HD agent partitioning from a 'contaminated' polyethylene surface into FK-5-1-12. Despite evidence that FK-5-1-12 was indeed capable of decontaminating surfaces by removal of HD, the fates of the agent and of simulants were not fully elucidated because of incomplete recovery and mass balance. The third phase was to conduct operational trials of solid-state COTS electronic memory devices contaminated with simulant and subjected to decontamination by immersion in various liquids, including aqueous media, aggressive redox reagents, and FK-5-1-12.

A.2 – Results

A.2.1 – Simulant–Fluid Interactions

In a simulant–fluid solubility study, FK-5-1-12 was determined to have apparent solubility limits one to two orders of magnitude greater than HFE-7200 for four CW agent simulants: 2-chloroethyl ethyl sulfide (CEES), methyl salicylate (MES), dimethyl methylphosphonate (DMMP) and diethyl phthalate (DEP). The fifth simulant, 2-(butylamino)ethanethiol (BAET), reacted with FK-5-1-12 at 10 % by volume dilution. Higher limits of contaminant solubility are useful from the perspectives of military operations and logistics, in that they minimise the need for *in situ* solvent recycling or resupply whilst maintaining a specified level of decontamination throughput. Thus, the apparently large limits of simulant solubility (less BAET) in FK-5-1-12 motivated further study of the FK in the decontaminant role. HFE-7200 was not used in any subsequent studies. This interpretation of solubility limits was later determined to be erroneous.

A.2.2 – Kinetic Studies

As previously discussed, a fundamental operational requirement is to minimise the time needed to achieve a desired extent of decontamination, since any such improvement will contribute directly to the critical path of

ensuring decontamination throughput. A further motivation, which had not yet been fully quantified by this stage of the research, was the ability of contaminated sensitive electronic equipment to tolerate exposure to a liquid for any given time interval. Thus, kinetic studies were undertaken in laboratory conditions in an effort to determine the time-dependency of contaminant partitioning into FK-5-1-12 and establish constraints on process feasibility.

A typical result for HD recovery in normalised mass v. time is shown in Figure A–1.

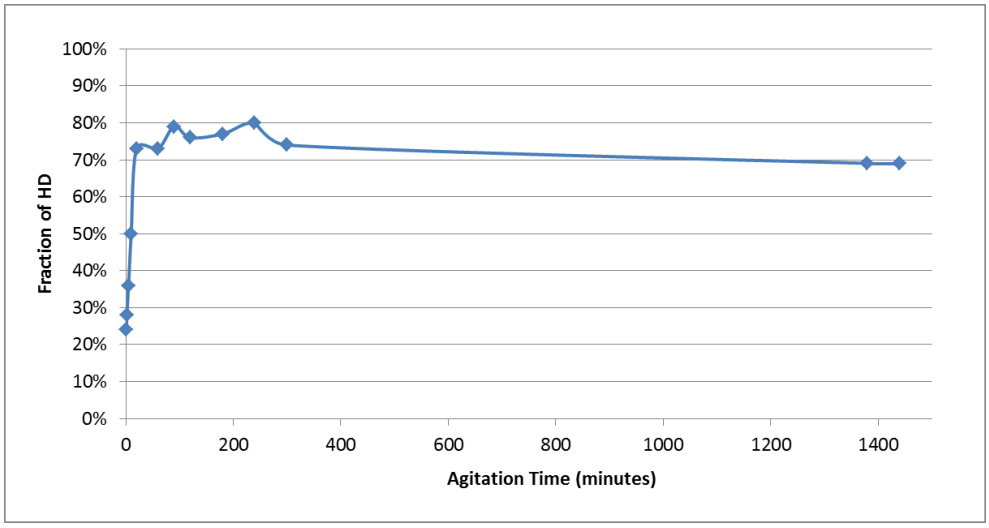

Figure A-1: Fraction of HD Removed into FK-5-1-12 v. Agitation Time

Approximately 75 % of the initial load of HD was recovered from FK-5-1-12 within 20 min of agitation as determined by GC-MS, and this quantity, subject to minor oscillations, appears to equilibrate or be gradually removed or transformed over 24 hours. At no time was HD 100 % recoverable, and the recovery did not increase monotonically.

One possible mechanistic explanation for the behaviour is offered in the form of two series processes: mass transfer (desorption from the LDPE substrate) and another process (whether reaction, e.g. hydrolysis or oxidation in FK-5-1-12, or another mass transfer step, such as re-sorption onto the substrate). These processes are represented by Equation A–1, which is generalised to Equation A–2.

$$[\mathrm{HD}]_{\mathrm{LDPE}} \overset{k_1}{\rightarrow} [\mathrm{HD}]_{\mathrm{FK}} \overset{k_2}{\rightarrow} [\mathrm{Products}]_{\mathrm{FK}}$$

Equation A-1: Desorption–Reaction Process

$$A \overset{k_1}{\rightarrow} B \overset{k_2}{\rightarrow} C$$

Equation A-2: General Mechanism of Observed HD Behaviour

When the mechanism is solved with first-order behaviour in the first step and zeroth-order behaviour in the second, Equation A–3 is obtained.

$$B = -e^{-k_1 t} - k_2 t + Constant$$

Equation A-3: Process Equation

In applying a constant of integration of 0.85, whose deviation from unity is within the 20.1 % systematic error of the method,[1] k_1 retains a value of 0.0534 min^{-1} and k_2 takes a value of 10^{-4} min^{-1}, yielding the function in Figure A–2, a qualitative fit.

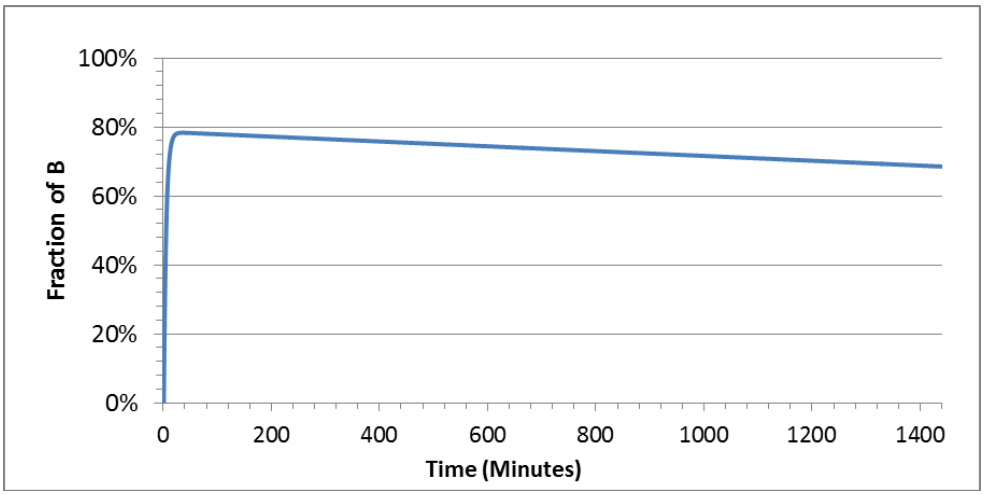

Figure A-2: Fraction of B v. Time

In order to obtain a quantitative best fit under these assumptions of process order, nonlinear least-squares regression in the parameters k_1, k_2, and the constant was performed over the entire 1440-min time domain and permitting any constant of integration within [0, 1].

Resultant parameters and derived half-lives are presented in Table A-1 and observed and fitted functions in Figure A–3.

Table A-1: Process Parameters

Parameter:	Value:	Units:
k_1	0.2269	min^{-1}
k_2	0.0001	min^{-1}
$Constant$	0.786	(–)
$t_{0.5\|1}$	3.055	min
$t_{0.5\|2}$	7150	min
R^2	0.736	(–)

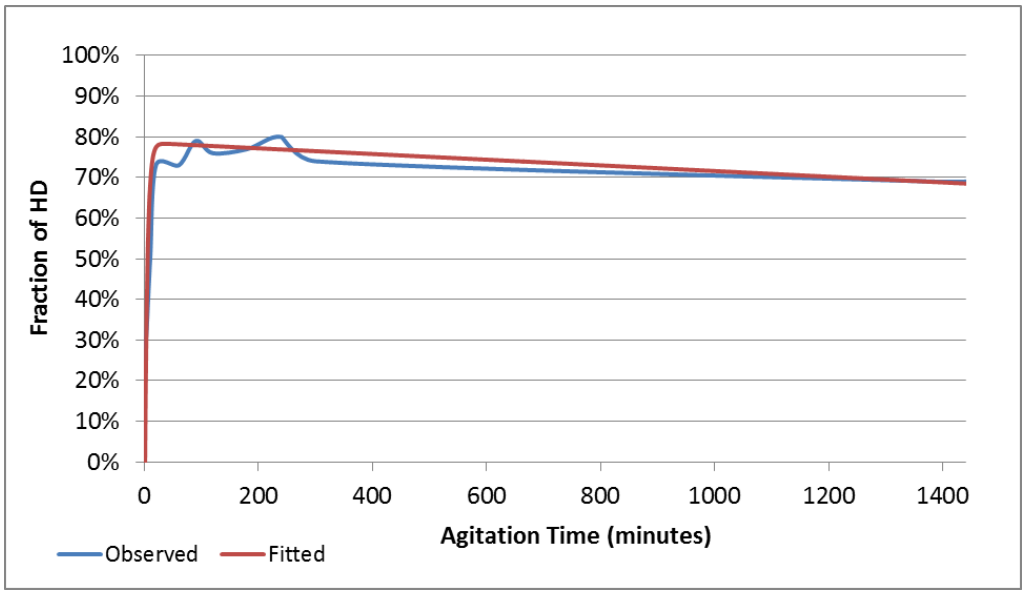

Figure A-3: Fit of HD Recovered from FK-5-1-12 by GC-MS v. Agitation Time

The constant of integration lies just outside the absolute value of the systematic error of the determination method. The remaining 20-30 % of HD not recovered could have remained adsorbed onto the LDPE surface throughout the 24 hours, or there could have been further systematic errors in the apparatus summing to this residual value. A future trial with HD as the challenge contaminant could attempt recovery in a known sorbent in series or parallel in an effort to obtain a less-uncertain mass balance.

Selected results of kinetics studies of all contaminants, with best-fit parameters within the operationally relevant time domain of [0, 20] min and initial concentrations of 4500 µmol contaminant·mol^{-1} fluid, are summarised

in Table A-2. Equations express the normalised concentration c as a function of time t.

Table A-2: Summary of Contaminant Removal Kinetics Determined by GC-MS

Contaminant:	Agitation Angular Velocity: (ω, rpm)	Linearised Equation:	Correlation Coefficient: (R^2)	Half-Life: ($t_{0.5}$, min)
HD	150	$c = -0.0536t - 0.1975$	0.9934	12.9
CEES	120	$c = -0.0006t - 0.0018$	0.9096	1160
MES	120	$c = 0.2775t - 0.8727$	0.9933	0.794
DEP	150	$c = -0.0541t - 0.4951$	0.3769	12.8
DMMP	150	$c = -0.0035t - 0.0721$	0.3188	198
DIMP	150	$c = -0.00002t - 0.0002$	0.6692	34657

Rates of contaminant partitioning into FK-5-1-12 were analysed using least-squares regression to integer-power curves. Within the initial 20-min time domain, all partitioning functions were regressed to first-order kinetics, except for MES, which was regressed to a second-order kinetic expression. DEP (a phthalic acid ester) and MES (a phenolic acid ester) both caused visible, plastic deformations of the polyethylene substrate surfaces when spiked at 4500 μmol·mol^{-1}, which is consistent with their expected behaviour as primary and secondary plasticisers.[2] Although CEES was selected as a simulant for HD on the basis of its similar physical and chemical properties, and favourable representation in the literature for this purpose,[3] its apparent mass-transfer parameters in FK-5-1-12 diverged by orders of magnitude from those of HD in determinations by GC-MS.

To attain a more complete accounting of the fate of the initial contaminant load, parallel analyses were attempted: HD samples from the liquid phase were determined by GC-MS, and HD (as Cl atoms) on the substrate surfaces were determined by INAA (SLOWPOKE-2 reactor at RMCC, Kingston, Ontario). Background Cl abundances were first determined and subtracted from the final responses, and internal chloride standards were used. Removal of HD from surfaces after 30 min of treatment time, as determined by INAA, is shown in Table A-3. Results appeared promising from the perspective of decontamination.

Table A-3: Surface Removal of HD Determined by INAA

Initial Load of HD: (µg)	Loading Density of HD: (µg·cm^{-2})	HD Fraction Remaining on Surface:
1.72	0.275	6.70%
17.2	2.75	2.62%
172	27.5	0.78%
1720	275	0.34%

However, no more than 55 % of initial HD loads of 172 µg and 1720 µg were recovered in the liquid phase by GC-MS, which confounded a mass balance. Two possible mechanistic explanations for the persistent lack of HD recovery by GC-MS were hydrolysis and oligomerisation, although an insufficiently homogeneous sampling technique for dispersed HD in the FK-5-1-12 phase was more likely.

FK-5-1-12 is reported by the manufacturer to dissolve 20 µg of water per g at 20 °C, giving a maximum of 480 µg (26 µmol) of water in a 15-mL vial of FK-5-1-12. Since the largest initial load of HD was 1720 µg (10.81 µmol), and HD may be hydrolysed stoichiometrically to thiodiglycol and hydrochloric acid (Equation A–4), water could have been in excess in any of the loadings considered.

$$C_4H_8Cl_2S_{(l)} + 2H_2O_{(l)} \rightarrow C_4H_{10}O_2S_{(aq)} + 2HCl_{(aq)}$$

Equation A-4: Hydrolysis of HD

Karl Fischer titration was not conducted at this stage, but was recommended in the scope of any future work. FK-5-1-12 was not dehydrated before use, and thus the possibility of hydrolysis was not discounted. Moreover, in the presence of a polar solvent, HD (and CEES) can form cyclic sulfonium cations in addition to chloride salts,[4] which may avoid detection by GC-MS. Methods for the determination of thiodiglycol and thiodiglycol sulfoxide by GC-MS are possible, given preliminary derivatisation with a suitable reagent, such as 1-(trifluoroacetyl)imidazole.[5]

A.2.3 – Operational Trials

Next, operational trials were conducted on 12 COTS 2-GB electrically erasable, programmable read-only memory (EEPROM) Universal Serial Bus (USB) devices (Verbatim, Charlotte, North Carolina) in order to observe system-level behaviour and to assign preliminary reliability metrics to different decontamination processes. Performance was evaluated using the HDDScan 3.3 programme as the number of memory blocks whose access time increased

(degradation) or decreased (improvement) during a 'butterfly read' stress test of sequential read–write operations in 32-kB increments to all accessible memory blocks. In baseline testing, each device was confirmed to have 15255 accessible memory blocks in total, with a typical proportion of 80 % of all blocks accessible in < 10 ms and 20 % of blocks in < 20 ms. Proportions of memory blocks accessible at the <10-ms and <20-ms thresholds varied quasi-sinusoidally in successive tests of the control device.

All other devices were connected to a host laptop computer via USB interface. Some were contaminated with the simulant CEES, either neat or in solution, spiked at 33 µL onto the exposed surface of the PrCB of the device before stress-testing. All were then immersed in 15 mL of various liquid decontamination media for the duration of the stress test. Results of the operational trials are summarised in Table A-4.

Table A-4: Summary of Trials of COTS Memory Devices

Device #:	Contaminant:	Decontaminant:	Blocks Affected**:	Fraction of Total Memory:
1	None	FK-5-1-12	-53	-0.35%
2	450 ppm CEES	FK-5-1-12	-81	-0.53%
3	4500 ppm CEES	FK-5-1-12	-235	-1.54%
4	98 % CEES	FK-5-1-12	-245	-1.61%
5	None	Distilled–deionised water	1439	9.43%
6	None	Municipal supply water (MSW)	-480	-3.15%
7	None	5% by volume domestic bleach in MSW	-15129	-99.17%
8	None	Domestic bleach, 6 % by weight sodium hypochlorite	-15255	-100.00%
9	None	1.5 mol·L^{-1} butane-2,3-dione monoximate in MSW	-650	-4.26%
10	None	5 % by weight benzoyl peroxide in anhydrous EtOH	263	1.72%
11	None	20 % by weight benzoyl peroxide in anhydrous EtOH	-397	-2.60%
12*	None	None	-116	-0.76%
		Amplitude of 30 successive stress tests	869	5.70%

*Control
** Positive values denote reduction in memory access time (performance improvement)

Process effluents of devices #5 to 8, from left to right, are depicted in Figure A–4. Liquid phases of the effluents were not sampled, but a qualitative increase in turbidity, changes in colour, and the presence of insoluble particulates were evident.

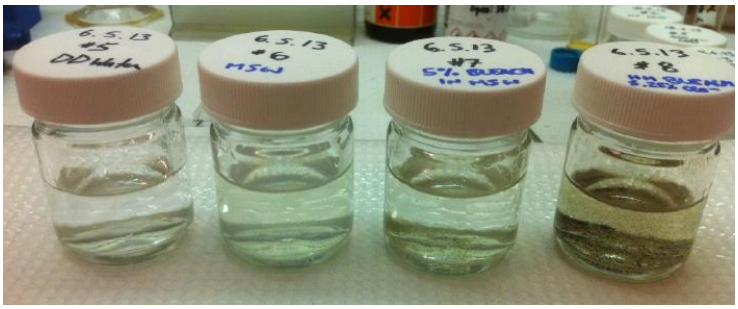

Figure A-4: USB Device Decontamination Process Effluents

Upon completion of the stress test for device #7, the host computer could recognise fewer than 1 % of the total number of memory blocks.

Within 2 min of the start of treatment of device #8, there was visible evidence of corrosion within its reactor vial; after 7 min, its light-emitting diode began pulsing on–off. Device #8 failed catastrophically, that is, it was no longer recognised as a peripheral by the host computer and its light-emitting diode was extinguished, at 15 min of treatment time. Surface effects are illustrated in Figure A–5, with corrosion of soldering points particularly evident in the lower right-hand quadrant. Corrosion could have been either electrochemical or galvanic in character given the uninsulated contact between the serial bus, energised to a maximum potential drop of 5 V_{DC}, and the liquid.

Figure A-5: Corroded USB Device

In summary, solid-state electronic memory devices demonstrated varying levels of operability when subjected to contamination by a CW simulant and decontamination by several different media. Consequences ranged in severity

from improvement in memory access times greater than the amplitude of test-to-test variation, in the case of distilled–deionised water, to over 99 % degradation in memory access and to catastrophic device-level failure before the conclusion of a single stress test in the cases of diluted and retail-strength bleach. Neither contamination with neat CEES nor decontamination by immersion in FK-5-1-12 resulted in a variation in memory performance larger than the amplitude of the control device.

Notwithstanding these apparently favourable results for single-pass treatment of solid-state electronic devices, the family of sensitive equipment is sufficiently diverse to warrant much broader investigation. Follow-on research, which has been the focus of the current project, assessed the ability of FK-5-1-12 to remove multiple challenge contaminants from a wider variety of substrate surfaces and from more complex sensitive equipment, with a correspondingly greater number of possible failure modes.

References

1. Determination of Bis-(2-Chloroethyl) Sulfide in Water by Liquid–Liquid Extraction and Analysis by Gas Chromatography–Mass Spectrometry, Method ASG 070a, Issue 1.7. Kingston, Ontario: Analytical Sciences Group; 2013.

2. Billmeyer FW. Textbook of Polymer Science. 2nd Edition. New York, New York: John Wiley & Sons; 1971.

3. Willis MP, Varady MJ, Pearl TP, Fouse JC, Riley PC, Mantooth BA, Lalain TA. Physics-Based Agent-to-Simulant Correlations for Vapour-Phase Mass Transport. Journal of Hazardous Materials 2013;263(2):479-85.

4. Somani SM. Chemical Warfare Agents. San Diego, California: Academic Press, Inc.; 1992.

5. Popiel S, Nawała J, Dziedzic D, Söderström M, Vanninen P. Determination of Mustard Gas Hydrolysis Products Thiodiglycol and Thiodiglycol Sulfoxide by Gas Chromatography-Tandem Mass Spectrometry After Trifluoroacetylation. Analytical Chemistry 2014;86:5865-72.

Appendix B

Mathematical Methods

B.1 – Statistics and Error Propagation

B.1.1 – Statistics

Statistics provides a mathematical framework to test a hypothesis without determining all the physical parameters that could influence it. The relative accuracy of a hypothesis is decided based upon the strength of an association between independent and dependent variables, while controlling for the effects of random chance.

The framework for statistical testing of hypotheses is as follows. First, a null hypothesis is formulated. This hypothesis will be either rejected or not rejected (but not 'accepted') as a result of a statistical test applied to it. A level of significance α is assigned to set the threshold for excluding random chance. Typically this value is a fraction of unity, e.g. 0.10, 0.05, or 0.01. A lower level is more restrictive on the influence of random chance. The next step is to apply a statistical test, such as a two-tailed t-test. The purpose of a two-tailed t-test is to evaluate the probability p of a significant influence, but without a prior expectation of the direction of the influence. Independent and dependent variables are then measured in a real system and the probability p computed based upon the formula for the given statistical test. A p-value that falls within the region(s) of the statistical function bounded by α (the rejection region(s)) means that the null hypothesis of an association between the independent and dependent variables may be rejected. If a p-value is not enclosed in the rejection region, then the null hypothesis, as it was written, cannot be rejected.[1] In addition to the results of a test, the mathematical assumptions of a given statistical distribution may also be tested using experimental data to judge the fitness of the distribution for the data at hand.[2]

For instance, a treatment is hypothesised to have no effect on the behaviour of a small sample and α of 0.05 is assigned. The behaviour of a sample is monitored for a short time as the baseline. Then, a treatment is applied to the members of the sample, but neither a positive nor a negative change in behaviour is expected. The behaviour of the sample is monitored again, after treatment, and compared to the baseline by a two-tailed t-test. The resulting probability p is computed according to Equation B-1, in which t is the test statistic, $\bar{X}$ the 'treatment' mean, μ_0 the 'baseline' mean, s_x the treatment sample standard deviation, and n the number in the sample.

$$t = \frac{\bar{X} - \mu_0}{\frac{s_x}{\sqrt{n}}}$$

Equation B-1: *t*-Test Statistic

The statistic t associated with n-1 degrees of freedom is interpolated from tabulated values of probability density functions to arrive at a probability. Suppose that the value of p, computed from t and n-1 degrees of freedom, is 0.001. Since this value is less than $\frac{\alpha}{2}$ (for two equally probable tails or regions), the null hypothesis may be rejected. In other words, the treatment had an effect on the behaviour of the sample which could not be explained by random chance alone.

The extent to which a set of empirical data corresponds to a theoretical distribution may be determined through a quantile–quantile plot.[2] The empirical data are normalised and the resulting quantiles (the fraction of data below a certain value) are plotted against the normalised quantiles of a theoretical distribution. The magnitude of the correlation coefficient of linear regression between the empirical and theoretical quantiles then corresponds to the overall closeness of the empirical data to that distribution. For instance, a set of data which skewed in a certain direction would result in a lower linear regression correlation coefficient when compared to a symmetrical Gaussian distribution. Any significant departure of real data from a theoretical (particularly Gaussian) distribution may be determined in this way. Hence, it can be used to validate assumptions of normality in statistical modelling.

B.1.2 – Error Propagation

All measurements of physical phenomena are associated with errors (departures from accuracy) and uncertainties (finite precision). The two are not identical, but they may be computed and compared in the same statistical terms as the standard deviation about the mean value of a variable.[3]

Standard deviations themselves are not additive. However, they are additive in quadrature (when squared), as variances about the mean. A general function $W = f(X)$ may be described by the influence of a measurable independent variable x on the predicted behaviour of a dependent variable w, provided the errors and uncertainties about x are also conveyed. This is done through the variance formula, in which $f(X)$ is evaluated at the mean value of the sample of x.

$$variance(w) \doteq \left[\frac{df}{dX}\right]^2 \cdot variance(x)$$

Equation B-2: Variance Formula

Variances of n independent variables x_i may then be added according the error propagation formula.

$$variance(w) \doteq \sum_{i=1}^{n} \left(\left[\frac{\partial f}{\partial X_i}\right]^2 \cdot variance(x_i) \right)$$

Equation B-3: Error Propagation Formula

If a sample of three or more determinations is available, then their mean value and standard deviation may be calculated through statistical formulae. For a single determination, there is no value for the sample standard deviation. Hence, the value itself and the propagated error on the measurements used to determine it are reported.

An example of the propagated error determined for the decontamination of bromophos-methyl (as Br) from plastic coupons is shown in Table B-1. The measurement errors (Δ) divided by the masses (m) of the coupon, the background of Br in the system, and the Br post-decontamination, are all summed in quadrature as relative error contributions. The product of the square root of this quantity and the Br residual on the coupon (in this case, 82 %) gives the error in the Br residual (18 %).

Table B-1: Example of Propagated Error

$$Error_{Residual\,\%} = Residual\,\% \cdot \sqrt{\left(\frac{\Delta m_{coupon}}{m_{coupon}}\right)^2 + \left(\frac{\Delta m_{Br-bkgd}}{m_{Br-bkgd}}\right)^2 + \left(\frac{\Delta m_{Br-post\ decon}}{m_{Br-post\ decon}}\right)^2}$$

$$Error_{Residual\,\%} = 82\,\% \cdot \sqrt{\left(\frac{0.0001\ \text{g}}{0.7990\ \text{g}}\right)^2 + \left(\frac{0.0034\ \mu\text{g Br}\cdot\text{g}^{-1}\text{coupon}}{0.0155\ \mu\text{g Br}\cdot\text{g}^{-1}\text{coupon}}\right)^2 + \left(\frac{0.0249\ \mu\text{g Br}\cdot\text{g}^{-1}\text{coupon}}{3.7310\ \mu\text{g Br}\cdot\text{g}^{-1}\text{coupon}}\right)^2}$$

$$Error_{Residual\,\%} = 18\,\%$$

It can be seen, by dividing both sides by the residual and squaring, that the error formula aggregates the relative errors from each independent measurement and equates them to a relative error in the sought-after value, which must be calculated rather than measured directly. Another consequence is that the most uncertain measurement in relative terms will give the dominant contribution to the total error. For instance, in this approach, if there were large uncertainty in the background abundance of bromine in the system, then the extent of decontamination, i.e. the removal of bromine, could not be reported with a high certainty.

B.2 – Numerical Methods

B.2.1 – Finite Methods for Partial Differential Equations

Closed-form, analytical solutions to the equations governing or describing natural systems may be cumbersome or non-existent. Such equations are practically solved using numerical methods. To solve partial differential equations (e.g. governing heat conduction and mass diffusion), infinitesimals of any variable ∂x are replaced in every instance by small, finite differences δx. For instance, a heat flux is replaced by a finite quantity of thermal energy δQ flowing through a surface area δA per unit time δt, $\frac{\delta Q}{\delta A \cdot \delta t}$. A thermal gradient is replaced by a finite temperature difference δT in any direction in space δx, $\frac{\delta T}{\delta x}$. The system geometry is replaced by an arrangement of nodes in space or time over which the governing equations (in terms of finite differences) may be calculated algebraically. Initial and boundary conditions are input, and the resulting mathematical model is solved numerically. The solution is approximate and requires computational effort, particularly as the finite differences are made smaller to improve accuracy. However, with these caveats, an acceptable solution can be found for a well-defined problem.[4]

An explicit solution to a transient heat-conduction problem has the advantage of simplicity, but is susceptible to numerical errors, e.g. instability. For instance, even with the governing equations of Fourier's law and the First Law of Thermodynamics (energy balance) about a node, some physically spurious results in temperature may result if excessively large finite differences in time are used.[5] Hence, such solutions must be tested for mathematical convergence and for violations of other physical laws.

References

1. Blanchard BS, Fabrycky WJ. Systems Engineering and Analysis. 2nd Edition. Englewood Cliffs, New Jersey: Prentice-Hall; 1990.

2. Montgomery DC. Design and Analysis of Experiments. 8th Edition. Hoboken, New Jersey: John Wiley & Sons; 2009.

3. Ku HH. Notes on the use of Propagation of Error Formulas. Journal of Research of the National Bureau of Standards - C. Engineering and Instrumentation 1966;70C(4):263-73.

4. Farlow SJ. Partial Differential Equations for Scientists and Engineers. 2nd Edition. New York, New York: Dover; 1993.

5. Çengel YA. Heat Transfer: A Practical Approach. Boston, Massachusetts: WCB-McGraw-Hill; 1998.